Hypothalamic dopamine receptor D1 signaling mediates hedonic feeding-induced obesity

Qi Zhang

Advisor: Ali D. Güler

B.S., Nankai University, 2015

A dissertation presented to the Graduate Faculty of the University of Virginia in Candidacy for the Degree of Doctor of Philosophy

Department of Biology

University of Virginia

April 2022

Committee Members
Ali Güler
Ignacio Provencio
Christopher Deppmann
Eyleen O'Rourke
John Campbell
Michael Scott

Abstract

Obesity comorbidities such as diabetes and cardiovascular disease are pressing public health concerns. Overconsumption of calories leads to obesity; however, the neural mechanisms underlying excess food consumption and the resulting weight gain are poorly understood. Here, we find that similar to other addictive or compulsive behaviors, encoding of palatable food, via dopaminergic signaling in a homeostatic center of the brain, is responsible for short-circuiting the exquisite neural mechanisms in place to prevent overconsumption. We demonstrate that dopamine receptor D1 (Drd1) signaling is required for palatable diet induced hyperphagia outside of the regular meal time. Genetic ablation of Drd1 protects mice from diet-induced obesity and associated metabolic syndromes. Specifically, we identified a heterogeneous group of neurons expressing Drd1 in the arcuate hypothalamus (ARC) with a significant proportion co-expressing agouti-related peptide/neuropeptide Y (AgRP/NPY). We elucidated an orexigenic role of these Drd1-expressing neurons which regulate feeding behavior differently than the AgRP/NPY neurons. Furthermore, Drd1 expressed in the AgRP/NPY neurons is required for gating the severity of diet-induced obesity. Stimulation of the Drd1 and AgRP/NPY co-expressing arcuate neurons is sufficient to induce voracious feeding while genetic ablation of Drd1 in these neurons reduces hyperphagia and body weight gain induced by a palatable diet. In accordance with the orexigenic function of the Drd1-expressing neurons in the ARC, we revealed the dynamic DA release within the ARC, responding to changes of energy supplies. We identified a continuum of DA neurons in the hypothalamic areas projecting to the ARC, of which the genetically defined A13 DA group in the zona incerta (ZI) potentially promotes feeding by modulating ARC activity.

These results provide a new mechanism that influences overconsumption of rewarding foods and positions Drd1 signaling in the $ARC^{AgRP/NPY}$ neurons as an integrator of the hedonic and homeostatic neuronal feeding circuits.

Graphical Abstract

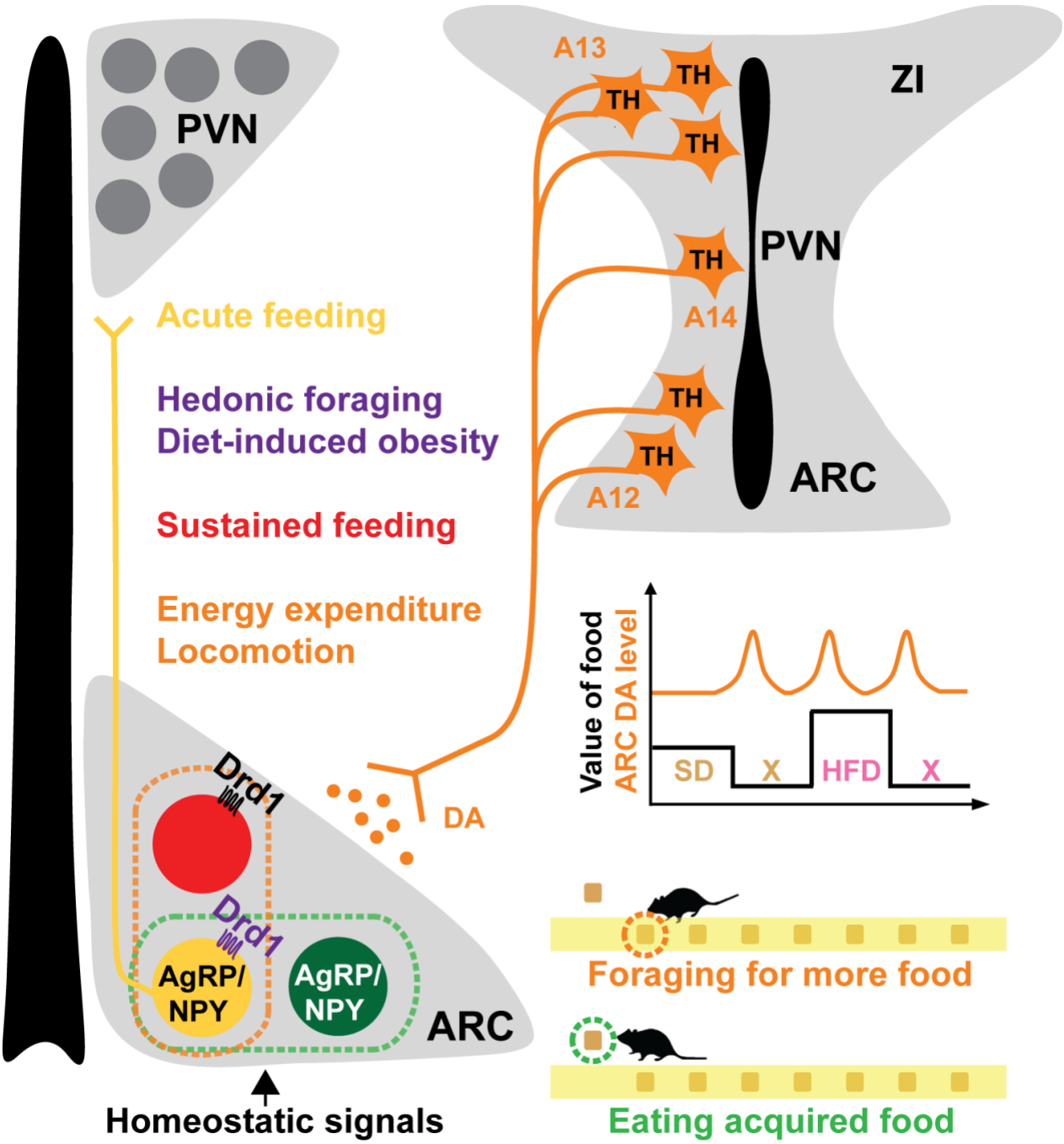

Acknowledgement

It is probably the most courageous, romantic, and meaningful thing for humans to pursue science against the enormous darkness of the unknown. I was very lucky to start a career as a researcher in one of the most interesting fields – neuroscience. I was even more lucky to join Ali Güler's lab to pusue my graduate training. Ali Güler is the best mentor I have met. He was dedicated to my project with endless intelligence and enthusiasm, while supporting me to explore science boundlessly. I would like to thank all the previous and current Güler members for their selfless technical and mental support: Qijun Tang, Ryan Grippo, Sean Chadwick, Everett Altherr, Elizabeth Godschall, Akin Odeleye, Aundrea Rainwater, Ricardo Salinas, Anthony Spano, and the marvelous undergraduate research assistants: Nidhi M. Purohit, Julia B. Davenport, Charles Brennan, Rahul K. Patel, and Aarti Purohit. They maximized the fun of research and minimized the pain. I am grateful for the whole Biology department in UVA especially for the labs studying neuroscience, now known as the Program in Fundamental Neuroscience. Their genuine love for science facilitates interactions and collaborations which bring us the infinity of possibilities. Many thanks to my committee members: Ignacio Provencio, Christopher Deppmann, Eyleen O'Rourke, John Campbell, and Michael Scott. They have been always supportive with both scientific inputs and humor.

Additionally, I would like to thank everyone who devote themselves to fighting the Covid-19 pandemic. They are the ones making everything possible.

Thanks to the dopamine system for being so fascinating and mysterious. Thanks for previous researchers that have not demonstrated everything and left something for me.

Thanks for my family and friends supporting or not supporting me pursuing a Ph.D. degree. Doesn’t matter anymore. Thanks to myself for not giving it up.

“Any man could, if he were so inclined, be the sculptor of his own brain.” — Santiago Ramón y Cajal

“Don’t forget the women.” — Qi Zhang

Table of Contents

Chapter I: Introduction

Obesity is a global pandemic that severely reduces lifespan. According to the World Health Organization, the prevalence of obesity nearly tripled since 1975 (World Health Organization. Obesity and overweight). In 2016, more than 1.9 billion (39%) adults were overweight, of which over 650 million (13%) adults were obese. In 2019, an estimated 38.2 million children under the age of 5 years were overweight or obese.

Being overweight and obese are linked to more deaths worldwide than being underweight. Obesity leads to comorbid conditions including type 2 diabetes, cardiovascular disease, and tumors (Piché et al., 2020; Chaput et al., 2011; Olson et al., 2017). Moreover, eating disorders, such as bulimia nervosa, are associated with elevated mortality risks (Gearhardt et al., 2012). Strikingly, recent studies indicate that COVID-19 patients with obesity are more severely ill and have a higher mortality rate, suggesting a role of obesity in aggravating COVID-19 (Yang et al., 2021).

One of the primary causes of obesity is the excessive intake of energy-dense foods that are high in fat and sugars (Jebb, 2004). The underlying drive to eat is a deficit in energy stores. Feeding initiated by energy deficiency and suppressed by satiety is referred to as “homeostatic feeding”. Nevertheless, there are times when palatability-associated sensory inputs provoke feeding regardless of energy surplus, such as opting for dessert following an energy-replete meal (Weingarten, 1983). Such intake, motivated by the rewarding palatability of energy-dense food is referred to as “non-homeostatic feeding” or “hedonic feeding”.

Energy homeostasis is maintained by integrating peripheral circulating signals reflecting energy homeostasis. Ghrelin, for example, is released from the stomach during

hunger and promotes feeding (Davis, 2018). Conversely, pancreas-derived insulin (Mitchell and Begg, 2021), adipose tissue-derived leptin (Blundell et al., 2001), and gut- and hindbrain-derived glucagon-like peptide-1 (Kreisler and Rinaman, 2016; Punjabi et al., 2011) are hormones that convey satiety in response to energy surplus to reduce food intake. The hypothalamus and hindbrain are two critical centers in the central nervous system responsible for integrating peripheral hormone signals. Both the hypothalamus and hindbrain are proximal to ventricular regions with a specialized permeable brain-blood barrier (Joly et al., 2007). This anatomical feature facilitates a high sensitivity for circulating hormones. The arcuate nucleus (ARC) within the ventromedial region of the hypothalamus, acts as a principal regulator of homeostatic feeding by responding to the various hunger and satiety hormones (Joly-Amado et al., 2014). Meanwhile, the hypothalamus also senses changes in levels of plasma fatty acids, which subsequently affects hepatic gluconeogenesis and glucose homeostasis (Kokorovic et al., 2009). In addition to blood-borne information, the caudal brainstem receives direct input from the vagus nerve that transmits information from the gastrointestinal tract about the nutritive, osmotic, and volumetric properties of food (Travagli and Anselmi, 2016). These ingestive inputs within the hindbrain contribute to the precise regulation of food intake.

Multiple central systems have been demonstrated to participate in the regulation of hedonic feeding including the dopamine (DA) system (Palmiter, 2007), the cannabinoid system (Harrold and Williams, 2003), and the opioid system (Nogueiras et al., 2012). The DA system is well established for encoding the incentive and motivational aspects driving feeding (Palmiter, 2007); (Narayanan et al., 2010); (Coccurello and Maccarrone, 2018). DA projections from the ventral tegmental area (VTA) to downstream brain targets

including the prefrontal cortex (PFC), central amygdala (CEA), hippocampus, and nucleus accumbens (NAc) form the mesocorticolimbic system. Upon activation, the VTA DAergic neurons release DA in proportion to the reward value of food which encodes the appropriate level of motivation for consumption (Volkow et al., 2011). Additionally, the cannabinoid system is involved in hedonic aspects of eating by amplifying reward indices (Harrold and Williams, 2003). Cannabinoid receptors are expressed particularly in reward-related brain areas such as the NAc (Winters et al., 2012). A cannabinoid receptor antagonist selectively inhibits consumption of palatable food and drink (Freedland et al., 2000). Similarly, the opioid receptors are distributed in brain areas involved in hedonic feeding (Mansour et al., 1988), and an opioid receptor antagonist reduces food intake in diet-induced obese animals (Holtzman, 1979; Statnick et al., 2003).

Importantly, hedonic feeding has an evolutionary basis. Energy-dense foods facilitate survival by buffering against food shortage and starvation. Nevertheless, as food acquisition is easy to achieve in modern society, overconsumption of palatable foods imposes a huge burden on human health. Mammals have evolved exquisite neural mechanisms to consume an appropriate level of calories, yet the basis by which energy-dense foods short-circuit these mechanisms remains unclear. Identifying the neural mechanisms by which palatable foods alter feeding behavior is a necessary step toward developing effective therapies against obesity.

The arcuate nucleus in homeostatic feeding

The ARC integrates peripheral signals to regulate energy homeostasis (Joly-Amado et al., 2014) via a fenestrated endothelium in the median eminence which allows

for the entry of nutrients, hormones, and other molecules from the blood (Rodríguez et al., 2010), and thus is characterized as the first sensor of peripheral signals. Neurons that synthesize both the agouti related peptide (AgRP) and neuropeptide Y (NPY) are the predominant orexigenic population in the ARC (Hahn et al., 1998). During states of energy deficit, these $ARC^{AgRP/NPY}$ neurons are activated by orexigenic signals such as ghrelin (Hahn et al., 1998; Liu et al., 2012; Takahashi and Cone, 2005; Andrews et al., 2008; Chen et al., 2004). The increased activity of $ARC^{AgRP/NPY}$ neurons promotes feeding and suppresses energy expenditure (Krashes et al., 2011; Small et al., 2001; Ruan et al., 2014; Aponte et al., 2011) via downstream targets including the bed nucleus of the stria terminalis (BNST), the paraventricular nucleus of hypothalamus (PVH), the lateral hypothalamus (LHA), and the paraventricular nucleus of thalamus (PVT) (Betley et al., 2013). Conversely, ablation of $ARC^{AgRP/NPY}$ neurons in adults leads to starvation (Luquet et al., 2005).

Given the broad projections from the $ARC^{AgRP/NPY}$ neurons, one can postulate that $ARC^{AgRP/NPY}$ neurons are involved in complex behavioral regulation underlying their potent orexigenic function. Stimulation of $ARC^{AgRP/NPY}$ neurons in the absence of food forces mice to forage (Dietrich et al., 2015). The foraging and repetitive behaviors triggered by $ARC^{AgRP/NPY}$ neurons are coupled with decreased anxiety (Li et al., 2019). In addition, the elevated activity of $ARC^{AgRP/NPY}$ neurons abrogates inflammatory pain, indicating an antinociceptive effect of hunger that prioritizes survival needs (Alhadeff et al., 2018). Besides the role in control of feeding, activation of $ARC^{AgRP/NPY}$ neurons leads to a rapid switch in substrate use from fat to carbohydrates and increases systemic glucose use independent of food intake (Cavalcanti-de-Albuquerque et al., 2019).

Interestingly, $ARC^{AgRP/NPY}$ neurons not only respond to food, but also display hyperactivity on exposure to dietary doses of ethanol (Cains et al., 2017). Moreover, the activity of $ARC^{AgRP/NPY}$ neurons is essential for ethanol-induced overeating in mice in the absence of societal factors (Cains et al., 2017).

The activity of $ARC^{AgRP/NPY}$ neurons are dynamically regulated during feeding behaviors. As hunger excites $ARC^{AgRP/NPY}$ neurons, eating drives $ARC^{AgRP/NPY}$ neuronal activity toward baseline activity (Betley et al., 2015; Chen et al., 2015; Beutler et al., 2017). The reduction of $ARC^{AgRP/NPY}$ neuronal activity by feeding can be considered on three distinct timescales: 1) transiently, following detection of food cues, 2) slowly and longer-lasting, in response to food ingestion, and 3) permanently, with restoration of energy balance (Berrios et al., 2021).

Recent studies have implicated $ARC^{AgRP/NPY}$ neurons in learning. Similar to the unpleasant feeling of hunger in humans, it was demonstrated that the increased activity of $ARC^{AgRP/NPY}$ neurons is aversive and transmits a negative valence signal (Betley et al., 2015). The reduction of $ARC^{AgRP/NPY}$ neuronal activity by food abates the negative signal and therefore could affect motivation-associated behaviors. It was recently reported that a lateral hypothalamic glutamatergic → dorsomedial hypothalamic GABAergic → $ARC^{AgRP/NPY}$ neuron circuit mediates $ARC^{AgRP/NPY}$ neuron-guided motivation (Berrios et al., 2021). This food-specific circuit facilitates the learning of sensory cue-initiated food-acquisition tasks by decreasing the aversive $ARC^{AgRP/NPY}$ neuron activity, while interfering with this circuit impairs food cue inhibition of $ARC^{AgRP/NPY}$ neurons, obstructing the learning process.

Like ARC$^{AgRP/NPY}$ neurons, there are other orexigenic populations in the ARC that promote food intake including neurons expressing somatostatin (SST), tyrosine hydroxylase (TH), or prepronociceptin (PNOC). SST, TH, and PNOC neurons are activated by energy deficit signals, and when stimulated, drive robust food consumption (Zhang and van den Pol, 2016; Luo et al., 2018; Jais et al., 2020).

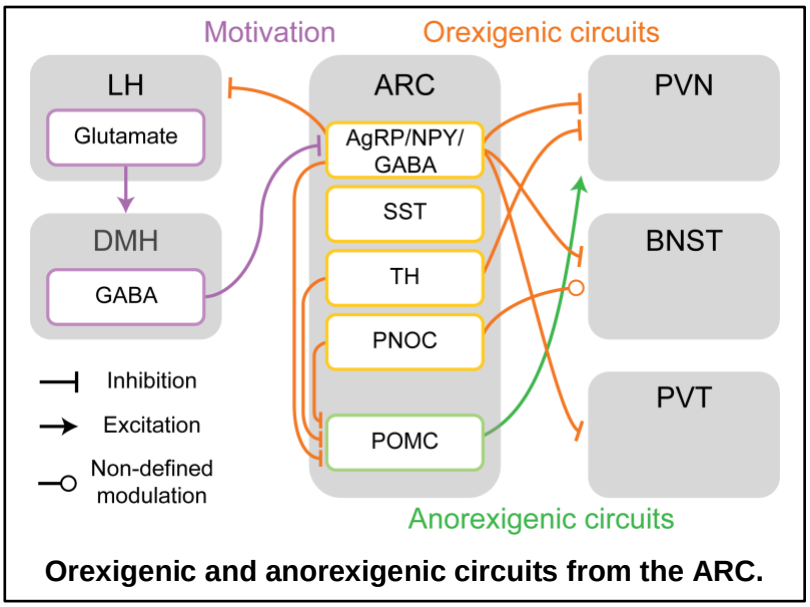

Orexigenic and anorexigenic circuits from the ARC.

Conversely, proopiomelanocortin (POMC) neurons are anorexigenic, suppressing food intake. POMC neurons are activated by satiety signals including leptin and insulin (Dodd et al., 2018; Cowley et al., 2001), and when stimulated, reduce the amount of calories ingested (Zhan et al., 2013). Recently, an unexpected feature of POMC neurons was revealed by fiber photometry; they are activated rapidly after the presentation of regular chow or palatable food, even before the food is actually consumed (Chen et al., 2015). This finding raises the possibility that POMC neurons contribute to anticipatory behaviors by responding to food-related sensory cues. Interestingly, cannabinoids stimulate a group of POMC neurons and subsequently increase food intake (Koch et al., 2015). In addition, it has been revealed that selective activation of POMC neurons that indirectly innervate the liver increases glucose concentrations (Kwon et al., 2020). The

role of POMC neurons in metabolic homeostasis appears to be complex and deserves further studies.

Previously undefined neuronal populations in the ARC also participate in feeding regulation. Hypothalamic non-AgRP, non-POMC GABAergic neurons are required for postweaning feeding (Kim et al., 2015), and chronic activation of the non-AgRP GABAergic ARC neurons leads to obesity (Zhu et al., 2020). Additionally, a group of fast acting anorexigenic, glutamate-releasing ARC neurons complement the slow POMC satiety response (Fenselau et al., 2017).

The dopamine system: motivation and addictive feeding

Transient increases of DA generally enhance salient environmental signals while suppressing irrelevant signals, helping an animal to attend to the environment and respond appropriately (Palmiter, 2007). Specifically, DA is a key neurotransmitter in reinforcement. It is believed that DA signaling encodes valence signals to generate appropriate behaviors such as eating (Namburi et al., 2016).

The DA system signals through D1-like receptors (D1 and D5 subtypes) and D2-like receptors (D2, D3 and D4 subtypes). D2-like receptors have a 10- to 100-fold greater affinity for DA than the D1-like receptors (Marcellino et al., 2012), suggesting that DA levels affect the balance of D2-like *vs.* D1-like receptor signaling. DA neurons fire either in a stable tonic mode (1–8 Hz) or in a transient high-frequency phasic mode (<500 msec; >15 Hz) (Atcherley et al., 2015). As a simplified conventional model, tonic firing causes DA release from extrasynaptic release sites, where it acts on high-affinity Drd2 (Richfield et al., 1989) and determines motivational arousal (Bromberg-Martin et al., 2010).

On the other hand, phasic DA firing results in high synaptic DA concentrations (Garris et al., 1994), which are able to stimulate the low-affinity Drd1 and are associated with the conditioning to positive and negative reinforcers (Schultz, 1998). Additionally, phasic DA firing concomitantly signals through Drd2 (Richfield et al., 1989).

The DA system plays an essential role in encoding feeding behaviors, especially considering the motivational aspects of DA signaling. Central ablation of DA synthesis impairs the ability of mice to eat and leads to death (Szczypka et al., 1999), while stimulation of the DA neurons rescues the $ARC^{AgRP/NPY}$ neuron ablation-induced starvation (Denis et al., 2015). The mesolimbic DA system is well-established in reinforcing the value of rewarding food and facilitating motivated behaviors (Salamone and Correa, 2012; Wise, 2004; Coccurello and Maccarrone, 2018; Salamone et al., 2003; Fields et al., 2007; Berridge, 2007). Midbrain DAergic neurons project to multiple limbic brain regions. These DA circuits are critical for reinforcement and reward prediction (Keiflin and Janak, 2015). DAergic neurons that originate in the VTA and project to the NAc are associated with hedonic feeding. Upon activation, these neurons release DA in proportion to the reward value of food which encodes the appropriate level of motivation for its consumption (Cameron et al., 2014; Hernandez and Hoebel, 1988). VTA DA neurons also send projections to the CEA and PFC, which participate in the encoding and gating the salient cues (Ellwood et al., 2017; Lutas et al., 2019). In addition, DA neurons in the substantia nigra (SN) that project to the dorsal striatum traditionally have been associated with action selection and goal-directed behaviors (Howard et al., 2017; Wise, 2009). Notably, stimulation of the midbrain DA neurons failed to affect the amount of food

consumed (Boekhoudt et al., 2017), but resulted in smaller and shorter meals, indicating a role for mesolimbic DA in meal continuation and cessation.

Beyond the mesolimbic system, DA neurons in hypothalamic areas participate in energy homeostasis. The genetically defined A12 group of DA neurons in the ARC is involved primarily in prolactin secretion (Gudelsky, 1981; Stagkourakis et al., 2019), and recently was reported to promote feeding by inhibiting POMC neurons without affecting the activity of the $ARC^{AgRP/NPY}$ neurons (Zhang and van den Pol, 2016). Of note, peripheral DA might also be involved in feeding. Peripheral DA blockade by pimozide, a D2-like receptor antagonist, disrupts feeding and attenuates the value of food rewards (Wise and Colle, 1984; Wise et al., 1978).

The functional relevance of other central DA neurons in feeding remains obscure. For example, both A13 DA neurons in the zona incerta (ZI) and A14 DA neurons in the PVN are situated in brain nuclei known to control food intake and these neurons project to the ventral hypothalamus (Moriya and Kuwaki, 2021; Romanov et al., 2017); yet their respective functions are poorly understood.

Among the 5 subtypes of DA receptors, Drd1 is the most abundant in sites receiving DAergic projections. Drd1 plays a significant role in reward processing (Beninger and Miller, 1998; Luca et al., 2007; Batel et al., 2008; Huang et al., 2008; Jenni et al., 2017). Drd1-expressing neurons in multiple brain regions regulate consumption of regular or palatable food including the medial prefrontal cortex (Land et al., 2014), nucleus accumbens (Durst et al., 2019), and paraventricular hypothalamic nucleus (Mirmohammadsadeghi et al., 2018). Moreover, Drd1-null mice are resistant to diet-induced obesity and metabolic syndromes (Grippo et al., 2020). Notably, recent studies

have demonstrated Drd1 expression in the ARC (Romero-Fernandez et al., 2014) and increased activity of $ARC^{AgRP/NPY}$ neurons in response to DA and Drd1 agonists (Zhang and van den Pol 2016; Alhadeff et al. 2019). Together, these studies suggest a novel role for Drd1 signaling in ARC-dependent energy homeostasis.

The interaction between homeostatic and hedonic systems

Although the homeostatic and hedonic systems mediate feeding behaviors via disparate mechanisms, these two systems are not isolated from each other but rather tightly interacted. As a pivotal center of hedonic feeding, DA neurons are directly modulated by homeostatic hormones transmitting peripheral energy states including insulin, leptin, and ghrelin. Leptin modulates VTA neurons, and its administration reduces feeding and DA release within the NAc (Leinninger et al., 2009). Additionally, long-term RNAi-mediated knock-down of leptin receptors in the VTA increases food intake and sensitivity to highly palatable food (Hommel et al., 2006). Insulin also alters the activity of midbrain DA neurons (Könner et al., 2011). Administration of insulin to the VTA reduces food intake and suppresses consumption of palatable diets (Bruijnzeel et al., 2011). On the contrary, ghrelin excites the VTA DA neurons and promotes appetite (Abizaid et al., 2006).

At the crossroads of the mesolimbic reward circuit and the ARC homeostatic system, the lateral hypothalamus (LH) contributes to homeostatic feeding and the incentive salience of food (Coccurello and Maccarrone, 2018). The LH receives inputs for $ARC^{AgRP/NPY}$ neurons to increase food consumption and modify preferences for both appetitive and aversive tastes (Betley et al., 2013; Fu et al., 2019). VTA-projecting GABAergic neurons in the LH robustly promote feeding (Betley et al., 2013; Marino et al.,

2020). Neurons expressing orexins (OX) in the LH integrate homeostatic signals such as leptin and ghrelin (Liu et al., 2017; Yamanaka et al., 2003) with reward processing (Borgland et al., 2009; Harris et al., 2005; Sharf et al., 2010). In addition, OX neurons or melanin-concentrating hormone (MCH)-expressing neurons in the LH communicate with the VTA or NAc, respectively, to modulate reward-associated feeding behaviors (Cason et al., 2010; Georgescu et al., 2005).

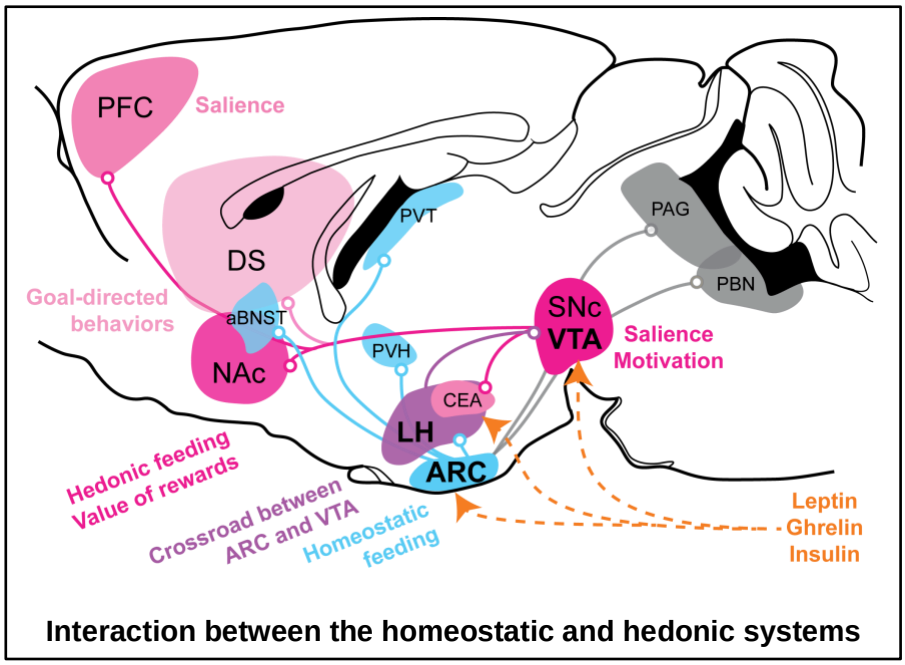

Interaction between the homeostatic and hedonic systems

The ARC is a potential integrator of homeostatic and hedonic inputs. Studies have posited a role of ARC$^{AgRP/NPY}$ neurons in modulating DA signaling in the VTA. Impairment of AgRP circuitry by Sirt1 knockdown in ARC$^{AgRP/NPY}$ neurons or early postnatal ablation of ARC$^{AgRP/NPY}$ neurons excites the VTA DA neurons by enhancing spike timing–dependent long-term potentiation and correspondingly increases exploratory behaviors (Dietrich et al., 2012). It is further demonstrated that GABA is the main effector of the ARC$^{AgRP/NPY}$ neurons in modulating VTA DA functions (Dietrich et al., 2012). The disinhibition of the VTA DA neurons by reduced activity of ARC$^{AgRP/NPY}$ neurons may contribute to maintaining the value of palatable food during energy surplus. In addition to these GABAergic inputs to the midbrain, metabolic sensing in ARC$^{AgRP/NPY}$ neurons is also

required for proper DA function. Impaired metabolic sensing in AgRP neurons caused by deletion of carnitine acetyltransferase (Crat) reduces acute DA release to palatable food consumption in the NAc while suppressing motivated operant responses to sucrose rewards during fasting (Reichenbach et al., 2022).

Conversely, DA signaling also mediates the activity of $ARC^{AgRP/NPY}$ neurons. The ARC receives projections from an array of DA neurons in hypothalamic and subthalamic areas (Moriya and Kuwaki, 2021; Romanov et al., 2017; Zhang and van den Pol, 2016). DA receptors including Drd1 are expressed in the ARC (Alhadeff et al., 2019; Romero-Fernandez et al., 2014; Zhang and van den Pol, 2016). Moreover, $ARC^{AgRP/NPY}$ neurons exhibited increased activity in response to DA and Drd1 agonists (Alhadeff et al., 2019; Zhang and van den Pol, 2016). These findings suggest that Drd1-dependent DA signaling contributes to ARC-dependent energy homeostasis. Further investigation into the interaction between $ARC^{AgRP/NPY}$ neurons and the DA system will be necessary to understand the underlying mechanisms of homeostatic and hedonic feeding.

The impact of high-fat and high-sugar diets on feeding

Energy-dense food is encoded to be preferred for survival purposes. In humans, the prevalence of obesity is positively correlated with dietary fat and sugar consumption (Hill et al., 2000; Ravussin and Tataranni, 1997; Stanhope, 2016). In animal models, access to high-fat and/or high-sugar food provokes overconsumption or compulsive-like eating behavior, which leads to body weight increase (la Fleur et al., 2007; Hariri and Thibault, 2010; Musselman et al., 2011). Moreover, short food deprivation periods caused a binge-like eating behavior in animals fed on energy-dense diets (Oswald et al., 2011). The

hyperphagia effects of diets enriched in fat and sugar could be attributed to their energy density and palatability. Due to the difficulty in controlling the variable micronutrients in diets, probing the mechanism by which fat and sugar content individually mediate feeding microstructure is challenging. Preliminary studies suggest that the fat content of a diet has weaker satiating feedback signals than protein or carbohydrate, and thus leads to passive overconsumption. High-fat diet (HFD) promoted larger bout size and greater total kilocalorie intake than high-carbohydrate diet in rats, suggesting that HFD is associated with weaker satiation (suppression of meal size) and satiety (suppression of total daily intake) (Warwick et al., 2003). On the other hand, it has been demonstrated that high-sugar diets but not HFDs increase eating rates, which implies an elevated palatability of high-sugar diets (Lee et al., 2020). In studies of obesity, diets called “high-fat” are usually also high in sugar. Therefore, we refer to the high-fat and high-sugar diets as HFDs for the following discussion.

A notable impact of HFDs is the subsequent devaluation of standard diets (SDs). The urge to consume HFD is accompanied by a reduced desire to eat SD that is potentially perceived as less palatable. For example, when receiving limited access to HFD with SD provided for the rest of the day, mice showed significantly increased HFD intake and reduced SD intake (Mazzone et al., 2020), suggesting that they ‘wait’ for their preferred food instead of compensating the caloric intake.

Another effect of HFD on feeding patterns is the altered feeding rhythms. Feeding and fasting drive daily rhythms, while the coupling between circadian oscillators and the feeding-associated metabolic regulators is necessary for maintaining energy balance (Turek et al., 2005). Disruption of diurnal rhythms is commonly found in animal models of

diabetes and obesity. HFD perturbs circadian feeding and activity rhythms (Grippo et al., 2020). Moreover, mice fed a HFD ad libitum exhibit dampened oscillations of circadian clock components (Kohsaka et al., 2007). Conversely, time-restricted access to HFD improves body weight regulation and metabolism (Hatori et al., 2012; Chaix et al., 2019a; Sutton et al., 2018).

Paralleling with the impact on feeding behaviors, HFD consumption persistently alters neural feeding circuits. For example, access to HFD enhances the activity of $ARC^{AgRP/NPY}$ neurons (Ewbank et al. 2020), which may promote sustained overconsumption. Longitudinal recordings revealed that the SD devaluation following HFD consumption is encoded at the level of $ARC^{AgRP/NPY}$ neurons and mesolimbic DA signaling. Prior HFD consumption vastly diminished the capacity of SD to alleviate $ARC^{AgRP/NPY}$ neuron-induced negative valence (Mazzone et al., 2020). The altered response of $ARC^{AgRP/NPY}$ neurons toward energy content in food potentially contributes to animals' potent preference toward HFD. On the other hand, the DA system is also affected by HFD consumption. High fat diet diminishes mesolimbic dopamine responses to SD while disrupting the functional capacity of VTA DA neurons to potentiate SD consumption (Mazzone et al., 2020)..

In addition, HFD-induced obesity is associated with altered expression levels of DA receptors. Repeated exposure to HFDs downregulates Drd2 in the striatum in rats (Hamdi et al., 1992; Johnson and Kenny, 2010). Similarly, in patients with obesity or binge eating disorders, brain imaging studies have reported decreased Drd2 or Drd3 availability in the dorsal and ventral striatum (Wang et al., 2001; de Weijer et al., 2011). On the other hand, long-term exposure to palatable foods reduces the expression level of Drd1 in the NAc of

rats (Alsiö et al., 2010). The extent to which changes in Drd1 contribute to obesity in humans has been less investigated. Identifying the neural mechanisms by which palatable foods alter feeding behavior will be a necessary step toward rationalizing effective therapies against obesity.

Current anti-obesity therapeutic strategy targeting the DA system: limitations and implications

With the global syndemic of obesity and comorbid conditions, current therapeutic approaches for patients with obesity remain largely insufficient. The main strategy adopted by obese individuals for long-term weight maintenance is the interventions to their life-style including dietary modifications, high levels of physical activity, and self-monitoring of body weight. However, diets aimed to reduce body weight by restricting the amount of food consumed commonly cause anxiety and mood disorders (Gearhardt et al., 2012; Piccinni et al., 2021) and are ineffectual for long-term weight loss in a significant fraction of obese individuals (Montesi et al., 2016). Most obese people are unable to regulate their food intake constantly and exhibit the cycle of overconsumption, dieting and relapse, which is reminiscent of the cycle of drug addiction (Volkow et al., 2017). In these patients who relapse toward their elevated body weight after repeated dieting attempts, drug treatments become an essential approach.

The major medical target against obesity is the central nervous system to enhance satiety responses or to suppress appetites. For example, Liraglutide, a glucagon-like peptide 1 receptor (GLP-1R) agonist, is an approved drug for obesity treatment. It has been found effective for weight reduction in patients with and without type 2 diabetes through its effects on satiety and gastric emptying (Isaacs et al., 2016). As the key node

in encoding reinforcement, the DA system is one of the most important central groups targeted by anti-obesity drugs. The complexity of manipulating the DA system lies in the widespread DA receptors that regulate various functions. Although DA is essential for feeding, and Drd1 signaling in multiple brain regions increases palatable food intake (Durst et al., 2019; Land et al., 2014; Mirmohammadsadeghi et al., 2018; Szczypka et al., 1999), stimulation of Drd2 results in a reduction in food consumption (Azevedo et al., 2019; Cooper and Al-Naser, 2006; Kern et al., 2012). As with the high affinity of Drd2, elevated DA levels have a dominant anorexigenic effect (Davis et al., 2012). Therefore, the main mechanism of targeting the DA system in obesity treatment is to increase DA levels by inhibiting DA reuptake. It is demonstrated that inhibition of DA reuptake results in an anorectic effect (van der Hoek and Cooper, 1994), suggesting that enhanced DA levels are sufficient to reduce food intake. In addition, increased DA signaling results in greater locomotor activity (van der Hoek and Cooper, 1994), which may contribute to weight loss by increasing energy expenditure. The current drugs acting as DA reuptake inhibitors include Contrave (bupropion with naltrexone), Empatic (bupropion with zonisamide), and Tesofensine (Adan, 2013). However, they all have multiple side effects including cardiovascular side effects, nausea, headache, insomnia, anxiety, and depressed mood (Adan, 2013).

Novel anti-obesity drugs target catecholaminergic and noradrenalinergic systems simultaneously in addition to the DA system. For example, Sibutramine, one of the few centrally acting drugs currently approved for long-term treatment of obesity in adults, inhibits reuptake of norepinephrine, 5HT, and DA (Lean, 2001). It is effective in weight loss by reducing hunger and increasing satiety and thermogenesis (Hansen et al., 1998;

James et al., 2000; Rolls et al., 1998; Seagle et al., 1998). Nevertheless, Sibutramine also causes adverse effects including anorexia, insomnia, headache, and hypertension (Florentin et al., 2008). In 2002, Sibutramine was temporarily withdrawn from the market in Italy because of adverse cardiovascular events including two deaths (Bosello et al., 2002).

Targeting DA receptors is an alternative strategy to manipulating DA levels. Therapy with Bromocriptine, a Drd2 agonist, is associated with weight loss and improved glucose tolerance (Cincotta and Meier, 1996), although it may cause side effects including nausea, vomiting and depression (Holt et al., 2010). On the other hand, Ecopipam, a selective Drd1 antagonist, is effective in achieving and maintaining weight loss in obese patients (Astrup et al., 2007). However, again, the receptor's widespread expression causes adverse side effects including depression and anxiety making its use problematic (Astrup et al., 2007). A treatment strategy that more precisely controls the activity of DA or DA receptor expressing neurons in specific brain areas would lead to safer therapeutic strategies against obesity.

Chapter II: Drd1-dependent signaling is required for high fat diet induced obesity and associated metabolic syndromes

This work was in collaboration with Ryan Grippo and QIjun Tang and was published as a research article in Current Biology (Grippo et al., 2020). My contributions are described below.

Abstract

The widespread availability of energy-dense, rewarding foods is correlated with the increased incidence of obesity across the globe. Overeating during mealtimes and unscheduled snacking disrupts timed metabolic processes, which further contribute to weight gain. We demonstrated that Drd1 signaling is required for palatable diet induced obesity. Drd1-null mice are resistant to diet-induced obesity, metabolic syndromes, and circadian disruption associated with energy-dense diets.

Introduction

Obesity and its comorbid conditions, including type 2 diabetes, cardiovascular disease, and metabolic syndrome, are global pandemics that severely reduce lifespan (Eckel et al., 2011; Guh et al., 2009; Hurt et al., 2010; de Mutsert et al., 2014). Excessive consumption of palatable foods high in sugar and/or fat is one of the primary contributors to the development of obesity. Nevertheless, dietary interventions by restricting the amount of food intake remain ineffective for long-term weight maintaining (Montesi et al., 2016). Energy-rich, rewarding foods encourage snacking outside of regular mealtimes, lowering adherence to dietary interventions and therefore preventing sustained weight loss (Del Corral et al., 2011; Webb and Wadden, 2017). Determining the neural

mechanisms by which palatable foods alter feeding amount and meal timing is a necessary step toward developing effective therapies against obesity.

The DA system plays an essential role in encoding feeding behaviors, especially with the incentive and motivational aspects. Central ablation of DA synthesis impairs the ability of mice to eat and leads to death (Szczypka et al., 1999), while stimulation of the DA neurons rescues the $ARC^{AgRP/NPY}$ neuron ablation induced starvation (Denis et al., 2015). DA signals through a group of G-protein-coupled receptors expressed in anatomically distinct regions throughout the CNS and peripheral nervous system. Both D1-like (Gs-coupled) and D2-like (Gi-coupled) receptors have been implicated in non-homeostatic consumption of palatable foods and obesity. Drd1 plays a significant role in reward processing. Drd1-expressing neurons in multiple brain regions regulate consumption of regular or palatable food including the medial prefrontal cortex (Land et al., 2014), nucleus accumbens (Durst et al., 2019), and paraventricular hypothalamic nucleus (Mirmohammadsadeghi et al., 2018). Moreover, treatment with a Drd1 antagonist reduces food intake in rodents and causes weight loss in humans.

In this study, we demonstrate that Drd1 expression is necessary for overconsumption of a high-fat diet (HFD). Drd1-knockout mice were resistant to HFD-induced weight gain and the associated metabolic syndromes. Moreover, Drd1-null mice are resistant from HFD-restructured feeding time with attenuated dampening of peripheral clocks. These findings solidify the role of Drd1-dependent DA signaling in the regulation of pathological calorie consumption.

Result

Genetic ablation of Drd1 protects mice from high fat diet-induced weight gain

HFD and metabolic syndromes

Mice with *ad libitum* access to high fat diets (HFDs) rapidly develop obesity, diabetes, and metabolic diseases (Hariri and Thibault, 2010; Winzell and Ahrén, 2004). To investigate the role of Drd1 signaling in obesity development, in collaboration with Ryan Grippo and Qijun Tang, we monitored the response to high fat dietary challenge in mice with genetic ablation of Drd1 (KO), in which both *Drd1a* alleles were replaced by Cre recombinase (Cre) (Heusner et al., 2008). We measured weekly changes in body weight (BW) between adult male wild-type (WT) and KO mice during *ad libitum* access to either standard diet (SD) (19% fat and 0% sucrose) or HFD (45% fat and 17% sucrose; Figure 1A). When fed on SD, BW change was indistinguishable between WT and KO groups (WT: 5.0% ± 2.6% increase; KO: 5.9% ± 1.1% increase; Student's two-tailed *t*-test; $P = 0.8$). As expected, when switched to HFD, WT mice increased BW; however, KO mice were completely resistant to BW gain (WT: 29.5% ± 3.1% increase; KO: 5.4% ± 1.6% increase; Student's two-tailed *t*-test; $P < 0.001$; Figures 1B and 1C).

Obesity from HFD consumption also results in increased fat mass, glucose intolerance, and insulin resistance. As expected, after 6-week access to the HFD, WT mice accumulated significant adiposity in gonadal white adipose tissue (GWAT) and posterior subcutaneous adipose tissue (SCAT), while KO mice maintained similar fat composition to SD controls in these tissues (Figure 1D). Most strikingly, KO mice were protected from HFD-induced glucose intolerance and insulin resistance, two hallmarks of obesity-associated metabolic syndromes (Figures 1E and 1F). Taken together, these data

demonstrate that, unlike WT mice, KO mice represented complete resistance to HFD-induced obesity while persisting robust responsiveness to glucose and insulin fluctuations.

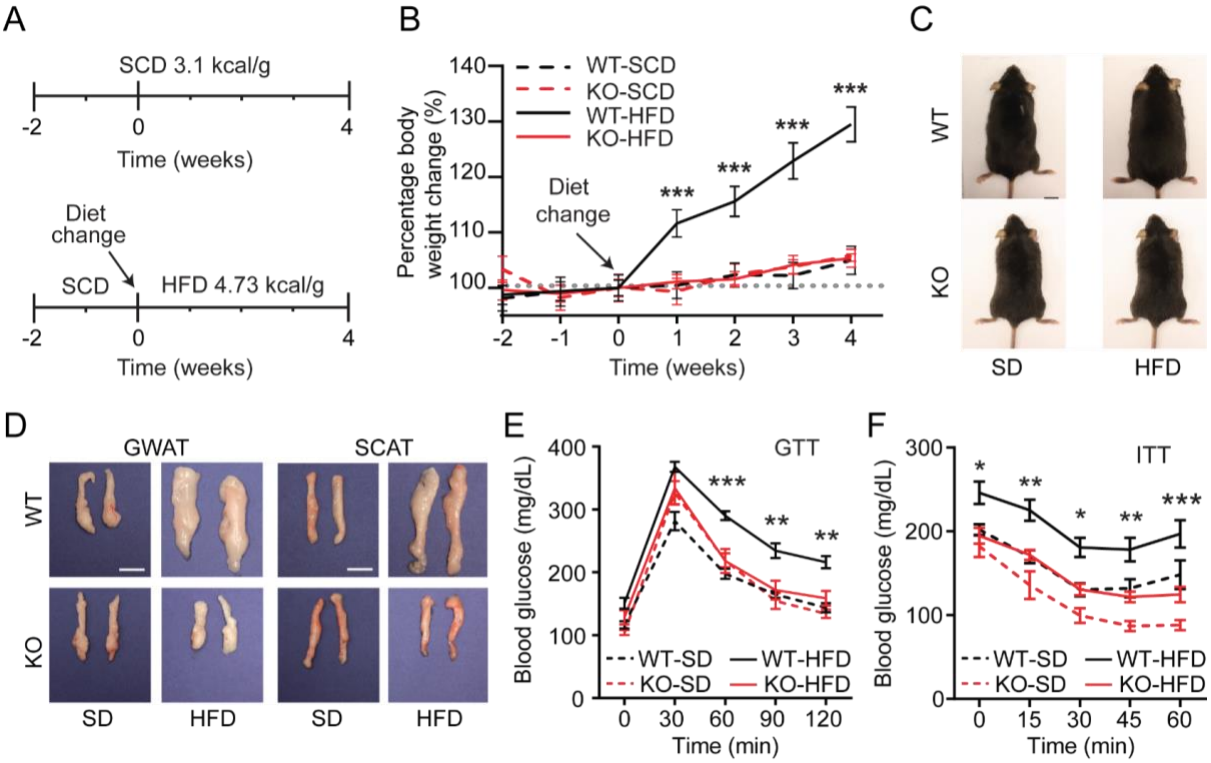

Figure 1 Drd1-null mice are resistant from high fat diet-induced weight gain and metabolic syndromes

(A) Food access paradigm. Diet switch from SD to HFD (week 0) is shown.

(B) Percent BW change relative to week 0 for WT and KO mice on SD or HFD. Repeated-measures three-way ANOVA with Bonferroni post hoc comparison; n = 7 - 13/group; $F_{genotype}(1, 37) = 4.8$, $P = 0.03$; $F_{diet}(1, 37) = 5.9$, $P = 0.02$. Arrow marks diet switch from SD to HFD. (Ryan Grippo, Qijun Tang, Qi Zhang)

(C) Representative images of WT or KO mice from A and B. Scale bar represents 1 cm. (Ryan Grippo, Qijun Tang, Qi Zhang)

(D) Representative dissected GWAT (left) and SCAT (right) images of WT or KO mice from a and b. Scale bar = 1 cm. (Qi Zhang, Qijun Tang, Ryan Grippo)

(E) Blood glucose levels during glucose tolerance test (GTT) (repeated-measures three-way ANOVA with Bonferroni post hoc comparison; n = 8 - 12/group; $F_{genotype}(1, 35) = 5.5$, $P = 0.03$; Fdiet(1, 35) = 21.9, $P < 0.001$). (Qi Zhang)

(F) Blood glucose levels during insulin tolerance test (ITT). Repeated-measures three-way ANOVA with Bonferroni post hoc comparison; n = 9 - 12/group; $F_{genotype}(1, 36) = 26.4$, $P < 0.001$; $F_{diet}(1, 36) = 18.4$, $P < 0.001$. (Qi Zhang)
Data are represented as mean ± SEM. ∗p < 0.05; ∗∗p < 0.01; ∗∗∗p < 0.001; ns, not significant.
Figure 1 was adapted from (Grippo et al., 2020).

Knock-out of Drd1 ablates HFD-restructured feeding time while attenuating dampened peripheral clock

HFDs not only increase food consumption but also alter feeding patterns, resulting in food intake that extends into the rest phase (Arble et al., 2010; Espinosa-Carrasco et al., 2018). This disruption in feeding rhythms induces weight gain independent of overconsumption, highlighting the importance of maintaining robust feeding rhythms for proper metabolic regulation (Hatori et al., 2012). Although caloric intake of either diet was equivalent between WT and KO mice during the active (night) phase, my colleague Ryan Grippo observed that WT mice exhibited a significantly increased HFD consumption in the rest (day) phase, which was nearly absent in KO mice (Figures 2A and 2B). These findings indicate a specific role of Drd1 signaling in promoting palatable food induced hyperphagia during the resting phase.

Prolonged access to HFD also dampens circadian clock gene rhythms in peripheral tissues (i.e., WAT and liver) (Kohsaka et al., 2007). Because KO animals exhibited resistance to HFD-restructed feeding rhythms, we evaluated circadian clock gene (*Rev-erbα*, *Per2*, and *Bmal1*) expression in GWAT and liver of WT and KO mice at 6 time points with 4-hr intervals across the 24-h day. Similar to previous reports (Hatori et al., 2012; Kohsaka et al., 2007), WT mice exhibited a dampening of clock gene amplitudes in GWAT

on HFD compared to SD controls (Figures 2C and 2D). The reduced oscillatory amplitudes of clock genes were relatively mild in the liver. Notebly, we observed a general difference of oscillatory amplitudes between WT and KO mice. For example, the amplitude of Rev-erbα expression was significantly higher in the GWAT and liver in KO-SD mice compared with WT-SD mice. This suggests that Drd1 signaling participates in the regulation of clock gene expression regardless of diet contents. KO mice were protected from HFD-induced dampening of clock genes at specific time points (e.g Bmal 1 in GWAT at ZT 1), suggesting that HFDs affect peripheral clocks partially through the Drd1 signaling.

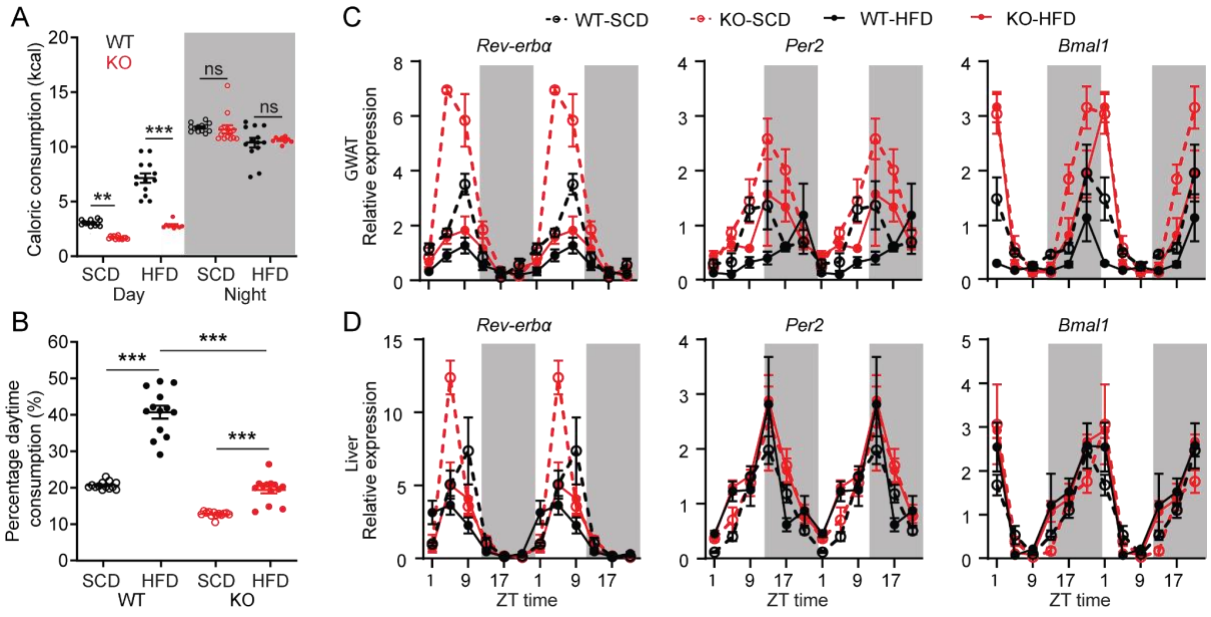

Figure 2 Drd1-null mice are resistant from diet-restructured feeding time but not peripheral clock

(A) Calorie intake during the 12-h light (day) or dark phases (night) for WT and KO mice on SD or HFD. Repeated-measures three-way ANOVA with Bonferroni post hoc comparison; n = 13/group; Ftime(1,96) = 1,544, $p < 0.001$; $F_{genotype}(1, 96) = 57.1$, $p < 0.001$; $F_{diet}(1, 96) = 12.6$, $p < 0.001$. (Ryan Grippo, Qijun Tang, Qi Zhang)

(B) Percent of total daily food intake during the day for WT and KO mice on SD or HFD. Two-way ANOVA with Bonferroni post hoc comparison; n = 13/group; $F_{genotype}(1, 48) = 203.2$, $p < 0.001$; $F_{diet}(1, 48) = 170.2$, $p < 0.001$. (Ryan Grippo, Qijun Tang, Qi Zhang)
(C, D) Double-plotted RNA expression level of circadian genes *Rev-erbα*, *Per2*, and *Bmal1* in GWAT (C) and liver (D). Three-way ANOVA with Bonferroni post hoc comparison; n = 3 at each time point in each group. Time is represented in ZT.
Data are represented as mean ± SEM. ∗p < 0.05; ∗∗p < 0.01; ∗∗∗p < 0.001; ns, not significant. (Qi Zhang)
Figure 2 was adapted from (Grippo et al., 2020).

Discussion

Excessive intake of palatable food in spite of energy surplus leads to obesity, however, the neuronal mechanism underlying HFD-induced overeating and weight gain is not clear. The DA system plays an essential role in encoding feeding behaviors, especially with the incentive and motivational aspects. Among the 5 subtypes of DA receptors, Drd1 is the most abundant in all dopaminergic neuron-projecting areas. With the significant role of Drd1 in reward processing, how Drd1 signaling contributes to diet-induced obesity is not fully understood. In our study, we demonstrated that the lack of Drd1 signaling imposes self-restricted, energy-rich food consumption predominantly during the active phase, and provide timely insight to how rewarding, energy-dense foods interfere with meal timing and diet adherence.

Consumption of food beyond regular activity periods generates peripheral circadian desynchrony (Hatori et al., 2012; Kohsaka et al., 2007). Even during conditions of isocaloric energy intake, high-fat food consumption out of phase with rhythmic metabolic processes leads to obesity through altered energy utilization and increased energy storage in mice. After 4-week access to HFD, we observed dampened peripheral clocks

in WT mice mainly occurring in the GWAT. This implies that the oscillation of clock genes in adipose tissue is primarily affected by HFD ingestion in the early stage of obesity development.

Conversely, time-restricted feeding paradigm reverse diet-induced weight gain and rescues peripheral rhythms of clock genes. Although the KO-HFD mice exhibited resistance for resting phase hyperphagia, their lean phenotype is not associated with a resilient amplitude of clock gene expression in the periphery. It is known that DA plays a dominant role in mediating circadian through Drd1. In mice, DA acting at Drd1 phase shifts the clock, while Drd1 antagonists block the phasing effect of light (Besharse and McMahon, 2016). In fact, we observed generally elevated amplitudes of clock genes in KO mice compared with WT mice. The baseline changes of peripheral clock genes induced by global knock-out of Drd1 makes it challenging to evaluate the impact of HFD. When gauged to KO-SD and WT-SD control groups respectively, the HFD-induced changes in peripheral clock amplitudes at most time points are indistinguishable between KO and WT animals, suggesting an overwhelming impact of dietary composition against the Drd1-ablation-induced time-restricted feeding. Alternatively, Drd1 signaling participates in pacing the peripheral clock following feeding time, thus global ablation of Drd1 might shield the effect of dietary contents. Interestingly, KO mice were protected from HFD-associated dampening of clock genes at a couple of time points. For example, KO mice show resistance of phase-shift of Per2 and dampening of Bmal1 in GWAT. These results indicate that the full extent of HFD-induced alterations in peripheral clocks requires Drd1 signaling.

Diet regimens that involve time-restricted feeding are growing in popularity because they attenuate BW gain and significantly improve metabolic profiles in rodents and humans (Chaix et al., 2019b; Gabel et al., 2018; Hatori et al., 2012; Sutton et al., 2018). Our findings implicate a significant role of targeting Drd1 signaling in enhancing the adherence of time-restricted dieting. Dissecting the role of Drd1 signaling in specific central or peripheral regions will be the focus of future investigations.

Materials and methods

Animals

All animal care experiments were conducted in concordance with the University of Virginia Institutional Animal Care and Committee. Mice were housed in a temperature and humidity controlled vivarium at 22-24°C and ~40% humidity with a 12h/12h light/dark cycle. Male adult animals older than 8 weeks were used in all behavioral experiments with the following genotypes: C57BL(The Jackson Laboratory Cat# JAX#000664; RRID: IMSR_JAX:000664), Drd1-Cre (Palmiter Lab, University of Washington).

Mouse Diets

Standard diet (SD):Teklad 8664 (Envigo, United Kingdom: 3.1 kcal/gram; 19% fat, 31% protein, 50% carbohydrates), Teklad 7912 (Envigo, United Kingdom: 3.1 kcal/gram; 17% fat, 25% protein, 58% carbohydrates) or PicoLab Rodent Diet 20 5053 (3.07 kcal/gram; 13% fat, 24% protein, 62% carbohydrates; 3.2% sucrose). High-fat, high-sugar diet (HFD): Open Source D12451 (4.73 kcal/gram; 45% fat, 20% protein, 35% carbohydrates; 17% sucrose).

Food Intake Measurements

Adult mice were housed individually in standard home cages with *ad libitum* access to SD food and water throughout all experiments. For longitudinal feeding experiments, 12-14 week old mice were then randomly assigned into two different feeding regimens, SD or HFD. All mice were maintained on SD for an additional two weeks to measure baseline food intake and weight change. SD animals remained on SD for an additional four weeks at the time of the "diet switch" while the HFD group was given *ad libitum* access to HFD. Pre-weighed food pellets were placed on the cage floor and refreshed weekly.

Glucose tolerance

Five weeks after the time of diet change, mice were fasted for 16 h (ZT 10 - ZT 2), and fasted glucose was recorded using a Glucometer (One Touch Ultra) by tail bleeds (Hatori et al., 2012). Subsequently, mice received an i.p injection of glucose (1g/kg BW in saline), and blood glucose was measured in intervals of 30 min for 2 h.

Insulin tolerance

Five weeks after the time of diet change, mice were fasted for 4 h (ZT 1 - ZT 5), and fasted glucose was recorded using a Glucometer (One Touch Ultra) by tail bleeds. Subsequently, mice received an i.p injection of insulin (0.75units/kg of BW in saline), and blood glucose was measured in intervals of 15 min for 1 h (Vinué and González-Navarro, 2015). The time of collection (ZT 2 for GTT and ZT 5 for ITT) was chosen during peak response to the glucose challenge which falls between ZT 2 and ZT 8 (la Fleur et al., 2001).

Body composition

Six weeks after the time of diet change SCAT, GWAT, and liver were harvested, weighed, placed into a chilled 4% PFA solution or Bouin's solution (fisher scientific) for fixation. Whole tissue was imaged (Canon EOS Rebel Xsi) before fixation. A ruler was used to scale each tissue.

QPCR

Six weeks after the time of diet change, WT-SD, KO-SD, WT-HFD, and KO-HFD mice were sacrificed by cervical dislocation every 4 h along the LD cycle (3 mice/time point: ZT 1,5,9,13,17,21). Tissues collected from mice during the Night phase were sacrificed in the dark under IR light with night-vision goggles. Dissected liver and GWAT tissue was flash frozen in liquid nitrogen. RNA was extracted with the RNeasy Lipid Tissue Mini Kit (QIAGEN). For liver and GWAT, 1100 ng of RNA was reverse-transcribed using a SuperScript IV First-Strand Synthesis System kit (Thermo Fisher). Quantitative PCR was performed using the iQ SYBR® Green Supermix system (BIO-RAD). Beta-actin was used as a housekeeping gene for the analysis of *Bmal1*, *Per2*, and *Rev-erbα*. The relative mRNA levels were calculated using the $2^{-\Delta Ct}$ method. The ΔCt values were obtained by calculating the differences: Ct(gene of interest) – Ct(housekeeping gene) in each sample. All groups were normalized relative to WT-SD median of 1.

Oligonucleotides:

Per2	Forward: GAAAGCTGTCACCACCATAGAA	Reverse: AACTCGCACTTCCTTTTCAGG
Bmal	Forward: TGACCCTCATGGAAGGTTAGAA	Reverse: GGACATTGCATTGCATGTTGG

Rev-erbα	Forward: TGGCATGGTGCTACTGTGTAAGG	Reverse: ATATTCTGTTGGATGCTCCGGCG
Actin	Forward: GGCTGTATTCCCCTCCATCG	Reverse: CAGTTGGTAACAATGCCATGT

Statistics

When comparing two groups of normally distributed data, a Student's two tailed t test was used. In experiments with a single variable across more than two groups, an one-way ANOVA was performed. To compare the effects of genotypes and treatments within 4 groups, a two-way ANOVA test was used. To compare the effects of genotype and treatment within 4 groups at multiple time points, a three-way ANOVA test was performed. Following a significant effect in the ANOVA test, Bonferroni's post hoc comparison was used to determine differences between individual data points. Analyses were conducted using the GraphPad Prism 8 statistical software for Windows. All data are presented as means ± standard error of the mean with $p < 0.05$ considered statistically significant.

Chapter III: The Drd1-expressing neurons in the ARC regulate energy homeostasis

Abstract

The decision to eat is informed by many factors including the peripheral energy balance signals, sensory inputs about the quality of the food, safety of the environment and time of day. Neuronal circuits that originate in the ARC process these inputs to initiate or cease feeding. The dopaminergic signaling in the brain is involved in many facets of feeding associated behaviors. DA receptors, including Drd1, are expressed in the ARC and Drd1 agonism modulates the activity of $ARC^{AgRP/NPY}$ neurons. Here, we demonstrate that dopamine receptor D1 (Drd1) expressed neurons in the ARC regulate energy homeostasis differentially from $ARC^{AgRP/NPY}$ neurons. The Drd1-expressing neurons in the ARC express genes involved in maintaining energy balance. Stimulation of these neurons promote feeding and energy expenditure simultaneously.

Introduction

Maintaining energy homeostasis is essential for survival. Excessive caloric intake beyond homeostatic need causes obesity and associated comorbid conditions including type 2 diabetes, cardiovascular disease, and metabolic syndrome. These conditions significantly reduce lifespan and create enormous burdens on healthcare systems. A mechanistic understanding of neuronal circuits that orchestrate energy homeostasis is necessary to develop effective therapeutic strategies to combat obesity and other eating disorders.

The arcuate nucleus of the hypothalamus (ARC) integrates peripheral signals to regulate energy homeostasis (Joly-Amado et al., 2014). Neurons that synthesize both the agouti-related peptide (AgRP) and neuropeptide Y (NPY) are the predominant orexigenic population in this nucleus (Hahn et al., 1998). During states of energy deficit, these $ARC^{AgRP/NPY}$ neurons are activated by orexigenic signals such as ghrelin (Hahn et al., 1998; Liu et al., 2012; Takahashi and Cone, 2005; Andrews et al., 2008; Chen et al., 2004). The increased activity of $ARC^{AgRP/NPY}$ neurons promotes feeding and suppresses energy expenditure (Krashes et al., 2011; Small et al., 2001; Ruan et al., 2014; Aponte et al., 2011) while ablation of $ARC^{AgRP/NPY}$ neurons in adults leads to starvation (Luquet et al., 2005). Whether $ARC^{AgRP/NPY}$ neurons are molecularly partitioned in orexigenic responses beyond homeostatic feeding remains an open question.

Other neuronal populations in the ARC that orchestrate food intake include neurons expressing proopiomelanocortin (POMC), tyrosine hydroxylase (TH), somatostatin (SST), or prepronociceptin (PNOC). TH, SST and PNOC neurons are activated by energy deficit signals, and when stimulated drive robust food consumption (Zhang and van den Pol, 2016; Luo et al., 2018; Jais et al., 2020). Conversely, POMC neurons are activated by satiety signals including leptin and insulin (Dodd et al., 2018; Cowley et al., 2001), and restrain the amount of calorie intake when stimulated (Zhan et al., 2013). Recent studies also revealed a group of fast acting anorexigenic glutamate-releasing ARC neurons that complement the slow POMC satiety response(Fenselau et al., 2017). Hypothalamic non-AgRP, non-POMC GABAergic neurons are required for postweaning feeding (Kim et al., 2015), and chronic activation of the non-AgRP GABAergic ARC neurons leads to obesity(Zhu et al., 2020).

Recent studies revealed Drd1 expression in the ARC (Romero-Fernandez et al., 2014) and increased activity of $ARC^{AgRP/NPY}$ neurons in response to DA and Drd1 agonists(Alhadeff et al., 2019; Zhang and van den Pol, 2016), suggesting that Drd1 signaling contributes to ARC-dependent energy homeostasis. Therefore, we sought to investigate the functional relevance of Drd1-expressing neurons in the ARC (ARC^{Drd1} neurons) in feeding behavior.

In this study, we show that the Drd1-expressing neurons in the ARC (ARC^{Drd1} neurons) comprise a heterogeneous population of cells including a subpopulation that expresses AgRP. Optogenetic or chemogenetic stimulation of the ARC^{Drd1} neurons induces acute and reversible food consumption. The ARC^{Drd1} neurons regulate feeding behavior differentially from the $ARC^{AgRP/NPY}$ neurons by promoting food exploration even after a food source has already been acquired and increasing energy expenditure. Our findings suggest that ARC^{Drd1} neurons contribute to the maintaining of energy balance and affect animals' decision between consumption of available food or seeking a different calorie source.

Result

The ARC^{Drd1} neurons express genes of energy homeostasis

To identify neuronal populations that potentially receive dopaminergic input in the ARC, we examined the RNA levels of DA receptors (*Drd1-5*) using previously obtained single-cell RNA sequencing data (Campbell et al., 2017). We found that *Drd1* expression is enriched in multiple molecularly distinct neuronal groups, which contrasts the low expression levels of *Drd2* to *Drd5* in the same dataset (Figure 3A). This analysis revealed that 53 out of the 173 *Drd1*-expressing neurons are from the $ARC^{AgRP/NPY}$ neuronal

clusters (Agrp/Gm8773 and Agrp/Sst) while 26 of them express two other orexigenic markers, *Sst* and *Th* (Figures 3B and 3C). Juxtaposing this, 45 of the Drd1-expressing cells are from two POMC neuronal clusters, Pomc/Ttr and Pomc/Anxa2. Since Drd1-dependent activation of $ARC^{AgRP/NPY}$ neurons has been previously observed (Zhang and van den Pol 2016), we confirmed that a subpopulation of $ARC^{AgRP/NPY}$ neurons expresses *Drd1* mRNA using RNAScope (Figure 3D). To quantify the colocalization between the ARC^{Drd1} neurons and $ARC^{AgRP/NPY}$ neurons, we generated the Drd1-tdTomato mice by crossing mice harboring the *Drd1*$^{tm1(cre)Rpa}$ (Drd1-Cre) (Heusner et al., 2008) and *Gt(ROSA)26Sor*$^{tm14(CAG-tdTomato)Hze}$ (Ai14 or TdTomato) (Madisen et al., 2010) alleles on the background of Tg(Npy-hrGFP)1Lowl/J (NPY-GFP) mice since NPY has been demonstrated to co-localized with the AgRP neurons in the ARC (Hahn et al., 1998). 38.3 ± 2.2% of the tdTomato-expressing ARC^{Drd1} neurons co-express NPY-GFP, while 68.6 ± 1.5% of the NPY-GFP neurons co-express Drd1:tdtomato in the ARC (Figure 3E). Therefore, we sought to investigate the relative contribution of the $ARC^{AgRP/NPY}$ positive or negative ARC^{Drd1} neurons on energy homeostasis and determine the role of Drd1 signaling in the $ARC^{AgRP/NPY}$ neurons.

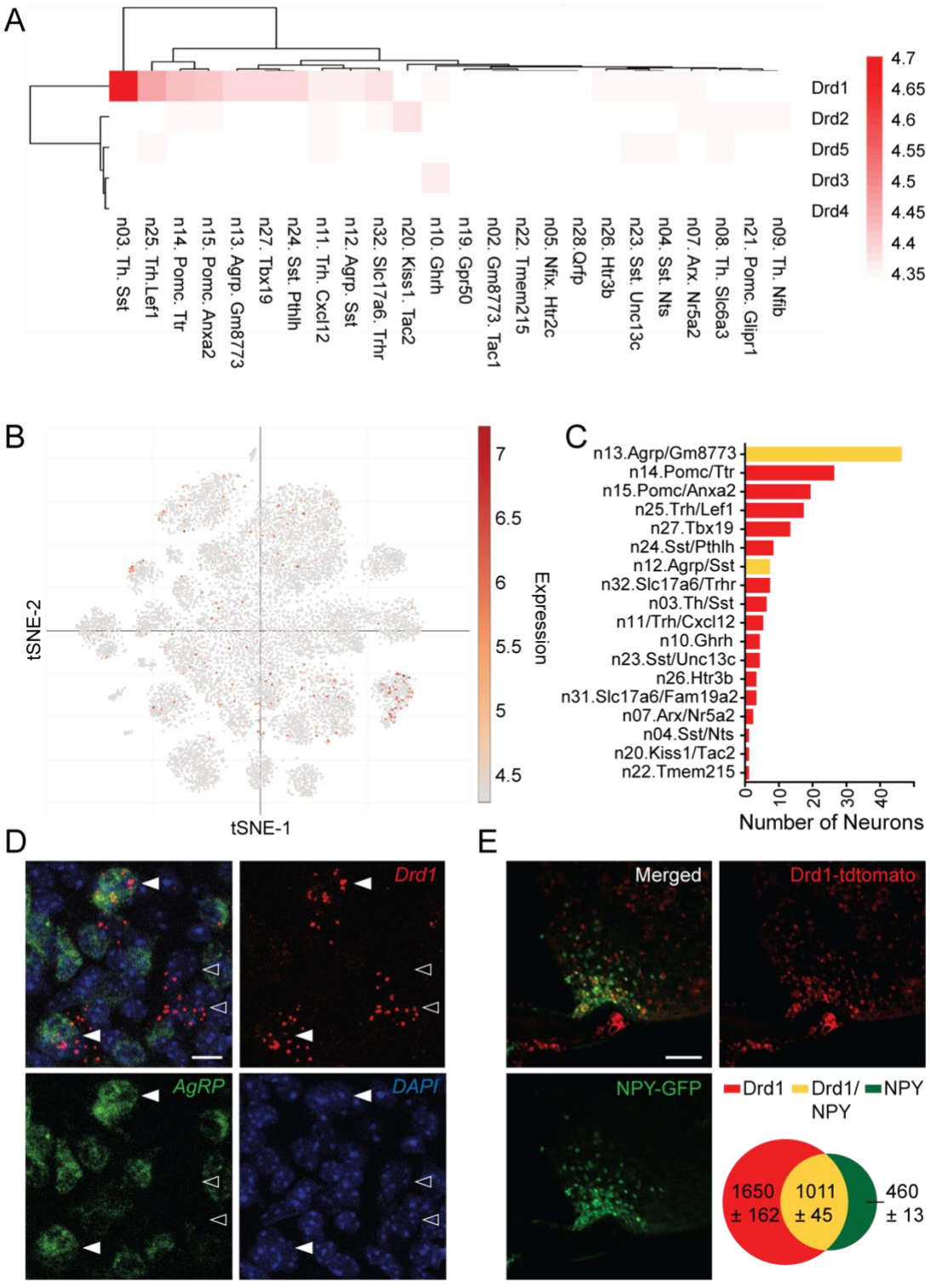
A
Drd1
Drd2
Drd5
Drd3
Drd4
4.7
4.65
4.6
4.55
4.5
4.45
4.4
4.35
n03. Th. Sst
n25. Trh.Lef1
n14. Pomc. Ttr
n15. Pomc. Anxa2
n13. Agrp. Gm8773
n27. Tbx19
n24. Sst. Pthlh
n11. Trh. Cxcl12
n12. Agrp. Sst
n32. Slc17a6. Trhr
n20. Kiss1. Tac2
n10. Ghrh
n19. Gpr50
n02. Gm8773. Tac1
n22. Tmem215
n05. Nfix. Htr2c
n28.Qrfp
n26. Htr3b
n23. Sst. Unc13c
n04. Sst. Nts
n07. Arx. Nr5a2
n08. Th. Slc6a3
n21. Pomc. Glipr1
n09. Th. Nfib
B
tSNE-2
tSNE-1
Expression
7
6.5
6
5.5
5
4.5
C
n13.Agrp/Gm8773
n14.Pomc/Ttr
n15.Pomc/Anxa2
n25.Trh/Lef1
n27.Tbx19
n24.Sst/Pthlh
n12.Agrp/Sst
n32.Slc17a6/Trhr
n03.Th/Sst
n11/Trh/Cxcl12
n10.Ghrh
n23.Sst/Unc13c
n26.Htr3b
n31.Slc17a6/Fam19a2
n07.Arx/Nr5a2
n04.Sst/Nts
n20.Kiss1/Tac2
n22.Tmem215
0
10
20
30
40
Number of Neurons
D
Drd1
AgRP
DAPI
E
Merged
Drd1-tdtomato
NPY-GFP
Drd1
Drd1/ NPY
NPY
1650 ± 162
1011 ± 45
460 ± 13

Figure 3. The genetic profile of ARC neurons reveals an orexigenic neuronal population expressing Drd1

(A) Batch-corrected, normalized expression values for *Drd* genes in each arcuate-median eminence (Arc-ME) neuron cluster from the Campbell *et al*., 2017 dataset.

(B) A t-Distributed Stochastic Neighbor Embedding (t-SNE) plot showing the expression level of Drd1 in the molecular census of the hypothalamic arcuate-median eminence complex (Arc-ME).

(C) Number of *Drd1* positive neurons from each cluster of Arc-ME neurons from A. *Drd1* positive neurons from AgRP-expressing clusters are depicted in yellow.

(D) RNAscope images showing representative Drd1-expressing cells in the ARC with (▶) or without (▷) *Agrp* expression. Scale bar represents 10 μm.

(E) Representative images showing the ARC of Drd1-tdtomato;NPY-GFP mice. Scale bar represents 100 μm. Venn diagram indicates the average number of cells expressing only the Drd1-tdtomato (red), only the NPY-GFP (green), and both Drd1-tdtomato and NPY-GFP (yellow) in each mouse (8 brain sections × 3 mice).

Optogenetic and chemogenetic activation of the ARC^{Drd1} neurons increases food intake

Given the genetic profile of the ARC^{Drd1} neurons, we sought to investigate the relative contribution of the AgRP/NPY positive or negative ARC^{Drd1} neurons on energy homeostasis and determine the role of Drd1 signaling in the $ARC^{AgRP/NPY}$ neurons (Figure 4A). To test whether increased activity of the ARC^{Drd1} neurons stimulate feeding, we targeted them by infusing an adeno-associated virus (AAV) that Cre recombinase dependently express Channelrhodopsin-2 (ChR2; AAV2-DIO-ChR2-EYFP) to the ARC of adult Drd1-cre mice. After at least 3 weeks of postoperative recovery, the ARC^{Drd1} neurons were activated by a 473nm laser at 20 Hz with a 2s-on-3s-off pattern delivered via a fiber optic cannula implanted above the ARC (Figure 4B). We measured food

consumption in these mice pre-, post- and during 1-h laser stimulation. Similar to optogenetic stimulation of $ARC^{AgRP/NPY}$ neurons, activation of ARC^{Drd1} neurons induced rapid and reversible food intake (1-hr intake in Drd1 stimulated: 0.60 ± 0.13 g versus AgRP stimulated: 0.56 ± 0.03 g. Two-way ANOVA with Bonferroni post hoc comparison, $F_{genotype}$ (1, 9) = 0.08617, P = 0.7758; Figure 4C).

To determine the effect of extended stimulation of the ARC^{Drd1} neurons, we expressed the designer receptor hM3Dq (AAV8-DIO-hM3Dq-mcherry) in the ARC of Drd1-cre mice (Drd1-hM3Dq; Figure 4E). We activated the ARC^{Drd1} neurons with i.p. injection of 0.3 g/kg clozapine N-oxide (CNO). At the beginning of the light phase when mice normally refrain from eating, this stimulation significantly increased food consumption in the Drd1-hM3Dq mice (4-h food consumption, saline: 0.24 ± 0.033 g versus CNO: 1.14 ± 1.127 g; repeated-measures three-way ANOVA with Bonferroni post hoc comparison, P < 0.001; Figure 4H). Reflecting the increased daily food intake, three consecutive days of CNO injections led to a significant amount of body weight gain in these animals (body weight change, Drd1-hM3Dq: 3.17 ± 0.677 % versus Drd1-mcherry:-1.29 ± 0.487 %; Student's two-tailed *t*-test, P < 0.001; Figure 4I). The temporal pattern of food consumption over 24 hours (Figures 4K-N) and the body weight gain across three days of CNO treatment (Figure 4O) were similar between chemogenetic stimulation of $ARC^{AgRP/NPY}$ (AgRP-hM3Dq) and the ARC^{Drd1} neurons.

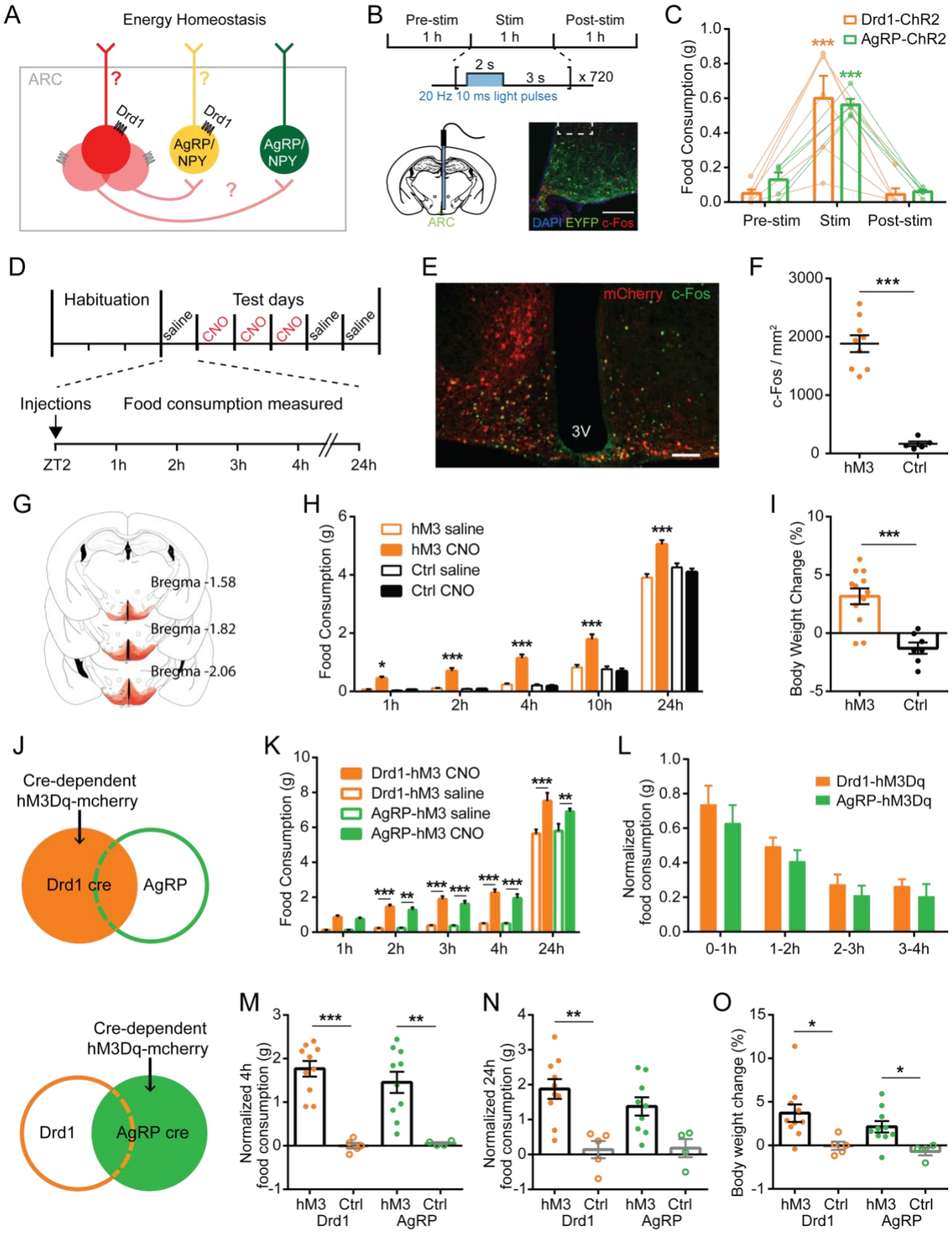
A
Energy Homeostasis
ARC
Drd1
AgRP/
NPY
B
Pre-stim
Stim
Post-stim
1 h
2 s
3 s
x 720
20 Hz 10 ms light pulses
ARC
DAPI EYFP c-Fos
C
Drd1-ChR2
AgRP-ChR2
Food Consumption (g)
Pre-stim
Stim
Post-stim
D
Habituation
Test days
saline
CNO
Injections
Food consumption measured
ZT2
1h
2h
3h
4h
24h
E
mCherry c-Fos
3V
F
c-Fos / mm²
hM3
Ctrl
G
Bregma -1.58
Bregma -1.82
Bregma -2.06
H
hM3 saline
hM3 CNO
Ctrl saline
Ctrl CNO
Food Consumption (g)
1h
2h
4h
10h
24h
I
Body Weight Change (%)
hM3
Ctrl
J
Cre-dependent
hM3Dq-mcherry
Drd1 cre
AgRP
K
Drd1-hM3 CNO
Drd1-hM3 saline
AgRP-hM3 saline
AgRP-hM3 CNO
Food Consumption (g)
1h
2h
3h
4h
24h
L
Drd1-hM3Dq
AgRP-hM3Dq
Normalized
food consumption (g)
0-1h
1-2h
2-3h
3-4h
Cre-dependent
hM3Dq-mcherry
Drd1
AgRP cre
M
Normalized 4h
food consumption (g)
hM3 Ctrl
Drd1
AgRP
N
Normalized 24h
food consumption (g)
hM3 Ctrl
Drd1
AgRP
O
Body weight change (%)
hM3 Ctrl
Drd1
AgRP

Figure 4 Optogenetic or chemogenetic activation of the ARC^{Drd1} neurons increases food intake

(A) Hypothetical model of the ARC^{Drd1} neurons involved in inducing orexigenic responses.

(B) Schematic depicting optogenetic experiment schedule. Photostimulation was conducted for 1 hr with 20 Hz 10 msec light pulses applied for 2 sec followed by a 3-sec break. Representative images showing the expression of ChR2-EYFP in the ARC of Drd1-Cre mice. Scale bar represents 100 μm.

(C) Food consumption before, during, and after the 1-hr photostimulation in Drd1-Cre (orange) or AgRP-Cre (green) mice expressing Cre-dependent ChR2-EYFP in the ARC. Two-way ANOVA with Bonferroni post hoc comparison; n = 5 - 6 /group; $F_{genotype}$ (1, 9) = 0.08617, $P = 0.7758$; $F_{treatment}$ (2, 18) = 54.99, $P < 0.001$.

Data are represented as mean ± SEM. ∗$P < 0.05$; ∗∗$P < 0.01$; ∗∗∗$P < 0.001$.

(D) Food intake experiment schedule. Mice were individually caged for at least 3 days and habituated to i.p. injections on the last day. During test days, mice were injected with saline on day 1, 5, 6, and with CNO on days 2 through 4 at ZT 2. Food intake was measured 1, 2, 3, 4, and 24 hrs after the injections.

(E) Representative image of hM3Dq:mCherry and c-Fos expression after CNO administration in Drd1-hM3Dq mice. Scale bar represents 100 μm.

(F) Number of c-Fos-expressing cells in the ARC after CNO administration in Drd1-hM3Dq or control mice. Student's two-tailed *t*-test; n = 7 - 9 / group.

(G) Expression pattern of hM3Dq:mCherry in the brain sections of Drd1-hM3Dq mice.

(H) Food consumption in Drd1-hM3Dq (orange; hM3) or control (black; Ctrl) mice 1, 2, 3, 4, and 24 hrs after saline (hollow) or CNO (solid) administration. Repeated-measures three-way ANOVA with Bonferroni post hoc comparison; n = 7 - 12 / group; $F_{transgene}$ (1, 17) = 17.84, $P < 0.001$; $F_{treatment}$ (1, 17)= 37.31, $P < 0.001$; F_{time} (2.504, 42.58) = 1120, $P < 0.001$.

(I) Percentage body weight change after 3 consecutive days of CNO injections in Drd1-hM3Dq mice Student's two-tailed *t*-test; n = 7 - 12 / group.

(J) Schematic depicting Cre-dependent hM3Dq-mCherry expression in the ARC of Drd1-Cre or AgRP-Cre mice.

(K) Food consumption in the Drd1-hM3Dq (orange) or AgRP-hM3Dq mice (green) 1, 2, 3, 4, and 24 hrs after saline (hollow) or CNO (solid) administration. Repeated-measures three-way ANOVA with Bonferroni post hoc comparison; n = 4 - 10 / group; $F_{genotype}$ (1, 18) = 0.8829, P = 0.3598; $F_{treatment}$ (1, 18) = 115.2, P < 0.001; F_{time} (4, 72) = 703.2, P < 0.001.

(L) Hourly food consumption following CNO administration in Drd1-hM3Dq or AgRP-hM3Dq mice. Responses were normalized by subtracting the average food consumption on day 1, 5, 6 after saline injections. Two-way ANOVA with Bonferroni post hoc comparison; n = 10 / group; $F_{genotype}$ (1, 18) = 1.071, P = 0.3145; F_{time} (3, 54) = 27.04, P < 0.001.

(M) Normalized 4-hr food consumption following CNO administration in Drd1-hM3Dq, AgRP-hM3Dq, or control mice (Ctrl). Control mice are Drd1-Cre or AgRP-Cre mice with cre-dependent mCherry targeted to the ARC. Two-way ANOVA with Bonferroni post hoc comparison; n = 4 - 10 / group; $F_{genotype}$ (1, 25) = 0.2998, P = 0.5889; $F_{transgene}$ (1, 25) = 46.38, P < 0.001.

(N) Normalized 24-hr food consumption following CNO administration in Drd1-hM3Dq, AgRP-hM3Dq, or control mice. Two-way ANOVA with Bonferroni post hoc comparison; n = 4 - 10 / group; $F_{genotype}$ (1, 24) = 0.5300, P = 0.4736; $F_{transgene}$ (1, 24) = 22.01, P < 0.001.

(O) Percentage body weight change after 3 consecutive days of CNO administrations in Drd1-hM3Dq or AgRP-hM3Dq mice. Two-way ANOVA with Bonferroni post hoc comparison; n = 4 - 10 / group; $F_{genotype}$ (1, 25) = 1.377, P = 0.2517; $F_{transgene}$ (1, 25) = 12.25, P = 0.0018.

Data are represented as mean ± SEM. ∗P < 0.05; ∗∗P < 0.01; ∗∗∗P < 0.001.

The ARC^{Drd1} neurons promote food exploration

As activation of ARC$^{AgRP/NPY}$ neurons in the absence of food triggers foraging and repetitive behaviors, which are reverted by food consumption, we aimed to investigate the role of ARC^{Drd1} neurons in foraging behavior. To this end, we evaluated the food seeking behavior of AgRP-hM3Dq and Drd1-hM3Dq mice in an open field where 8 pellets of the standard chow (PicoLab Rodent Diet 20 5053) were buried under the corn bedding (Figure 5A). AgRP-hM3Dq and Drd1-hM3Dq mice exhibited similar latency of finding the first food pellet (Figure 5B). The total number of food pellets found within the 20 min test was also comparable in AgRP-hM3Dq and Drd1-hM3Dq mice (Figure 5C). Strikingly, stimulated AgRP-hM3Dq mice spent significantly more time eating the firstly acquired pellet compared to Drd1-hM3Dq mice which quit consumption of the first pellet rapidly and instead continued to search for the next pellet (Figures 5E-G). These results suggest that the ARC^{Drd1} and ARC$^{AgRP/NPY}$ neurons differentially regulate food consumption and activation of ARC^{Drd1} neurons promotes food exploration even after a food source has already been acquired.

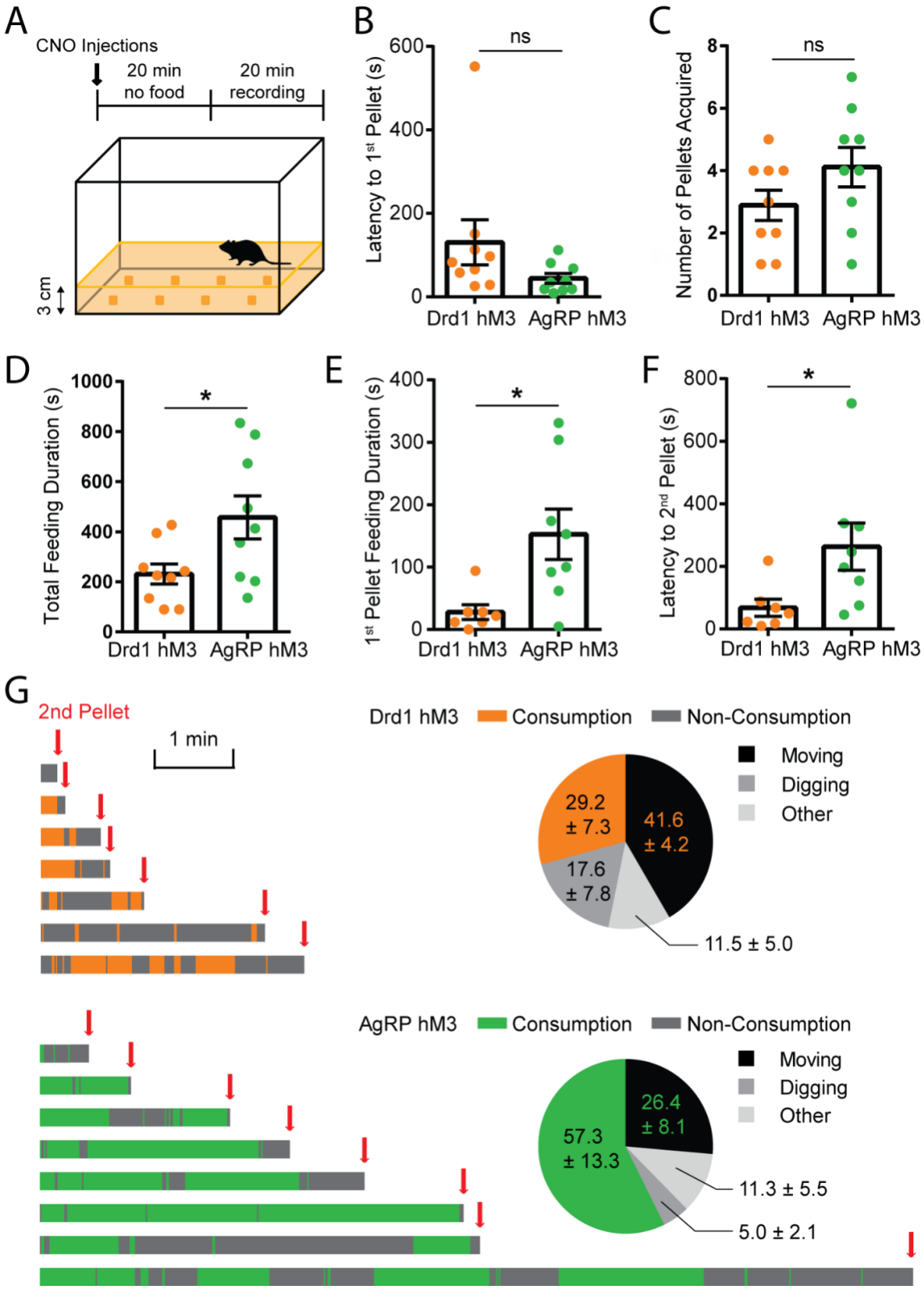
A
CNO Injections
20 min
no food
20 min
recording
3 cm
B
ns
Latency to 1st Pellet (s)
600
400
200
0
Drd1 hM3
AgRP hM3
C
ns
Number of Pellets Acquired
8
6
4
2
0
Drd1 hM3
AgRP hM3
D
*
Total Feeding Duration (s)
1000
800
600
400
200
0
Drd1 hM3
AgRP hM3
E
*
1st Pellet Feeding Duration (s)
400
300
200
100
0
Drd1 hM3
AgRP hM3
F
*
Latency to 2nd Pellet (s)
800
600
400
200
0
Drd1 hM3
AgRP hM3
G
2nd Pellet
1 min
Drd1 hM3
Consumption
Non-Consumption
Moving
Digging
Other
29.2
± 7.3
41.6
± 4.2
17.6
± 7.8
11.5 ± 5.0
AgRP hM3
Consumption
Non-Consumption
Moving
Digging
Other
26.4
± 8.1
57.3
± 13.3
11.3 ± 5.5
5.0 ± 2.1

Figure 5 Chemogenetic activation of the ARC^{Drd1} neurons facilitate foraging instead of continuous feeding

(A) Foraging paradigm: Habituated mice were injected with CNO and placed in an arena with 8 pellets of SD buried under 3cm-thick corn bedding on the cage floor and video recorded for 20 min.

(B) Latency to the acquisition of the first pellet. Student's two-tailed *t*-test; n = 7 - 8 / group.

(C) Total numbers of food pellets acquired during the 20 min test. Student's two-tailed *t*-test; n = 7 - 8 / group.

(D) Total feeding duration during the 20 min test. Student's two-tailed *t*-test; n = 7 - 8 / group.

(E) First pellet feeding duration. Student's two-tailed *t*-test; n = 7 - 8 / group.

(F) Latency to the acquisition of the second pellet after the acquisition of the first pellet. Student's two-tailed *t*-test; n = 7 - 8 / group.

(G) Annotated consumption or non-consummatory behaviors of each mouse during the test after the acquisition of the first pellet and before the acquisition of the second pellet. Consumption time of Drd1-hM3Dq and AgRP-hM3Dq mice is shown as orange and green, respectively. Time spent performing non-consummatory behaviors is shown as dark gray. Pie charts indicated the percentage time spent consuming food (orange or green), moving (black), digging (gray) and other non-consummatory behaviors (light gray).

Data are represented as mean ± SEM. $*P < 0.05$; $**P < 0.01$; $***P < 0.001$; ns, not significant.

The ARC^{Drd1} neurons promote energy expenditure and locomotion

To gain further insight into how energy homeostasis is regulated by ARC^{Drd1} neurons, we monitored the metabolic activity during their chemogenetic activation using the homecage Comprehensive Lab Animal Monitoring System (CLAMS). Paralleling the increased food consumption, we observed increased respiratory exchange rates (RER) in Drd1-hM3Dq and AgRP-hM3Dq mice following CNO administration (4-hr average RER, Drd1-hM3Dq: 0.91 ± 0.010 versus AgRP-hM3Dq: 0.92 ± 0.010; Student's two-tailed *t*-test, $P = 0.44$; Figures 6A-D). This reflects the rapid switch of substrate utilization from fats to carbohydrates as the animals begin to consume food. Consistent with the previous reports (Cavalcanti-de-Albuquerque et al., 2019), we did not observe increased energy expenditure following ARC$^{AgRP/NPY}$ neuron stimulation (Figure 6E). However, stimulation of the ARC^{Drd1} neurons significantly increased energy expenditure (Figure 6E) and locomotion (Figure 6F) suggesting a distinct role for these neurons in energy homeostasis.

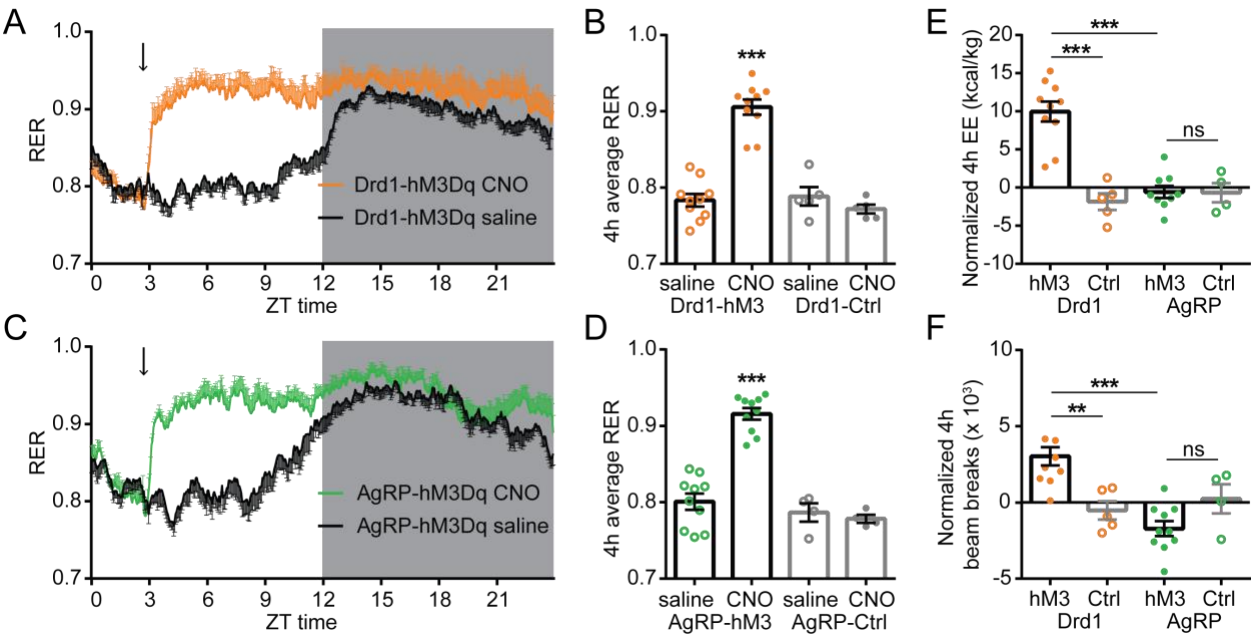

Figure 6. ARC^{Drd1} neurons regulate energy homeostasis

(A, C) 24-hr RER in Drd1-hM3Dq (A) or AgRP-hM3Dq mice (D) following saline (black line) or CNO (orange line) administration. The night period is shown as the gray square. Arrows indicate the time of injections.

(B) Average 4-hr RER in Drd1-hM3Dq and control mice following saline or CNO administration. Two-way ANOVA with Bonferroni post hoc comparison; n = 5 - 10 / group; $F_{transgene}$ (1, 26) = 38.09, $P < 0.001$; $F_{treatment}$ (1, 26) = 25.81, $P < 0.001$.

(D) Average 4-hr RER AgRP-hM3Dq and control mice following saline or CNO administration. Two-way ANOVA with Bonferroni post hoc comparison; n = 4 - 10 / group; $F_{transgene}$ (1, 24) = 45.15, $P < 0.001$; $F_{treatment}$ (1, 24) = 22.39, $P < 0.001$.

(E) Normalized 4-hr EE in Drd1-hM3Dq, AgRP-hM3Dq, or control mice. Responses were normalized by subtracting the EE after saline injections. Two-way ANOVA with Bonferroni post hoc comparison; n = 4 - 10 / group; $F_{genotype}$ (1, 24) = 13.11, $P = 0.0014$.

(F) Normalized 4-hr beam breaks in Drd1-hM3Dq, AgRP-hM3Dq, or control mice. Responses were normalized by subtracting the beam breaks after saline injections. Two-way ANOVA with Bonferroni post hoc comparison; n = 4 - 10 / group; $F_{genotype}$ (1, 25) = 8.372, $P = 0.0078$.

Data are represented as mean ± SEM. $*P < 0.05$; $**P < 0.01$; $***P < 0.001$.

Discussion

The ARC controls energy balance through molecularly distinct cell types, many of which remain unknown. Our RNA-seq analysis revealed a heterogeneous composition of the ARC^{Drd1} neurons with both orexigenic and anorexigenic neuronal populations. Chemogenetic activation of the ARC^{Drd1} neurons promote feeding to a similar degree with the $ARC^{AgRP/NPY}$ neurons, suggesting a dominant impact of the orexigenic groups during feeding regulation. This is consistent with previous finding that simultaneous activation of both $ARC^{AgRP/NPY}$ neurons and POMC neurons increases food consumption, which probably facilitates animals' survival as starvation is more likely lethal than overconsumption.

Chemogenetic activation of the ARC^{Drd1} neurons induces distinct metabolic phenotypes from the stimulation of the $ARC^{AgRP/NPY}$ neurons including increased energy expenditure and locomotion (Figures 6E and 6F). These responses are likely associated with the simultaneous activation of multiple ARC dependent circuits including the neurons coexpressing POMC which is known to promote energy expenditure and ambulatory movements. Expression of Drd1 in both $ARC^{AgRP/NPY}$ and POMC neurons might be a reflection of their shared hypothalamic progenitor origin (Padilla et al., 2010); however, the role of Drd1 signaling in POMC neurons remains unclear. Another unique feature of the ARC^{Drd1} neuron stimulation is the increased food seeking following the acquisition of the first food item (Figures 5E-G). The decision process between consumption of available food or seeking a different food item triggers foraging behavior in the absence of food, which is reversed by feeding because food consumption rapidly suppresses the activity of $ARC^{AgRP/NPY}$ neurons. The continuous foraging induced by the ARC^{Drd1} neuron

might be mediated by the non-AgRP neurons that are not inhibited by food acquisition. It is possible that when activated by Drd1-dependent DA signaling, the ARC^{Drd1} neurons affect the animals' decision by increasing the value of an unacquired but potentially "better" food item. Further probing of the heterogeneity of ARC^{Drd1} neurons will increase the depth in understanding the central control of animals' complex feeding behaviors.

Materials and methods

Animals

All animal care experiments were conducted in concordance with the University of Virginia Institutional Animal Care and Committee. Mice were housed in a temperature and humidity controlled vivarium at 22-24°C and ~40% humidity with a 12h/12h light/dark cycle. Male adult animals older than 8 weeks were used in all behavioral experiments with the following genotypes: C57BL(The Jackson Laboratory Cat# JAX#000664; RRID: IMSR_JAX:000664), Drd1-Cre (Palmiter Lab, University of Washington), $Gt(ROSA)26Sor^{tm14(CAG-tdTomato)Hze}$ (The Jackson Laboratory Cat# JAX#007914; RRID: IMSR_JAX:007914), Tg(Npy-hrGFP)1Lowl (The Jackson Laboratory Cat# JAX#006417; RRID: IMSR_JAX:006417), $Agrp^{tm1(cre)Lowl}$ (The Jackson Laboratory Cat# JAX#012899; RRID: IMSR_JAX:012899).

Mouse diets

Standard diet (SD): Teklad 8664 (Envigo, United Kingdom: 3.1 kcal/gram; 19% fat, 31% protein, 50% carbohydrates. PicoLab Rodent Diet 20 5053 (3.07 kcal/gram; 13% fat, 24% protein, 62% carbohydrates; 3.2% sucrose).

RNAseq analysis

The batch-corrected and normalized cluster-level expression values for Drd1, Drd2, Drd3, and Drd5 were downloaded from the Broad Single Cell Atlas and read into the R package to generated a heatmap with the following code:

```
expr <- read.csv(file = "ForAli_v4_heatmap.csv", header = TRUE, row.names = 1)
expr_mat <- data.matrix(expr)
cols = colorRampPalette(c("white", "red"))(30)
pheatmap(expr_mat,border_color="NA", scale="none", show_rownames = TRUE, main="Dopamine Receptor Isoforms Expressed by Arc-ME Neurons",cluster_rows = T, cluster_cols = T, legend = T, color = cols)
```

The number of Drd1 positive neurons from each molecular cluster according to the Broad Single Cell Atlas was quantified to make the bar graph.（**John Campbell**）

RNAscope

Mice were anesthetized with ketamine and xylazine (i.p.) and perfused transcardially with PBS followed by 4% paraformaldehyde. Brains were harvested and fixed overnight in 4% paraformaldehyde at 4°C. Coronal sections were cut at 30 μm on a vibratome and dried on slides overnight in the dark and a hydrophobic barrier was applied to the slides. *In situ* hybridization was performed using the RNAscope® Multiplex Fluorescent Reagent Kit v2 Assay (ACD) in accordance with the manufacturer's instruction. Probes were used against mouse Drd1 (RNAscope® Probe- Mm-Drd1-C2, Cat No. 461901) and mouse AgRP (RNAscope® Probe- Mm-AgRP, Cat No. 400711). Sections were immersed with RNAscope® hydrogen peroxide to block the activity of endogenous peroxidases. After a wash in distilled water, sections were permeabilized with RNAscope® protease IV for 30 min at 40°C. Sections were hybridized with the Drd1 and AgRP probe at 40°C for 2 h,

followed by amplification incubation steps: Amp 1, 30 min at 40°C; Amp 2, 30 min at 40°C; Amp 3, 15 min at 40°C. HRP signals were developed with RNAscope® Multiplex FL v2 HRP and TSA® Plus fluorophores (HRP-C1 and 1:1500 TSA® Plus fluorescein for AgRP; HRP-C2 and 1:750 TSA® Plus Cy3 for Drd1). Sections were washed with the provided washing buffer 2 × 2 min in between each step. Sections were then coverslipped with DAPI Fluoromount-G (Southern Biotech). Confocal microscope imaging was performed in W.M. Keck Center for Cellular Imaging, University of Virginia, with Leica SP5 X imaging system.

Stereotaxic Surgery

For stereotaxic injections of virus vectors, mice older than 8 weeks were anesthetized with 5% gaseous isoflurane in a closed container, and then placed into the Kopf Small Animal Stereotaxic Frame on a heating pad to maintain body temperature. The isoflurane level was lowered to 2-3% when breathing rhythms steadily reached one breath per 1-2 seconds. The skull was exposed via a small incision after 0.8 mL bupivacaine injection under the scalp. A small hole in the skull was drilled above the targeted injection site. A 26 gauge Hamilton syringe was inserted into the ARC (coordinates: bregma: AP: -1.40 mm, DV: -5.90 mm, L: 0.30 mm) and 500 nl of the virus was bilaterally injected at a flow rate of 100 nl/min using an automated delivery system (World Precision Instruments microsyringe controller). For optogenetic surgeries, a fiber optic cannula was implanted above the ARC following the injection of the virus (coordinates: bregma: AP: -1.40 mm, DV: -5.65 mm, L: 0.30 mm). The exposed end of the fiber optic cannula was fixed to the skull with Metabond. Mice were allowed to recover for 3 weeks before any behavioral

tests. All surgical procedures were performed in sterile conditions and in accordance with University of Virginia IACUC guidelines.

Viral constructs

AAV8-hSyn-DIO-hM3Dq-mcherry (Addgene 44361-AAV8; 9 × 10ˆ12 viral genomes/µl), AAV8-hSyn-DIO-mcherry (Addgene 50459-AAV8; 1.2 × 10ˆ13 viral genomes/µl), AAV-EF1a-DIO-hChR2(H134R)-EYFP-WPRE-pA (University of North Carolina at Chapel Hill Gene Therapy Center Vector Core Services; 2.1 × 10ˆ13 viral genomes/µl) were injected to the ARC (ML: ± 0.30 mm, AP: - 1.40 mm, DV: −5.90 mm). All coordinates are relative to bregma (George Paxinos and Keith B. J. Franklin).

Immunohistochemistry

Mice were anesthetized with ketamine and xylazine (i.p.) and perfused transcardially with PBS followed by 4% paraformaldehyde. Brains were harvested and fixed overnight in 4% paraformaldehyde at 4℃ and then were then placed into 30% sucrose for around 24h until they sank to the bottom of the container. The tissue was sectioned coronally at 30 µm on a cryostat and immersed in PBS with 0.004% sodium azide. Sections were treated with 3% donkey serum in 0.3% Triton X-100 in PBS for 30 minutes, and then incubated with primary antibodies overnight at 4℃. After washing with PBS (5 min × 2), brain sections were incubated with secondary antibodies for 2 hrs at room temperature. Sections were washed in PBS (5 min × 2) and mounted using DAPI Fluoromount-G (Southern Biotech). Images were captured on a Zeiss Axioplan 2 Imaging microscope equipped with an AxioCam MRm camera using AxioVision 4.6 software (Zeiss). Brightness and contrast were corrected with imageJ. The manipulation of the images between control and experimental conditions were kept consistent.

For c-Fos staining, mice were i.p. injected with 0.3mg/kg CNO two hours before anesthesia. Brain sections were treated with 5% donkey serum in 0.3% Triton X-100 in PBS for 1 hour, and then incubated with rabbit anti-c-Fos (1:200) for 20h at room temperature. After washing with PBS, brain sections were incubated with secondary donkey anti-rabbit Cy2 (1:250) for 3h at room temperature. The counting of c-Fos-labeled neurons was done manually and blindly.

The following primary antibodies were used for fluorescent labeling: rabbit anti-c-Fos (1:200, Santa Cruz Sc-52), rabbit anti-DsRed (1:1000, Clontech 632496), chicken anti-mCherry (1:500, NOVUSBIO NBP2-25158). The secondary antibodies (Jackson ImmunoResearch) used were Cy2- or Cy3- conjugated donkey anti-rabbit (1:250), and donkey anti-chicken (1:250).

Food intake analysis

For optogenetic food intake analysis, adult Drd1-Cre and AgRP-Cre mice were single-housed for at least 3 days and habituated to the head-tether before the test. During the test day, after a brief habituation mice were given no laser stimulation for 1h, laser stimulation for 1h, and no laser stimulation for another hour. One pellet of the SD around 4 g was provided. The amount of food consumption within each hour was manually measured. The laser stimulation was 20 Hz 473nm blue light with a 2s-on-3s-off pattern.

For chemogenetic food intake analysis, adult mice were single-housed for at least 3 days and habituated to i.p. injection of saline before the test. During the test, mice were i.p. injected with saline on days 1, 5, and 6, and i.p. injected with 0.3 mg/kg CNO on days 2, 3 and 4. The injections occur at the beginning of the light cycle, from ZT2 to ZT3. Three pellets of SD were placed on the floor of the home cages with the total weight of food

around 13 g. Food consumption was manually measured at 1h, 2h, 3h, 4h, and 24h after the injections. Body weights were measured 24h after injections.

Open Field 8-pellet SD foraging analysis

Drd1-hM3Dq mice and AgRP-hM3Dq mice were habituated to the test conditions on day 1. On day 5, mice were placed in the open field before the test for 20 min. During the test, Drd1-hM3Dq mice and AgRP-hM3Dq mice were injected with 0.3mg/kg CNO and placed into the open field without food for 20 min for CNO to take effect. Mice were put into their home cage without food when 8 pellets of the SD were buried under the 3cm-thick corn bedding in the open field, and then placed back into the open field. Behavior was recorded with a camera above the open-field chamber for 20 min. The total number of food pellets found within 20 min, the latency to the first and second food pellets, the feeding time of the first food pellet, and the total feeding time were quantified offline. Mice that failed to find the second food pellet were not included in the analysis of the latency to the second food pellet (Drd1-hM3Dq: n = 2; AgRP-hM3Dq: n = 1).

Comprehensive Lab Animal Monitoring System (CLAMS)

The CLAMS system (Columbus Instruments) was used for indirect calorimeter and ambulatory locomotor activity measurements during ad libitum access to SCD or HFD. Mice were acclimated to metabolic cages for 3 days and habituated to i.p. injection on the second day. During test day, mice were injected with saline or CNO between ZT 3 to ZT 4 and then monitored for 24 hrs following the manufacturer's instructions.

Energy expenditure (EE) in watts per kilogram of lean mass [W/kg] was calculated with the following formula described in (Fischer et al., 2018).

EE[W/kg]=1/60∗((0.2716[W∗min/ml]∗VO2[ml/kg/hour])+(0.07616[W∗min/ml]∗VCO2[ml/kg/hour])

The unit Watts was converted to kcal/h by multiplying factor of 0.86 to report EE as kcal/h/kg of lean mass.

Locomotor activity was reported as the sum of ambulatory beam breaks in x and y directions.

Statistics

When comparing two groups of normally distributed data, a Student's two-tailed *t*-test was used. In experiments with a single variable across more than two groups, an one-way ANOVA was performed. To compare the effects of genotypes and treatments within 4 groups, a two-way ANOVA test was used. To compare the effects of genotype and treatment within 4 groups at multiple time points, a three-way ANOVA test was performed. Following a significant effect in the ANOVA test, Bonferroni's post hoc comparison was used to determine differences between individual data points. Analyses were conducted using the GraphPad Prism 8 statistical software for Windows. All data are presented as means ± standard error of the mean with $p < 0.05$ considered statistically significant.

Chapter IV: The Drd1-signaling in the ARC$^{AgRP/NPY}$ neurons is required for gating the severity of high fat diet induced obesity

Abstract

Obesity comorbidities such as diabetes and cardiovascular disease are pressing public health concerns. Overconsumption of calories leads to obesity, however, the neuronal mechanisms underlying excess food consumption and weight gain are poorly understood. Here, we demonstrate that dopamine receptor D1 (Drd1) expressed in the agouti-related peptide/neuropeptide Y (AgRP/NPY) neurons of the arcuate hypothalamus is required for gating the severity of diet induced obesity. Stimulation of the Drd1 and AgRP/NPY co-expressing arcuate neurons is sufficient to induce voracious feeding while genetic ablation of Drd1 in these neurons reduces hyperphagia and body weight gain induced by a palatable diet. These results define a new mechanism that influences overconsumption of rewarding foods and positions Drd1 signaling in the ARC$^{AgRP/NPY}$ neurons as an integrator of the hedonic and homeostatic feeding neuronal circuits.

Introduction

Obesity resulting from overconsumption and a sedentary lifestyle often leads to diabetes, cardiovascular disease and metabolic syndrome (Piché et al., 2020); (Chaput et al., 2011). However, the treatment of obesity with anti-obesity medications often delivers insufficient efficacy and dubious safety (Müller et al. 2021).

Energy-dense foods increase appetite leading to consumption even in the absence of homeostatic need (Ferrario et al., 2016). Mammals have evolved exquisit neural mechanisms to consume a sufficient but not excess of calories, yet the basis by which HFD short-circuits these mechanisms remains unclear. Dopamine (DA) signaling is

necessary for encoding feeding associated behaviors, especially with the incentive and motivational aspects driving feeding (Palmiter, 2007; Narayanan et al., 2010; Coccurello and Maccarrone, 2018). DA-deficient mice fail to eat and die of starvation (Szczypka et al., 1999).

Dopamine receptor D1 (Drd1) is one of the five DA receptors in mammals and plays a significant role in reward processing (Beninger and Miller, 1998; Luca et al., 2007; Batel et al., 2008; Huang et al., 2008; Jenni et al., 2017). Drd1-expressing neurons in multiple brain regions regulate consumption of regular or palatable food. These regions include the medial prefrontal cortex (Land et al., 2014), nucleus accumbens (Durst et al., 2019), and paraventricular hypothalamic nucleus (Mirmohammadsadeghi et al., 2018). Moreover, Drd1-null mice are resistant to diet-induced obesity and metabolic syndrome (Grippo et al., 2020). Ecopipam, a selective Drd1 antagonist, is effective in achieving and maintaining weight loss in obese patients, however, the receptor's widespread expression causes adverse side effects including depression and anxiety, making its use problematic (Astrup et al., 2007). A treatment strategy targeting the activity of Drd1 expressing neurons that are selectively involved in food consumption would lead to safer therapeutic strategies against obesity. Although a potential role for Drd1 in $ARC^{AgRP/NPY}$ neuron activity has been postulated (Alhadeff et al., 2019; Romero-Fernandez et al., 2014; Zhang and van den Pol, 2016; Alhadeff et al., 2019; Zhang and van den Pol, 2016), the functional relevance of DA signaling in the ARC-dependent energy homeostasis is unknown. Therefore, we sought to evaluate the role of Drd1 signaling in the $ARC^{AgRP/NPY}$ neurons during feeding and diet induced obesity.

In this study, we show that the ARC^{Drd1} neuron-induced feeding is attenuated by blocking neurotransmitter release from ARC$^{AgRP/NPY}$ neurons. Correspondingly, activation of the ARC^{Drd1} neurons that do not express the ARC$^{AgRP/NPY}$ neuronal marker, NPY, fails to initiate feeding, while stimulation of the neurons that co-express Drd1 and NPY increases food intake robustly. Animals that lack Drd1 expression in ARC$^{AgRP/NPY}$ neurons (Drd1^{AgRP}-KO) when given *ad libitum* access to a high fat diet (HFD) are hypophagic and gain less weight compared to controls. Our findings suggest that the Drd1 signaling in the ARC$^{AgRP/NPY}$ neurons is a key contributor to palatable diet-induced obesity.

Result

Inhibition of ARC$^{AgRP/NPY}$ neuron neurotransmitter release dampens ARC^{Drd1} neuron induced food consumption

We sought to elucidate whether the ARC^{Drd1} neuron induced feeding is dependent on the ARC$^{AgRP/NPY}$ neurons. To this end, we utilized the Npy$^{tm1.1(flpo)Hze}$ (NPY-flp) mice which express Flp recombinase in the ARC$^{AgRP/NPY}$ neurons and crossed them with the Drd1-Cre mice to generate Drd1-cre; NPY-flp mice. This allowed us to express two independent transgenes in these two neuron populations simultaneously. By expressing cre-dependent AAV8-DIO-hM3Dq-mcherry in the ARC^{Drd1} neurons and Flp-dependent tetanus neurotoxin (AAV-fDIO-TeNT-GFP) in the ARC$^{AgRP/NPY}$ of the Drd1-cre; NPY-flp mice, we blocked neurotransmitter release in the ARC$^{AgRP/NPY}$ while being able to chemogeneticaly stimulate ARC^{Drd1} neurons (Figure 7A). We found that blocking the ARC$^{AgRP/NPY}$-neuron neurotransmission dramatically dampened the increased food consumption induced by stimulation of the ARC^{Drd1} neurons (Figures 7B and 7C), although a trend toward increased food consumption was still observed compared to the

saline control group (4-h food consumption, saline: 0.46 ± 0.06 g versus CNO: 0.81 ± 0.19 g; Student's two-tailed t test, P = 0.0677; Fig 7B). Likewise, following the CNO injection, we did not observe an increase in RER, energy expenditure, or locomotion in these animals (Figures 7D-F) unlike stimulation of ARC^{Drd1} neurons in the absence of $ARC^{AgRP/NPY}$ neurotransmission blockade. Taken together, these results demonstrate that intact $ARC^{AgRP/NPY}$ neuron signaling is required for the ARC^{Drd1} neuron induced changes in energy homeostasis.

The subpopulation of ARC^{Drd1} neurons expressing NPY is sufficient to induce voracious food consumption

Since ARC^{Drd1} neuron induced food consumption is dependent on the $ARC^{AgRP/NPY}$ neurons, either the ARC^{Drd1} neurons increase $ARC^{AgRP/NPY}$ neuron activity to induce feeding or activation of a subpopulation of the ARC^{Drd1} neurons that express AgRP/NPY are sufficient for this behavior. To distinguish between these two possibilities, we delivered an AAV in which hM3Dq expression is turned on by Cre recombinase but turned off by Flp recombinase (AAV-Con/Foff-hM3Dq), to the ARC of Drd1-cre;NPY-flp mice (Figure 7G). Activation of the ARC^{Drd1} neurons that do not express *Npy* failed to induce feeding or metabolic fluctuations including RER, energy expenditure and locomotion that were observed during activation of all ARC^{Drd1} neurons (Figures 7H, 7J-K). Interestingly, activation of these ARC^{Drd1} neurons that lack *Npy* still increased 24-h food consumption after CNO injections (24-h food consumption: saline injected: 5.79 ± 0.24 g, CNO injected: 6.33 ± 0.29 g, Student's two-tailed *t*-test, P = 0.003, Figure 7I), suggesting a role for these neurons in sustained feeding response.

To test the possibility that ARC^{Drd1} neurons expressing NPY are sufficient to induce food intake, we targeted these neurons by infusing an AAV that expresses hM3Dq only following Cre and Flp-dependent recombination (AAV-Con/Fon-hM3Dq), into the ARC of the Drd1-cre; NPY-flp (Drd1/NPY-hM3Dq) mice (Figure 8A). As positive control, we targeted the same virus to the ARC of the AgRP-cre; NPY-flp (AgRP/NPY-hM3Dq) mice (Figure 8A). CNO-stimulated Drd1/NPY-hM3Dq mice rapidly initiated voracious feeding within one hour (Figure 8B) which lasted at least for 4 hrs similar to the AgRP/NPY-hM3Dq mice (Figures 8C and 8D). However, 24-h food consumption in Drd1/NPY-hM3Dq mice was not as robust as AgRP/NPY-hM3Dq mice (normalized 24-h food consumption: Drd1/NPY-hM3Dq: 0.73 ± 0.26 g; AgRP/NPY-hM3Dq:2.30 ± 0.53 g; One-way ANOVA with Bonferroni post hoc comparison, P = 0.0251; Figure 8F). This suggests that the subset of ARC neurons that express AgRP, NPY and Drd1 ($ARC^{AgRP/NPY/Drd1}$) are engaged during acute feeding response. Consistent with this finding, Drd1/NPY-hM3Dq mice did not gain body weight after three consecutive days of CNO injections (body weight change: Drd1/NPY-hM3Dq: 0.62 ± 0.60 %; AgRP/NPY-hM3Dq: 6.38 ± 1.59 %; One-way ANOVA with Bonferroni post hoc comparison, P = 0.0079; Figure 8G). We next determine the role of the $ARC^{AgRP/NPY/Drd1}$ neurons in metabolic response using CLAMS. Similarly with AgRP/NPY-hM3Dq mice, Drd1/NPY-hM3Dq mice rapidly increased their RER in response to CNO injections (4-h average RER: saline: 0.79 ± 0.01; CNO: 0.92 ± 0.01; Two-way ANOVA with Bonferroni post hoc comparison, P < 0.001; Figures 8H and 8I). Neither Drd1/NPY-hM3Dq nor AgRP/NPY-hM3Dq mice showed changes in energy expenditure or locomotion (Figures 8J and 8K).

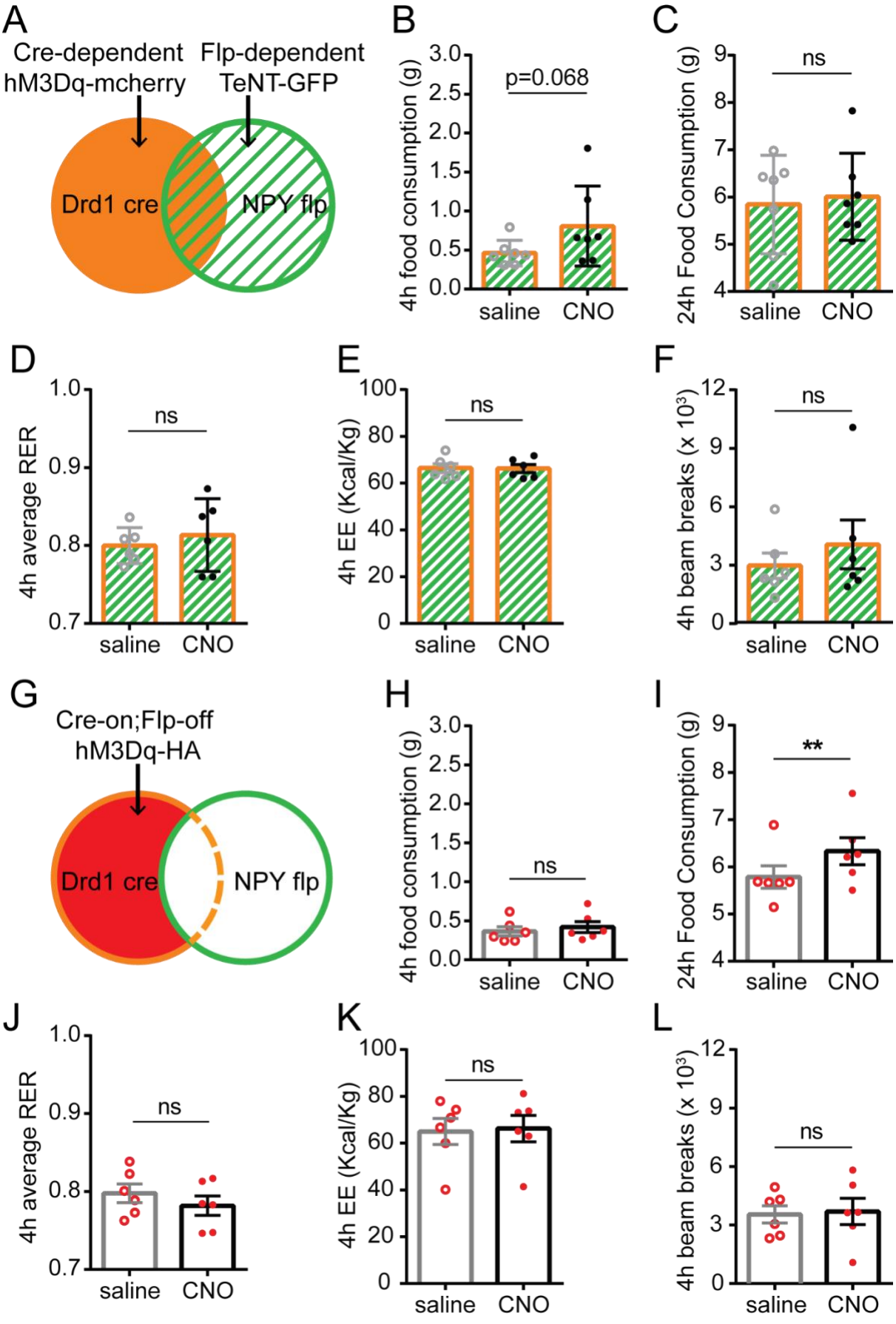
A
Cre-dependent
hM3Dq-mcherry
Flp-dependent
TeNT-GFP
Drd1 cre
NPY flp
B
4h food consumption (g)
p=0.068
saline
CNO
C
24h Food Consumption (g)
ns
saline
CNO
D
4h average RER
ns
saline
CNO
E
4h EE (Kcal/Kg)
ns
saline
CNO
F
4h beam breaks (x 10³)
ns
saline
CNO
G
Cre-on;Flp-off
hM3Dq-HA
Drd1 cre
NPY flp
H
4h food consumption (g)
ns
saline
CNO
I
24h Food Consumption (g)
**
saline
CNO
J
4h average RER
ns
saline
CNO
K
4h EE (Kcal/Kg)
ns
saline
CNO
L
4h beam breaks (x 10³)
ns
saline
CNO

Figure 7. Acute feeding requires ARC$^{AgRP/NPY}$ neuron signaling

(A, G) Schematic depicting Cre-dependent hM3Dq-mCherry and Flp-dependent TeNT-GFP expression (A), Cre-on;Flp-off hM3Dq-HA expression (G) in the ARC of Drd1-Cre;NPY-Flp mice.

(B-F) 4-hr food consumption (B), 24-hr food consumption (C), RER (D), EE (E), or beam breaks (F) in mice indicated in A following saline or CNO administration. Student's two-tailed *t*-test; n = 6 / group.

(H-L) 4-hr food consumption (H), 24-hr food consumption (I), RER (J), EE (K), or number of beam breaks (L) in mice indicated in F following saline or CNO administration. Student's two-tailed *t*-test; n = 6 / group.

Data are represented as mean ± SEM. $*P < 0.05$; $**P < 0.01$; $***P < 0.001$; ns, not significant**.**

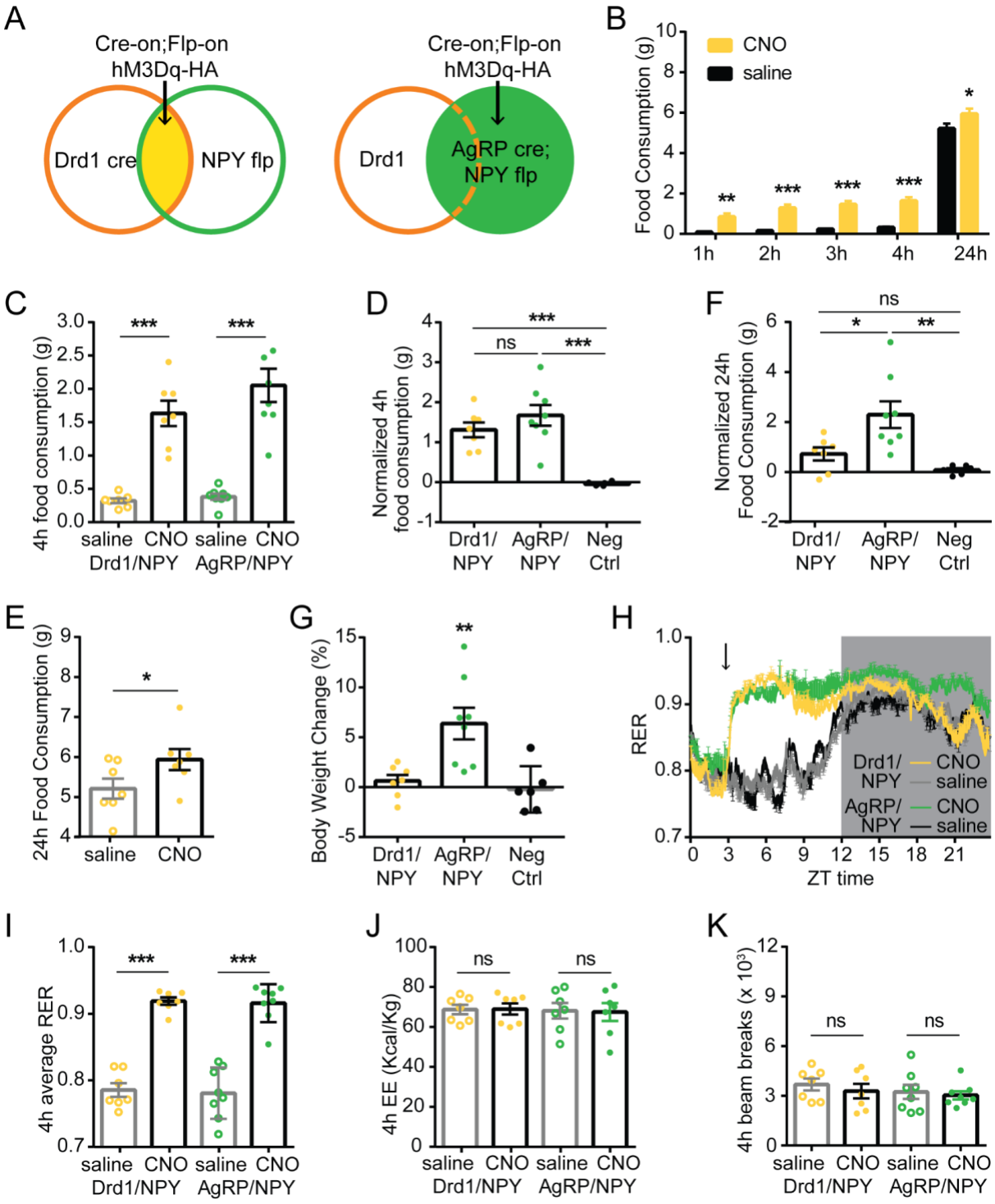

Figure 8. Stimulation of ARC neurons that co-express Drd1 and NPY induce feeding acutely

(A) Schematic depicting Cre-on;Flp-on hM3Dq-HA expression in the ARC of Drd1-Cre;NPY-Flp mice.

(B) Food consumption after 1h, 2h, 3h, 4h, and 24 hrs of saline or CNO injections in Drd1/NPY-hM3Dq mice. Two-way ANOVA with Bonferroni post hoc comparison; n = 7 / group; $F_{treatment}$ (1, 12) = 31.51, $P < 0.001$; F_{time} (4, 84) = 847.8, $P < 0.001$.
(C) 4-hr food consumption in Drd1/NPY-hM3Dq or AgRP/NPY-hM3Dq mice following saline or CNO administration. Two-way ANOVA with Bonferroni post hoc comparison; n = 7 - 8 / group; $F_{genotype}$ (1, 26) = 2.140, $P = 0.1555$; $F_{treatment}$ (1, 26) = 82.60, $P < 0.001$.
(D) Normalized 4-hr food consumption in Drd1/NPY-hM3Dq, AgRP/NPY-hM3Dq, or negative control mice (Neg Ctrl). Negative control mice are Drd1-Cre or NPY-Flp mice with Cre-on;Flp-on hM3Dq-HA delivered to the ARC. Responses were normalized by subtracting the average food consumption on day 1, 5, 6 after saline injections. One-way ANOVA with Bonferroni post hoc comparison; n = 6 - 8 / group; $F_{genotype}$ (2, 18) = 18.92, $P < 0.001$.
(E) 24-hr food consumption in Drd1/NPY-hM3Dq mice following saline or CNO administration. Student's two-tailed *t*-test; n = 7 / group.
(F) Normalized 24 -hr food consumption in Drd1/NPY-hM3Dq, AgRP/NPY-hM3Dq, or negative control mice. One-way ANOVA with Bonferroni post hoc comparison; n = 6 -8 / group; $F_{genotype}(2,18) = 8.844$, $P = 0.0021$.
(G) Percentage body weight change in Drd1/NPY-hM3Dq, AgRP/NPY-hM3Dq, or negative control mice after 3 consecutive days of CNO injections. One-way ANOVA with Bonferroni post hoc comparison; n = 6 - 8 / group; $F_{genotype}$ (2,18) = 9.278; $P = 0.0017$.
(H) 24-hr RER in the Drd1/NPY-hM3Dq mice following CNO (yellow line) or saline (grey line) administration, or the AgRP/NPY-hM3Dq mice following CNO (green line) or saline (black line) administration. Dark periods are shown as the gray square. Arrows indicate the time of injections.
(I) Average 4-hr RER in Drd1/NPY-hM3Dq or AgRP/NPY-hM3Dq mice following saline or CNO administration. Two-way ANOVA with Bonferroni post hoc comparison; n = 7 - 8 / group; $F_{genotype}$ (1, 26) = 0.1369, $P = 0.7144$; $F_{treatment}$ (1, 26) = 159.9, $P < 0.001$.
(J) Average 4-hr EE n Drd1/NPY-hM3Dq or AgRP/NPY-hM3Dq mice following saline or CNO administration. Two-way ANOVA with Bonferroni post hoc comparison; n = 7 / group; $F_{genotype}$ (1, 24) = 0.08857, $P = 0.7686$; $F_{treatment}$ (1, 24) = 0.002338, $P < 0.9618$.

(K) Average 4-hr number of beam breaks in Drd1/NPY-hM3Dq or AgRP/NPY-hM3Dq mice following saline or CNO administration. Two-way ANOVA with Bonferroni post hoc comparison; n = 7 - 8 / group; $F_{genotype}$ (1, 26) = 0.8812, P = 0.3565; $F_{treatment}$ (1, 26) = 0.6433, P = 0.4298.
Data are represented as mean ± SEM. ∗P < 0.05; ∗∗P < 0.01; ∗∗∗P < 0.001; ns, not significant.

Optogenetic stimulation of the Drd1/NPY neuron projections in the PVN induces robust food consumption

To investigate the potential downstream brain regions receiving projections from the Drd1/NPY neurons, we examined the distribution of hM3Dq-HA-labeled axons in brain regions of Drd1/NPY-hM3Dq mice (Figure 9A). We observed axons from the Drd1/NPY neurons in the BNST, PVN, PVT, and periaqueductal gray (PAG), among which the PVN is most densely innervated (Figure 9B). Therefore, we sought to evaluate the functional role of the Drd1/NPY neuron projections in the PVN. To this end, we targeted the ARC of Drd1-cre; NPY-flp mice by infusing an AAV that expresses ChR2 only following Cre and Flp-dependent recombination (AAV-Con/Fon-ChR2-EYFP). After at least 3 weeks of postoperative recovery, the axon terminals from the Drd1/NPY neurons in the PVN were activated by a 473nm laser at 20 Hz with a 2s-on-3s-off pattern delivered via a fiber optic cannula (Figure 9C). We measured food consumption in these mice pre-, post- and during 1-h laser stimulation. Strikingly, stimulation of the Drd1/NPY neuron projections in the PVN robustly increases food consumption, indicating that the $ARC^{Drd1/NPY} \rightarrow$ PVN circuit is sufficient to drive feeding (1-hr intake: pre-stimulation: 0.046 ± 0.01887 g; during stimulation: 0.624 ± 0.1067 g; post-stimulation: 0.0380 ±

0.01463 g; One-way ANOVA with Bonferroni post hoc comparison, *P* = 0.0045; Figure 9D).

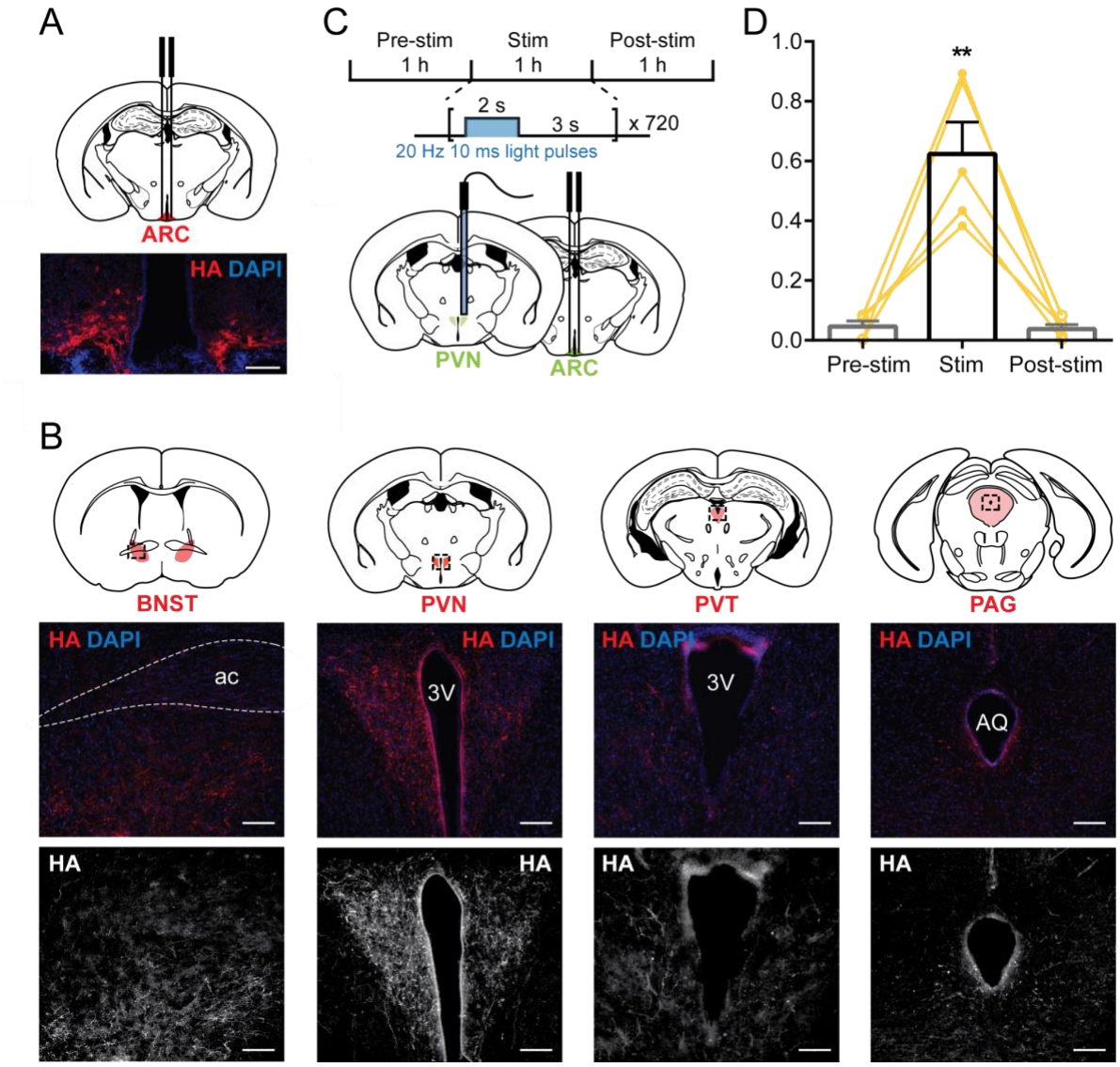

Figure 9. The projections from the subpopulation of ARC^{Drd1} neurons expressing NPY in the PVN is sufficient to induce voracious food consumption

(A) Schematic and representative image showing the Cre-on;Flp-on hM3Dq-HA expression in the ARC of Drd1-Cre;NPY-Flp mice. Scale bar represents 100 μm.

(B) Representative images showing hM3Dq-HA axons in the BNST, PVN, PVT, and PAG. Scale bar represents 100 μm. ac: anterior commission; 3V: third ventricle; AQ: cerebral aqueduct.
(C) Schematic depicting Cre-on;Flp-on ChR2-EYFP expression in the ARC of Drd1-Cre;NPY-Flp mice and optogenetic stimulation of the neuron fibers in the PVN.
(D) Food consumption before, during, and after the 1-hr photostimulation in Drd1-Cre;NPY-Flp mice expressing Cre-on;Flp-on ChR2-EYFP in the ARC.
Data are represented as mean ± SEM. ∗P < 0.05; ∗∗P < 0.01; ∗∗∗P < 0.001; ns, not significant.

Genetic ablation of Drd1 in the ARC$^{AgRP/NPY}$ neurons attenuates diet induced obesity

To investigate the function of Drd1 in the ARC$^{AgRP/NPY}$ neurons, we genetically ablated the Drd1 expression from these neurons by crossing the mice that carries the floxed Drd1 allele (*Drd1*$^{tm2.1Stl}$) with the AgRP cre mice (Drd1^{AgRP}-KO) (Figure 10A). Unlike the germline Drd1 knockout mice (Grippo et al., 2020), at 8 weeks of age, the Drd1^{AgRP}-KO mice had similar body weight compared to the control littermates (Figure 10B). To test whether genetic ablation of the Drd1 expression from the ARC$^{AgRP/NPY}$ neurons affects feeding, we monitored day and night food consumption in Drd1^{AgRP}-KO mice on a standard (SD) or high-fat diet (HFD) during a two-day period. We did not find any difference between the Drd1^{AgRP}-KO and control groups (Figure 10C). Next, we determined the meal microstructure of the Drd1^{AgRP}-KO and control mice fed on either of these diets. Meals were defined as feeding bouts clustering within 5 min intervals (Rathod and Di Fulvio, 2021), with consumption amount no less than 0.05g and duration no less than 5s. On SD, Drd1^{AgRP}-KO and control mice had similar feeding microstructures (Figures 10D-G). However, on HFD, the Drd1^{AgRP}-KO mice had significantly smaller

meals during the daytime (HFD meal size in day time: Drd1^{AgRP}-KO: 0.15 ± 0.007 g; Ctrl: 0.18 ± 0.004 g; Student's two-tailed *t* test, *P* = 0.0047; Figure 10H). Therefore, we further investigated the role of Drd1 in ARC$^{AgRP/NPY}$ neurons in HFD foraging. To this end, we assessed food seeking behavior where habituated mice were placed in an open field with one pellet of the HFD buried under the bedding (Figure 10L) (Grippo et al., 2020). The latency to find the pellet was significantly longer in the Drd1^{AgRP}-KO mice compared to controls (latency to food: Drd1^{AgRP}-KO: 486.9 ± 36.83 s; Ctrl: 244.9 ± 44.54 s; Student's two-tailed t test, *P* = 0.0006; Figure 10M), which implicates a role for Drd1^{AgRP}-signalling during hedonic feeding. To investigate the long-term consequences of this phenotype, we put the Drd1^{AgRP}-KO mice and controls on the HFD for 8 weeks and measured their food consumption and body weight weekly. Strikingly, the Drd1^{AgRP}-KO mice exhibited reduced food consumption (Figures 10N and 10O) and body weight (Figures 10P and 10Q) compared to the controls, which was most prominent within the first two weeks after the diet change (Figures 10O and 10Q. Our observations confirm that the Drd1 signaling in the ARC$^{AgRP/NPY}$ neurons is a contributor to the development of HFD-induced hyperphagia and obesity.

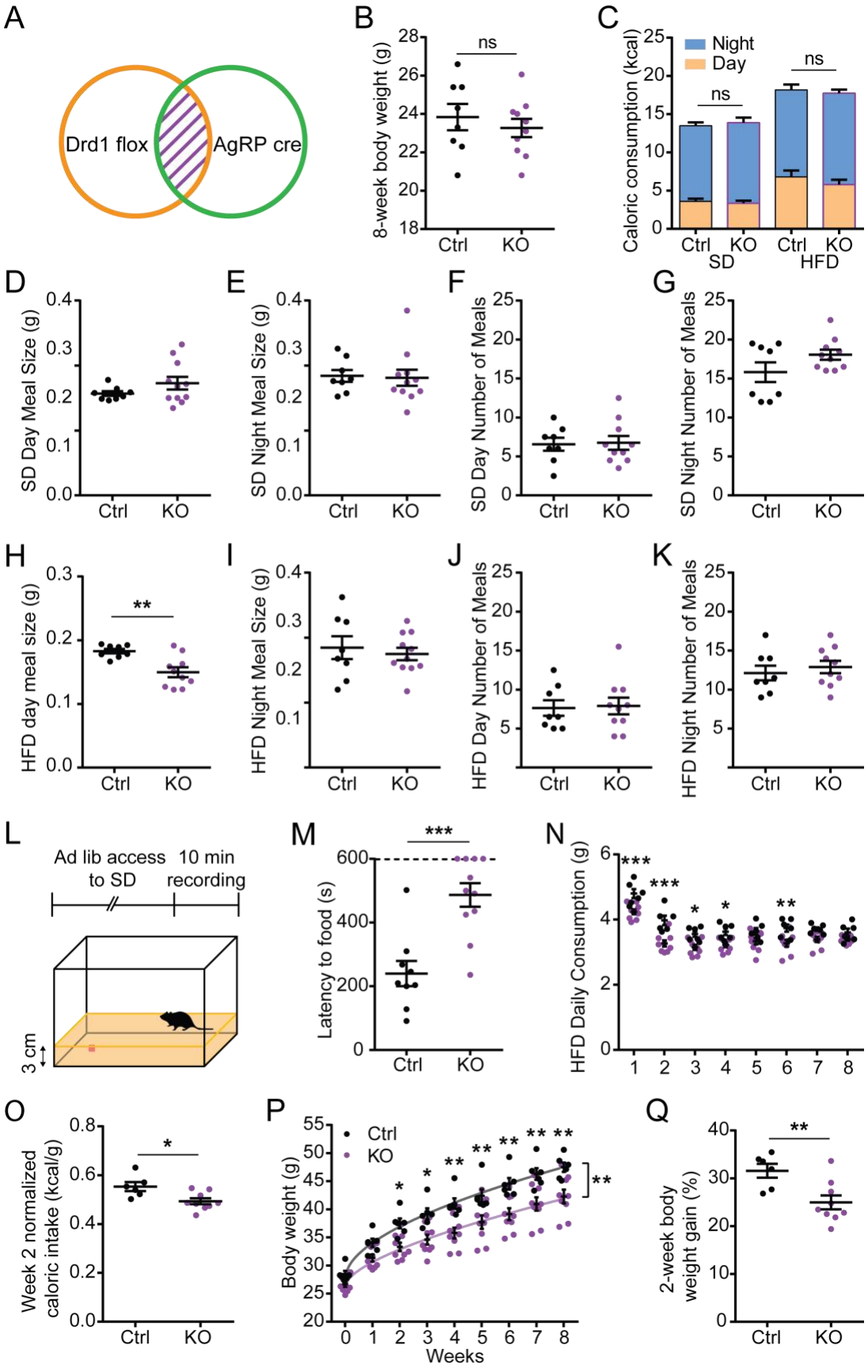
A
Drd1 flox
AgRP cre
B
8-week body weight (g)
ns
Ctrl
KO
C
Caloric consumption (kcal)
Night
Day
ns
ns
Ctrl
KO
Ctrl
KO
SD
HFD
D
SD Day Meal Size (g)
E
SD Night Meal Size (g)
F
SD Day Number of Meals
G
SD Night Number of Meals
H
HFD day meal size (g)
**
I
HFD Night Meal Size (g)
J
HFD Day Number of Meals
K
HFD Night Number of Meals
L
Ad lib access to SD
10 min recording
3 cm
M
Latency to food (s)
***
N
HFD Daily Consumption (g)
O
Week 2 normalized caloric intake (kcal/g)
*
P
Body weight (g)
Ctrl
KO
Weeks
Q
2-week body weight gain (%)
**

Figure 10. The Drd1 signaling in the ARC$^{AgRP/NPY}$ neurons is required for high fat diet induced hyperphagia

(A) Schematic indicating the genetic ablation of Drd1 from ARC$^{AgRP/NPY}$ cells in AgRP-Cre$^{cre/+}$;Drd1$^{fl/fl}$ mice (Drd1^{AgRP}-KO).

(B) Body weights of the control (Ctrl; AgRP-Cre$^{+/+}$;Drd1-Flox$^{fl/fl}$; black) and Drd1^{AgRP}-KO (KO; AgRP-Cre$^{cre/+}$;Drd1-Flox$^{fl/fl}$; purple) littermates at 8 weeks of age. Student's two-tailed *t-test*; n = 8 - 10 / group.

(C) Kilocalories (kcal) consumed by control or Drd1^{AgRP}-KO mice during day and night periods when provided with *ad libitum* access to SD or HFD. Repeated-measures three-way ANOVA with Bonferroni post hoc comparison; n = 8 - 10 / group; F_{time} (1, 16) = 198.7, $P < 0.001$; $F_{genotype}$ (1, 16) = 0.0007562, $P = 0.9784$; F_{diet} (1, 16) = 34.43, $P < 0.001$.

(D, E) Daily SD meal sizes of control (Ctrl) or Drd1^{AgRP}-KO (KO) mice during day time (D) or night time (E). Student's two-tailed *t*-test; n = 8 - 10 / group.

(F, G) Daily number of SD meals of control or Drd1^{AgRP}-KO mice during day time (F) or night time (G). Student's two-tailed *t*-test; n = 8 - 10 / group.

(H, I) Daily SD meal sizes of control (Ctrl) or Drd1^{AgRP}-KO (KO) mice during day time (H) or night time (I). Student's two-tailed *t*-test; n = 8 - 10 / group.

(J, K) Daily number of HFD meals of control or Drd1^{AgRP}-KO mice during day time (J) or night time (K). Student's two-tailed *t*-test; n = 8 - 10 / group.

(L) Open field foraging paradigm.

(M) Latency to food of control or Drd1^{AgRP}-KO mice during the 10 min recording. Mice that failed to find food are represented with latency of 10 min. Student's two-tailed *t*-test; n = 9 - 11 / group.

(N) Daily HFD consumption of control or Drd1^{AgRP}-KO mice through eight weeks of *ad libitum* access to the HFD. Two-way ANOVA with Bonferroni post hoc comparison; n = 6 - 9 / group; $F_{genotype}$ (1,13) = 20.22, $P < 0.001$; F_{time} (7,91) = 50.28, $P < 0.001$.

(O) Daily caloric consumption normalized to body weight of control or Drd1^{AgRP}-KO mice during the second week with *ad libitum* access to the HFD. Student's two-tailed *t*-test; n = 6 - 9 / group.

(P) Body weights of control or Drd1^{AgRP}-KO mice with *ad libitum* access to HFD for 8 weeks. Two-way ANOVA with Bonferroni post hoc comparison; n = 6 - 9 / group; $F_{genotype}$ (1, 13) = 11.58, $P = 0.0047$; F_{time} (8, 104) = 352.4, $P < 0.001$.
(Q) Percentage body weight change of control or Drd1^{AgRP}-KO mice after 2-week *ad libitum* access to HFD. Student's two-tailed *t*-test; n = 6 - 9 / group.
Data are represented as mean ± SEM. $*P < 0.05$; $**P < 0.01$; $***P < 0.001$; ns, not significant.

Discussion

The decision to eat is informed by many factors including the peripheral energy balance signals, sensory inputs about the palatability of the food, safety of the environment and time of day (Fulton, 2010; Arcis and Desor, 2003; Kim et al., 2020). Neuronal circuits that originate in the ARC process these inputs to initiate or cease feeding (Krashes et al., 2011; Zhang and van den Pol, 2016; Luo et al., 2018; Jais et al., 2020; Zhan et al., 2013; Fenselau et al., 2017). The varied functions of the ARC are supported by molecularly specialized neuron subtypes.

The ARC$^{AgRP/NPY}$ neurons are the predominant orexigenic neuronal population. Until recent studies, the functional heterogeneity of the ARC$^{AgRP/NPY}$ neurons was poorly explored. We demonstrated that a significant proportion of the ARC^{Drd1} neurons that express AgRP/NPY (ARC$^{AgRP/NPY/Drd1}$ neurons) are mostly within the Agrp/Gm8773 neuronal cluster. Although the second subset of the ARC$^{AgRP/NPY}$ neurons mediate control of glucoregulation and metabolism (e.g. the somatostatinergic Agrp/Sst neurons) (Campbell et al., 2017), whether Agrp/Gm8773 neurons have a unique role in energy homeostasis is unclear. We established that the stimulation of ARC$^{AgRP/NPY/Drd1}$ neurons is sufficient to initiate robust feeding and that genetic ablation of Drd1 in these neurons

disturbs food-seeking and reduces body weight gain on the HFD. These data support the notion that DA modulates the activity of a subpopulation of the $ARC^{AgRP/NPY}$ including some of the Agrp/Gm8773 neurons via Drd1 signaling and contributes to the development of diet-induced obesity.

The $ARC^{AgRP/NPY/Drd1}$ neuron stimulation-induced 24-hr food consumption response (Figure 8E) is not as robust as the stimulation of the entire $ARC^{AgRP/NPY}$ neuron population (Figure 8F). Notably, the stimulation of the ARC^{Drd1} neurons that lack NPY expression increases 24-hr food consumption without significant induction during the acute phase of the feeding response. These findings suggest that the non-AgRP ARC^{Drd1} orexigenic neurons (e.g. $ARC^{Sst/Drd1}$ or $ARC^{Th/Drd1}$ neurons) contribute to the sustained food consumption following the acquisition of food when the activity of the $ARC^{AgRP/NPY}$ neurons are dampened (Betley et al., 2015; Chen et al., 2015; Beutler et al., 2017).

The daily rhythm and the microstructure of feeding are two critical parameters that are required for maintaining energy balance. Energy-dense foods increase appetite and encourage snacking outside of regular mealtimes (Grippo et al., 2020). Mice fed *ad lib* HFD lose circadian rhythmicity of their food consumption which contributes to obesity and is reversible by time restricted feeding (Hatori et al., 2012). Larger portion sizes of food lead to significantly higher energy intake and weight gain (Rolls et al., 2004a; Rolls et al., 2002; Rolls et al., 2004b), while a greater number of smaller meals is associated with a lower risk of obesity (Ma et al., 2003). Wild type mice increase their meal caloric size during the resting phase when presented with a HFD (Figures 10D and 10H). Surprisingly, this diet induced meal size change is reduced in the $AgRP^{Drd1}$-KO mice, suggesting an

increased satiation. Thus, Drd1 signaling in the $ARC^{AgRP/NPY}$ neurons contributes to the diet-induced hyperphagia by affecting the temporal distribution of larger meals.

Excessive intake of the HFD regardless of energy surplus is an often cited cause of obesity in humans (Hill et al., 2000; Bray and Popkin, 1998). HFD increases the activity of $ARC^{AgRP/NPY}$ neurons (Baver et al., 2014). However, the molecular mechanism of how the HFD induces this change in the $ARC^{AgRP/NPY}$ neurons is unknown. G_s-coupled G protein-coupled receptors (GPCR) signaling in the $ARC^{AgRP/NPY}$ neurons triggers sustained increase in food intake (Nakajima et al., 2016) and Drd1, as a G_s-coupled GPCR, is likely one of the culprits. Although Drd1 is expressed in a fraction of the $ARC^{AgRP/NPY}$ neurons, we demonstrated that this signaling pathway is necessary for appropriate foraging behavior and diet induced obesity. In future studies, we will investigate the mechanism by which ARC DA inputs during consumption of HFD modulate the activity of $ARC^{AgRP/NPY}$ neurons through Drd1 signaling.

Materials and methods

Animals

All animal care experiments were conducted in concordance with the University of Virginia Institutional Animal Care and Committee. Mice were housed in a temperature and humidity controlled vivarium at 22-24°C and ~40% humidity with a 12h/12h light/dark cycle. Male adult animals older than 8 weeks were used in all behavioral experiments with the following genotypes: C57BL(The Jackson Laboratory Cat# JAX#000664; RRID: IMSR_JAX:000664), Drd1-Cre (Palmiter Lab, University of Washington), $Drd1^{tm2.1Stl}$ (The

Jackson Laboratory Cat# JAX#025700; RRID: IMSR_JAX:025700), Agrp$^{tm1(cre)Lowl}$ (The Jackson Laboratory Cat# JAX#012899; RRID: IMSR_JAX:012899), Npy$^{tm1.1(flpo)Hze}$ (The Jackson Laboratory Cat# JAX#030211; RRID: IMSR_JAX:030211).

Mouse diets

Standard diet (SD): PicoLab Rodent Diet 20 5053 (3.07 kcal/gram; 13% fat, 24% protein, 62% carbohydrates; 3.2% sucrose). High-fat diet (HFD): Open Source D12451 (4.73 kcal/gram; 45% fat, 20% protein, 35% carbohydrates; 17% sucrose).

Stereotaxic Surgery

Stereotaxic surgery was conducted as described in chapter III.

Viral constructs

AAV8-hSyn-DIO-hM3Dq-mcherry (Addgene 44361-AAV8; 9 × 10ˆ12 viral genomes/µl), AAV1-hSyn-FRT-TeNT-GFP (generated and produced in the Zweifel lab; 10ˆ12 viral genomes/µl), AAV1-ConFon-hM3-HA (ssAAV-1/2-hEF1alpha/hTLV1-Fon/Con[dFRT-HA_hM3D(Gq)(rev)-I-dlox-I-HA_hM3D(Gq)-I-dlox-I-HA_hM3D(Gq)(rev)-dFRT]-WPRE-hGHp(A); entry v605 at https://vvf.ethz.ch; 4.6 × 10ˆ12 viral genomes/µl), AAV1-ConFoff-hM3-HA (generated in the Güler lab, produced at the University of North Carolina at Chapel Hill Gene Therapy Center Vector Core Services; 2.2 × 10ˆ13 viral genomes/µl) were injected to the ARC (ML: ± 0.30 mm, AP: - 1.40 mm, DV: −5.90 mm). All coordinates are relative to bregma (George Paxinos and Keith B. J. Franklin).

Immunohistochemistry

Immunohistochemistry staining was conducted as described in chapter III.

The following primary antibodies were used for fluorescent labeling: rabbit anti-c-Fos (1:200, Santa Cruz Sc-52), rabbit anti-DsRed (1:1000, Clontech 632496), rabbit anti-HA

(1:500, Cell Signaling Technology C29F4), chicken anti-HA (1:500, Aves Labs ET-HA100), chicken anti-TH (1:500, Millipore AB9702), chicken anti-mCherry (1:500, NOVUSBIO NBP2-25158), goat anti-GFP (1:500, Rockland Immunochemicals Inc 600-101-215). The secondary antibodies (Jackson ImmunoResearch) used were Cy2- or Cy3-conjugated donkey anti-rabbit (1:250), and donkey anti-chicken (1:250).

Food intake analysis

Chemogenetic food intake analysis was conducted as described in chapter III.

For HFD intake and body weight measurements, 16-week to 22-week control and AgRP$^{Drd1\text{-}KO}$ littermates were provided with ad libitum access to HFD for 8 weeks. 10 pellets of pre-weighed HFD placed on the cage floor were weighed and refreshed weekly. Body weights were measured weekly.

Comprehensive Lab Animal Monitoring System (CLAMS)

The CLAMS system (Columbus Instruments) was used for indirect calorimeter and ambulatory locomotor activity measurements during ad libitum access to SCD or HFD. For chemogenetic activation experiments, mice were acclimated to metabolic cages for 3 days and habituated to i.p. injection on the second day. During test day, mice were injected with saline or CNO between ZT 3 to ZT 4 and then monitored for 24 hrs following the manufacturer's instructions. Control mice and AgRP^{Drd1}-KO mice were acclimated to metabolic cages for 2 days, and then monitored for 48 hrs with ad libitum access to SD. Mice were switched to HFD afterwards and then monitored for another 48 hrs with ad libitum access to HFD.

Energy expenditure (EE) in watts per kilogram of lean mass [W/kg] was calculated with the following formula described in (Fischer et al., 2018).

EE[W/kg]=1/60∗((0.2716[W∗min/ml]∗VO2[ml/kg/hour])+(0.07616[W∗min/ml]∗VCO2[ml/kg/hour])

The unit Watts was converted to kcal/h by multiplying factor of 0.86 to report EE as kcal/h/kg of lean mass.

Locomotor activity was reported as the sum of ambulatory beam breaks in x and y directions.

Open Field HFD foraging analysis

Open field HFD foraging analysis was conducted as described previously (Grippo et al., 2020). 8-week to 9-week old control and AgRP^{Drd1}-KO littermates were single-housed for at least one week and habituated to the HFD on day 1 and day 2 with 1-hr access to one pellet of the HFD provided each day. On day 3, mice were habituated to the open field for 10 min without food. On day 5, control mice and AgRP^{Drd1}-KO mice were placed into the open field with one pellet of the HFD buried under the 3cm-thick corn bedding. Behavior was recorded with a camera above the open-field chamber for 10 min and latency to food was quantified offline. The mice that failed to find the food pellet after 10 min were given a latency score of 10 min.

Statistics

When comparing two groups of normally distributed data, a Student's two-tailed *t*-test was used. In experiments with a single variable across more than two groups, an one-way ANOVA was performed. To compare the effects of genotypes and treatments within 4 groups, a two-way ANOVA test was used. To compare the effects of genotype and treatment within 4 groups at multiple time points, a three-way ANOVA test was performed. Following a significant effect in the ANOVA test, Bonferroni's post hoc comparison was

used to determine differences between individual data points. Analyses were conducted using the GraphPad Prism 8 statistical software for Windows. All data are presented as means ± standard error of the mean with $p < 0.05$ considered statistically significant.

Chapter V: The ARC potentially receives DA inputs from the Zona Incerta to regulate feeding

Abstract

The ARC neurons monitor and respond to blood-borne signals to initiate or cease feeding; however, the contribution of the central projections carrying sensory information to the ARC during feeding-associated behaviors remains obscure. Here we demonstrated that ARC receives projections from a continuum of DA neurons in the hypothalamus including the A12-A14 groups. We further revealed a potential functional pathway from the A13 group to the ARC to promote feeding.

Introduction

Energy-dense foods increase appetite leading to consumption beyond the homeostatic need (Ferrario et al., 2016). Dopamine (DA) signaling is necessary for encoding feeding behaviors, especially with the incentive and motivational aspects driving feeding (Palmiter, 2007; Narayanan et al., 2010; Coccurello and Maccarrone, 2018). DA-deficient mice fail to eat and die of starvation (Szczypka et al., 1999), while stimulation of the DA neurons rescues the $ARC^{AgRP/NPY}$ neuron ablation-induced starvation (Denis et al., 2015). The mesolimbic dopamine system is well-established for reinforcing the value of rewarding food and facilitating motivated behaviors (Salamone and Correa, 2012; Wise, 2004; Salamone et al., 2003; Coccurello and Maccarrone, 2018; Fields et al., 2007; Berridge, 2007; Salamone and Correa, 2012). However, counterintuitively, stimulation of the midbrain DA neurons fails to affect the amount of food consumption (Boekhoudt et al., 2017).

Beyond the mesolimbic system, hypothalamic DA neurons have been demonstrated to participate in energy homeostasis. DA neurons in the ARC (A12 group; Felten and Sladek, 1983; Fuxe et al., 1970) promote feeding by inhibiting POMC neurons without affecting the activity of the $ARC^{AgRP/NPY}$ neurons (Zhang and van den Pol, 2016). Additionally, DA in the paraventricular nucleus (PVN; A14 group) are situated in hypothalamic nuclei known to control food intake and these neurons project to the ventral hypothalamus (Moriya and Kuwaki, 2021; Romanov et al., 2017).

The functional relevance of DA neurons in the zona incerta (ZI; A13 group) in feeding is poorly explored. The ZI neurons extensively project to the neuraxis from cerebral cortex to spinal cord, including the ventral hypothalamus (Mitrofanis, 2005). Paralleling the widespread connectivity, ZI neurons are involved with diverse functions including controlling visceral activity, arousal, attention, and posture and locomotion (Mitrofanis, 2005). Patients receiving deep brain stimulation of the subthalamus, including the ZI, for the treatment of movement disorders can exhibit characteristics of binge eating (Amami et al., 2015; Zahodne et al., 2011). Correspondingly, the ZI cells were excited by food deprivation and the gut hunger signal ghrelin, while stimulation of ZI GABAergic neurons rapidly evokes binge-like eating (Zhang and van den Pol, 2017). Of note, prominent colocalization between the TH and VGAT-expressing neurons is observed in the ZI (Negishi et al., 2020), suggesting a robust orexigenic potential for A13 DA neurons.

Here we demonstrate that the ARC receives projections from a continuum of DA neurons in the hypothalamic areas including the dorsal ARC, PVN and ZI. DA is released in the ARC in feeding-associated events. Chemogenetic stimulation of the ZI neurons

including a group of TH neurons increases food consumption. Our findings suggest a functional pathway from the ZI DA neurons to the ARC that promotes feeding.

Result

The ARC receives projections from a continuum of DA neurons in the hypothalamic and subthalamic areas

To gain insight into the potential sources of DA inputs to the ARC, we targeted the ARC of adult wild type mice with retrogradely transported red fluorescent beads (retrobeads) (Figure 11A). One week after surgery, we examined the distribution of retrobeads in brain regions inhabited by dopaminergic neurons. We observed retrobeads in the dorsal ARC, zona incerta (ZI), and ventral tegmental area (VTA). There was notable colocalization of retrobeads and tyrosine hydroxylase (TH; the rate-limiting enzyme in DA synthesis) immunoreactivity in the ZI, but relatively lower in the VTA (Figure 11B). This suggests that the projections from the VTA to the ARC are non-dopaminergic and dopaminergic input to the ARC originates within the hypothalamus. To identify the dopaminergic neurons that make synaptic contacts within the ARC, we delivered a retrogradely transported AAV that Cre recombinase dependently expresses hM3Dq-mcherry (retrograde AAV-DIO-hM3Dq-mcherry) to the ARC of $Th^{tm1(cre/Esr1)Nat}$ (TH-IRES-creER) mice which express cre in TH-positive cells after five consecutive days of 75mg/kg tamoxifen injections (Figure 11C). In these mice, we observed robust mcherry and TH colocalization in the dorsal ARC, PVN and ZI (Figure 11D), but relatively sparsely in the VTA. This parallels our previous observation that the A12 and A13 dopaminergic neurons in the ARC and ZI are the likely sources of DA to the ARC.

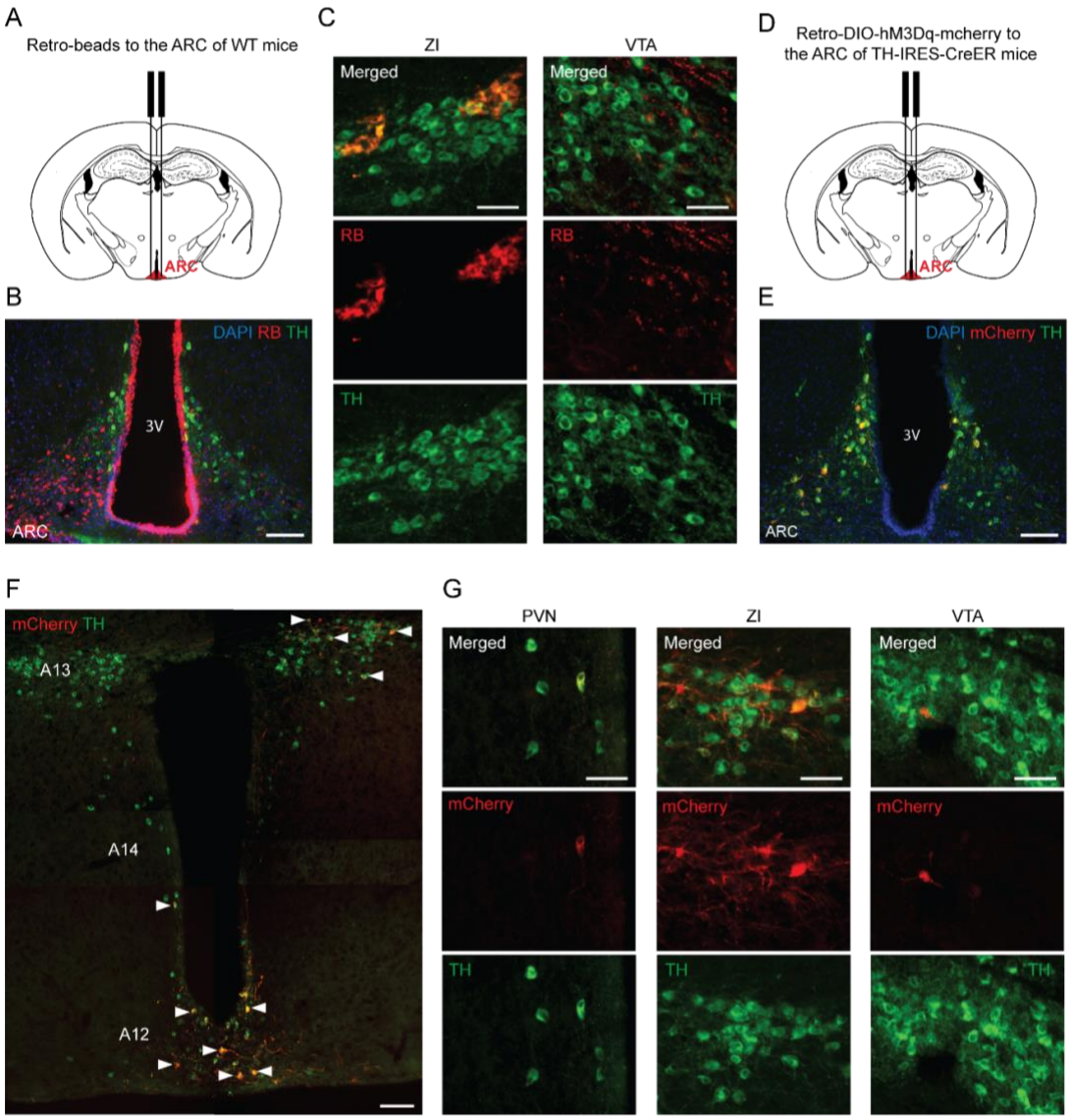

Figure 11. The ARC receives anatomical inputs from multiple dopaminergic neuronal populations

(A, D) ARC retrograde tracing paradigms: Retro-beads (A) or retrograde AAV-DIO-hM3Dq-mCherry (D) were delivered to the ARC of WT or TH-IRES-CreER, respectively. (B, E) Representative images showing retro-beads (B) or hM3Dq:mCherry expression (E) in the ARC. Scale bar represents 100 μm. c Representative images showing retro-beads

and their co-localization with TH-expressing cells in the ZI (left) and the VTA (right). Scale bar represents 50 μm.

(F) Representative stitched images showing expression of hM3Dq:mCherry and TH marking the A12-14 groups of DA neurons. Arrows indicate cells co-expressing hM3Dq:mCherry and TH. Scale bar represents 100 μm.

(G) Representative images of hM3Dq:mCherry- and TH-expressing cells in the PVN (left), the ZI (middle) and the VTA (right). Scale bar represents 50 μm.

Chemogenetic stimulation of the DA neurons in ZI increases food consumption

With the anatomical projections from the ZI DA neurons to the ARC, we sought to explore the role of ZI DA neurons in feeding regulation. To this end, we delivered the AAV-DIO-hM3Dq-mcherry to the ZI of TH-IRES-creER mice (TH-hM3Dq mice; Figure 12A). We confirmed the expression of hM3Dq-mecherry in the ZI after five consecutive days of 75mg/kg tamoxifen injections. However, besides a group of the hM3Dq-mecherry expressing neurons colocalized with TH in the lateral ZI, we observed hM3Dq-mCherry expression superior to the ZI DA neurons without TH expression (Figure 12A). We activated the hM3Dq-mCherry expressing neurons in the ZI with i.p. injection of 0.3 g/kg clozapine N-oxide (CNO) at ZT 3. This stimulation significantly increased food consumption in the TH-hM3Dq mice 4 hrs after CNO administration (4-hr intake: saline: 0.2458 ± 0.04999 g versus CNO: 0.5042 ± 0.04690 g; Student's two-tailed *t*-test, $P < 0.001$; Figure12B), but not in the control group (normalized 4-hr intake: hM3: 0.2583 ± 0.03826 versus Ctrl: -0.05378 ± 0.04290; Student's two-tailed *t*-test, $P < 0.001$; Figure 13C). These results suggest an orexigenic role of the ZI DA neurons paralleling their projections to the ARC.

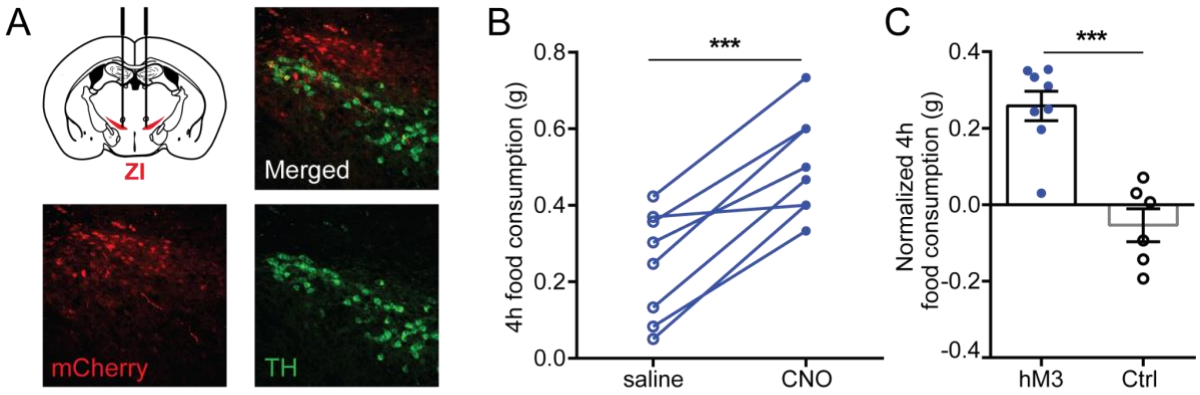

Figure 12. Chemogenetic stimulation of ZI neurons promote feeding

(A) Schematic depicting Cre-dependent hM3-mCherry expression in the ARC of TH-IRES-creER mice.

(B) 4-hr food consumption following saline or CNO administration in TH-hM3Dq mice. Student's two-tailed *t*-test; n = 8 / group.

(C) Normalized 4-hr food consumption following CNO administration in TH-hM3Dq or control mice (Ctrl). Control mice are TH-Cre:ER mice with cre-dependent mCherry targeted to the ZI. Student's two-tailed *t*-test; n = 6 - 8 / group.

DA is released in the ARC responding to the acute changes of energy supplies

To test when DA is released to the ARC during energy fluctuations, we next monitored the dynamics of DA levels in the ARC by delivering AAV that expresses the DA sensor, dLight 1.3b, to the ARC of adult male mice (Figure 13A). To reveal the dynamics of DA signaling in the ARC during food deficiency, we monitored the activity of the ARC Drd1 neurons expressing dLight during delivery and withdrawal of SD and HFD in overnight fasted mice (Figure 13B). To abolish the potential impacts induced by chronological order of diets on DA release, we switched the sequence of firstly delivered SD and HFD pellets in half of the animals. Surprisingly, the availability of SD failed to evoke DA release in the ARC (Figures 13C and 13D). Instead, DA release was enhanced acutely responding to the withdrawal of SD (Figure 13D), suggesting that DA signals to the ARC cells to prepare animals' seeking behavior following food deprivation. Consistently with this observation, DA was released after HFD withdrawal in a similar level with SD withdrawal (Figure 13E). Interestingly, when HFD was delivered, DA release was increased compared to SD delivery (Figures 13F), which revealed the potential of ARC DA signaling in encoding responses towards elevated energy density in food items. Altogether, these results suggest that DA signaling to the ARC cells senses the availability and energy contents in food.

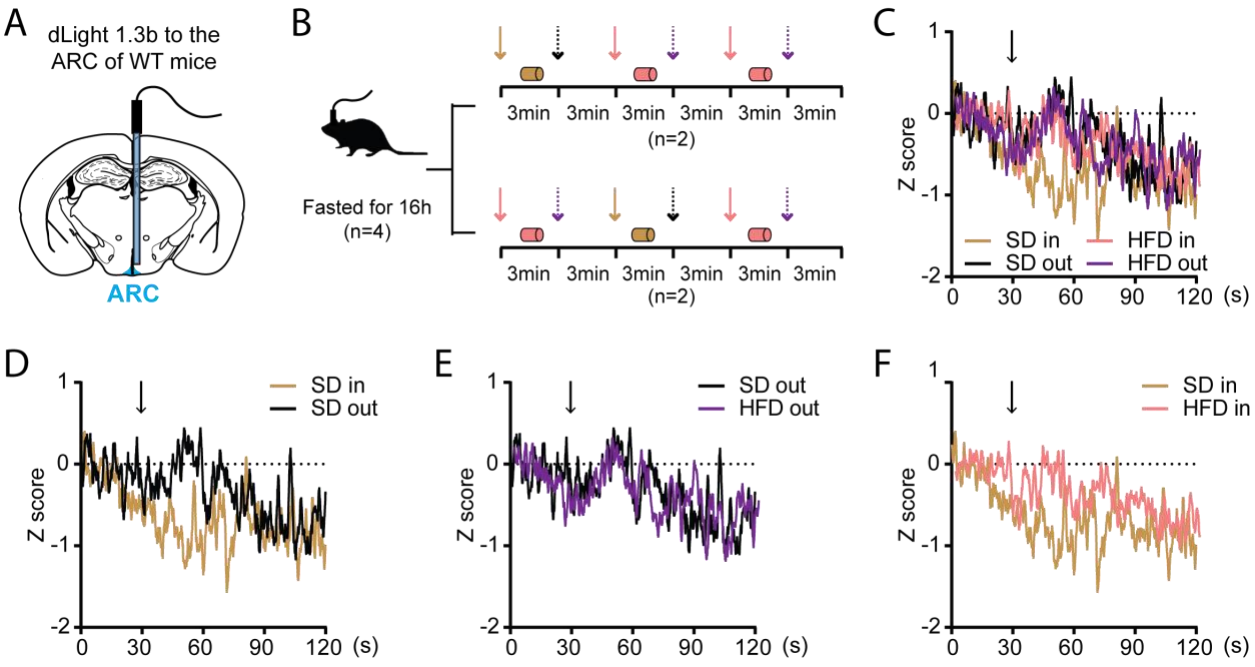

Figure 13. DA is acutely released in the ARC responding to changed energy supplies

(A) Schematic depicting dLight 1.3b expression in the ARC of wildtype mice.

(B) Food delivery and withdrawal paradigm: Mice previously habituated to HFD were overnight fasted for 16 hrs and refed with one pellet of SD and two pellets of HFD. The sequence of first two food pellets was switched for half of the animals. Each food pellet was available for 3 min and subsequently withdrawn for 3 min. Yellow and pink arrows indicate delivery of SD and HFD respectively; black and purple dashed arrows indicate withdrawal of SD and HFD respectively.

(C) Fiber photometry monitoring of fluorescent DA sensor dLight1.3b in the ARC in response to SD or HFD delivery and withdrawal in overnight-fasted mice.

(D) DA response to SD delivery and withdrawal from C.

(E) DA response to SD and HFD withdrawal from C.

(F) DA response to SD and HFD delivery from C.

Discussion

The nature of how ARC neurons monitor and respond to blood-borne signals are well described (Jais and Brüning, 2021); however, the contribution of the central projections carrying sensory information to the ARC during feeding-associated behaviors remains obscure (Chen et al., 2015). Dopaminergic signaling in the brain is involved in many facets of feeding-associated behaviors (Denis et al., 2015; Palmiter, 2007; Narayanan et al., 2010; Coccurello and Maccarrone, 2018). The ARC receives projections from a continuum of DA neurons in the hypothalamus (Figure 11) (Moriya and Kuwaki, 2021; Romanov et al., 2017; Zhang and van den Pol, 2016). DA receptors, including Drd1, are expressed in the ARC and Drd1 agonism modulates the activity of $ARC^{AgRP/NPY}$ neurons (Zhang and van den Pol, 2016). Although the relative contribution of ARC-projecting DA neurons to food consumption is yet to be discovered, this node represents a significant integration point for DA neurotransmission in energy homeostasis.

Of note, most of the rostral groups of TH-expressing neurons in the forebrain (A11, A13 − A15) showed little or no co-localization with markers of dopamine transporter (DAT) (Yip et al., 2018). One exception is the ARC A12 DA neurons with about 30% of the TH neurons expressing DAT (Yip et al., 2018). When monitoring DA activity in the ARC, we show that DA is released acutely responding to varied environmental changes including food deprivation and increased energy contents or palatability in available food items. As mentioned in Chapter I, Drd1 is dominantly regulated by phasic DA release, which requires rapid removal of DA from the synaptic cleft after excitatory bouts through DAT. One tentative model would be that the A12 DA neurons expressing DAT integrate hypothalamic DA inputs within the ARC by re-uptaking excessive DA. In this way, the

ARC-Drd1 neurons are manipulated by phasic DA release for precisely encoding feeding-associated behaviors towards energy fluctuations. Notably, the ARC DA activity levels in this study is much lower than the brain regions receiving midbrain DA inputs including NAc. It is possible that the DA dynamics in the ARC is relatively subtle, which in turn makes it challenging to study.

Because of the lack of DAT expression, the commonly used DATcre mouse line is not ideal for studying the hypothalamic clusters of DAergic neurons. Nevertheless, it has been reported that transgenes under control of the TH promoter, but not DAT, exhibit striking non-DA cell-specific expression patterns (Lammel et al., 2015; Lindeberg et al., 2004; Min et al., 1994). When the VTA of TH-Cre mouse lines targeted with a cre-dependent EYFP, only 48-59% of the EYFP-expressing cells were colocalized with TH expression (Lammel et al., 2015). Consistent with this report, when examining the function of the ZI DA neuron projections in the ARC, we observed very limited colocalization between expression of the Cre-dependent hM3-mCherry and TH immunoreactivity in TH-IRES-creER mice. This is possibly as a result of inappropriate expression driven by an exogenous promoter. Alternatively, there could be a dynamic expression pattern of TH in the ZI during development. Some precursor cells previously expressing TH and thus driving hM3 expression might not express TH in the later stage when visualizing the transgene expression. It is also possible that some cells have TH transcription but not expression as a consequence of post-transcriptional regulation of TH mRNA (Lindeberg et al., 2004). Regardless of the ectopic expression pattern of hM3 in THiresCre-ER mice, stimulation of ZI neurons including a subpopulation with TH

expression promotes food consumption, suggesting a potential of the A13 DA neurons in the ZI in directly manipulating the ARC neurons to induce feeding.

It has been demonstrated that the activation of DA-neurons supports feeding even in the absence of AgRP-neurons (Denis et al., 2015). This emphasizes the importance of the DA-dependent hedonic pathways in consummatory behaviors and their ability to override the homeostatic energy balance regulation. Our findings highlight the novel impacts of hypothalamic DA neurons in monitoring consumption of regular or hedonic food by signaling to the ARC. These findings will overhaul how we approach eating disorders and allow for the development of novel therapeutic strategies. Further study of the functional role of hypothalamic DA pathways in homeostatic and hedonic regulation of feeding will provide the much sought-after insight to how rewarding foods bypass the energy homeostasis neurocircuitry and promote food consumption even during times of energy surplus.

Materials and methods

Animals

All animal care experiments were conducted in concordance with the University of Virginia Institutional Animal Care and Committee. Mice were housed in a temperature and humidity controlled vivarium at 22-24°C and ~40% humidity with a 12h/12h light/dark cycle. Male adult animals older than 8 weeks were used in all behavioral experiments with the following genotypes: C57BL (The Jackson Laboratory Cat# JAX#000664; RRID: IMSR_JAX:000664), $Th^{tm1(cre/Esr1)Nat}$ (The Jackson Laboratory Cat# JAX#008532; RRID: IMSR_JAX:008532).

Mouse diets

Standard diet (SD): PicoLab Rodent Diet 20 5053 (3.07 kcal/gram; 13% fat, 24% protein, 62% carbohydrates; 3.2% sucrose).

Stereotaxic Surgery

Stereotaxic surgery was conducted as described in chapter III. For fiber photometry surgeries, a fiber optic cannula was implanted above the ARC following the injection of the virus (coordinates: bregma: AP: -1.40 mm, DV: -5.65 mm, L: 0.30 mm). The exposed end of the fiber optic cannula was fixed to the skull with Metabond. Mice were allowed to recover for at least 2 weeks before any behavioral tests.

Viral constructs

AAV8-hSyn-DIO-hM3Dq-mcherry (Addgene 44361-AAV8; 9 × 10ˆ12 viral genomes/µl), retrograde AAV-hSyn-DIO-hM3Dq-mcherry (Addgene 44361-AAVrg; 7 × 10ˆ12 viral genomes/µl), AAV-dLight 1.3b (Addgene) were injected to the ARC (ML: ± 0.30 mm, AP: - 1.40 mm, DV: −5.90 mm). All coordinates are relative to bregma (George Paxinos and Keith B. J. Franklin).

Retrograde tracing

Retro-beads tracing: 300 nL of fluorescent retrobeads (Lumafluor) were bilaterally injected to the ARC of wildtype mice. Brains were processed 3 days after retrobead delivery.

Retrograde AAV tracing: 500nl retrograde AAV-Con-hM3Dq-mcherry was bilaterally injected to the ARC of TH-IRES-CreER mice. Brains were processed three weeks after AAV delivery for immunohistochemistry as described in chapter III.

Immunohistochemistry

Immunohistochemistry staining was conducted as described in chapter III.

The following primary antibodies were used for fluorescent labeling: rabbit anti-c-Fos (1:200, Santa Cruz Sc-52), rabbit anti-DsRed (1:1000, Clontech 632496), chicken anti-mCherry (1:500, NOVUSBIO NBP2-25158). The secondary antibodies (Jackson ImmunoResearch) used were Cy2- or Cy3- conjugated donkey anti-rabbit (1:250), and donkey anti-chicken (1:250).

In vivo fiber photometry recording

Mice were previously habituated to HFD and were overnight fasted for 16 hrs before the test day. During the test day, mice were transferred to the recording room and individually housed in their home cage with the cage top left open. Implanted fiber-optic cannula (Thorlabs, 0.39 NA, Ø200 µm Core) on the animal is connected to fiber-optic cables (Doric Lenses, 0.37 NA, Ø200 µm Core) by the zirconia mating sleeve (Doric Lenses) connected to fiber-optic cables. The fiber-optic cable is connected to a commutator (Doric Lenses) to allow free-moving of the animals. Mice were allowed to acclimate to the experiment environment and fiber-optic tethering 10 min before recording. Fluorescent signals from both DA-dependent (465nm) and DA-independent isosbestic (405nm) excitation light wavelengths were recorded by the fiber photometry system. The isosbestic wavelength excitation signal was used to control for the artifacts from animal movement, fluorescent reporter expression and photobleaching. Signals were collected at 120Hz sampling rate. Mice were refed with one pellet of SD and 2 pellets of HFD. Access to each food pellet was 3 min following with a 3 min withdrawal period. The sequence of the firstly delivered SD and HFD was switched for half of the animal to abolish chronological effects.

Fiber photometry data analysis

Data was processed in Matlab with custom scripts. To eliminate the artifact from motion or protein expression, the DA-dependent isosbestic (405nm induced) signal was fitted to the DA-dependent (465nm induced) signal with a linear least-squares fit. The fluorescence change over baseline fluorescence (ΔF/F0) was calculated as (465nm induced signal - fitted 405nm induced signal) / (median of 465nm induced signal). To account for different photobleaching dynamics, each analyzed ΔF/F0 curve is further dentrended by an exponential fit. To normalize the variability caused by signal strength, Z-score ((signal-average of baseline signal) / standard deviation of baseline signal) is calculated to present the data. For DA response during the delivery and withdrawal of food, the first 30 seconds before the food delivery or withdrawal were used as baseline to calculate z-score. The DA responses within the 90-second period were displayed. (**Qijun Tang**)

Food intake analysis

Chemogenetic food intake analysis was conducted as described in chapter III.

Statistics

When comparing two groups of normally distributed data, a Student's two-tailed *t*-test was used. In experiments with a single variable across more than two groups, an one-way ANOVA was performed. To compare the effects of genotypes and treatments within 4 groups, a two-way ANOVA test was used. To compare the effects of genotype and treatment within 4 groups at multiple time points, a three-way ANOVA test was performed. Following a significant effect in the ANOVA test, Bonferroni's post hoc comparison was used to determine differences between individual data points. Analyses were conducted

using the GraphPad Prism 8 statistical software for Windows. All data are presented as means ± standard error of the mean with $p < 0.05$ considered statistically significant.

Chapter VI: Conclusions and future directions

Obesity resulting from overconsumption and increasingly common sedentary lifestyles leads to diabetes, cardiovascular, and metabolic diseases. Diets aimed to reduce body weight by restricting the amount of food intake commonly cause anxiety and mood disorders and remain largely ineffective for long-term weight loss. These observations have led clinicians to view overconsumption as an addiction, but whether restrictive dieting shares a neural basis with other forms of addiction and compulsive behaviors (*e.g.*, drugs of abuse, gambling) remains unknown. In our study, we find that similar to other addictive or compulsive behaviors, palatable food via dopaminergic signaling plays an essential role for short-circuiting the exquisite neural mechanisms governing weight maintenance and thereby leading to overconsumption. This work presents four major clinical and basic science implications: 1. Probing the genetic and functional heterogeneity of the DA system will largely increase the depth of understanding the mechanism of obesity development; 2. A treatment strategy targeting selective DA receptor expressing neurons is safer than global manipulation of DA levels or DA receptor activities; 3. The entanglement of homeostatic and hedonic feeding centers may be more intense than broadly believed; 4. The potential impact of hypothalamic DA neurons in energy homeostasis currently may be underestimated.

In collaboration with the Campbell lab, we identified a novel neuronal population expressing Drd1 in the ARC with heterogeneous gene expression profiles that had not been characterized previously. Beyond an orexigenic role of the ARC^{Drd1} in inducing voracious feeding, a striking difference was observed following stimulation of ARC^{Drd1} neurons or $ARC^{AgRP/NPY}$ neurons. Unlike the $ARC^{AgRP/NPY}$ neurons, increased activity of

the ARC^{Drd1} neurons facilitates potent foraging and locomotion which are not reversed by acquisition or consumption of a food item. This provocative example illustrates the complexity of overlapping neuronal circuits in encoding feeding-associated responses. Elevated activity of ARC$^{AgRP/NPY}$ neurons in hunger states emphasizes the value of food ingestion as it suppresses the aversion-like negative valence. However, when DA inputs influence the ARC neurons through Drd1 signaling, the value of an unacquired but potentially “better” food item is increased. Depending on the information carried by the inputs, different but potentially overlapping neuronal populations in the ARC are mediated to affect an animal’s decision toward sustained feeding or continuous foraging. We also demonstrated the functional diversity of the ARC^{Drd1} neurons which either express or do not express AgRP/NPY in acute or sustained feeding respectively. This type of research focusing on the functional diversity of neuronal subpopulations will be essential for future studies.

The clinical situation of obesity treatment is challenging. Current anti-obesity medications share the common problem of off-targeting instead of selectively controlling a precise central or peripheral target, thus often delivering insufficient efficacy and dubious safety. By revealing that the Drd1 signaling in the ARC$^{AgRP/NPY}$ neurons gates the severity of diet-induced hyperphagia and weight gain, we raised possibility that the Drd1 signaling in the ARC may be a prominent contributor to obesity development. Unlike the global Drd1 knockout mice, mice with ablation of Drd1 in the ARC$^{AgRP/NPY}$ neurons have no observable deficiencies during development compared to the wild type controls. These findings provide Drd1 signaling in the ARC$^{AgRP/NPY}$ neurons as a precise therapeutic target against obesity. Although patients with obesity and eating orders share the common

feature of overconsumption and being overweight, the pathology might be subtly different from case to case. We show that Drd1 in the $ARC^{AgRP/NPY}$ neurons is required for proper palatable food foraging, suggesting a specific role of this target in driving repetitive behaviors toward attaining and consuming palatable food.

For hedonic feeding, the Drd1-dependent DA system is well established for encoding the incentive and motivational aspects of feeding behaviors and is required for diet induced obesity. Using the DA system to override normal homeostatic setpoints for consumption represents an elegant solution for our evolutionary forerunners who lived in a world of unpredictable food availability resulting in feast or famine. However, this ancient adaptation has been disastrous in the face of persistent abundance of the high calorie foods that modernity offers and is the basis for the most rapidly increasing cause of mortality in developed countries. We demonstrated that the molecular players of the prototypical reward signaling cascade influence the activity of the most prominent neuron type that regulates homeostatic food intake: $ARC^{AgRP/NPY}$ neurons expressing Drd1 are sufficient to drive feeding, and Drd1 signaling in these neurons is necessary for diet induced changes in meal size and obesity. These findings have broad clinical and basic science implications. They contribute to the understanding of how palatable diets manipulate neuronal control of homeostasis during the development of obesity. A better understanding of the molecular underpinnings will have significant and immediate impact on therapies for obesity and its comorbidities.

In contrast to the well-established role of midbrain DA neurons in reinforcing the value of rewarding food and encoding the motivation towards hedonic feeding, the function of other DA systems including the hypothalamic A12-A15 DA neurons is less

explored. By showing a diversity of genetically defined DA neurons in the hypothalamic areas projecting to the ARC, we propose that hypothalamic DA neurons influence feeding by manipulating the activity of the ARC neurons. Even in the face of the imperfect expression pattern of hM3 in TH-IRES-creER mice, stimulation of ZI neurons promotes food consumption, suggesting that A13 DA neurons in the ZI directly interact with the ARC neurons to induce feeding, independently from the established role of midbrain DA neurons in driving feeding motivation. These findings highlight the importance in further understanding the function of hypothalamic DA neurons in obesity development.

Humans in modern society receive tremendous amounts of information every day. Multifarious ways of entertainments have been developed against emptiness. The DA system is one of the central systems largely affected by hedonic stimulus. Excessive excitement may disturb the DA system by attenuating its response to regular positive valence. In turn, humans may develop repetitive behaviors for novel or more intense exciters risking physiological and psychological health. Therefore, understanding the mechanism underlying the hedonic inputs-induced inertness in the DA system or other central systems will be critical to prevent human extinction over the booming civilization. Current knowledge of the role of DA system in hedonic feeding or obesity is very limited. A fundamental step will be dissecting the functional impact of heterogeneous DAergic circuits. Previous studies of neuronal groups were largely based on their locations or single genetic markers, which is arbitrary and ambiguous. Comprehensively analysis in a single-neuron level will be essential for future studies to subdivide functional relevance of selective neurons in detailed aspects of certain behaviors. Similarly, treatments against obesity by targeting a certain brain region or a specific gene may be insufficient to solve

the problem caused by off-targeting. One hypothetic model is to make advantage of the permeable median eminence and deliver DA receptor-targeting drugs from blood to the ventral hypothalamus. These drugs could be selectively activated by certain genes or peptides in order to precisely control DA activity in specific neuronal groups. For example, a Drd1-signaling suppressor transported via blood and absorbed by the ARC cells in an inactive form but activated under the procedure of AgRP production may restrain diet-induced obesity with minimal side effects. Furthermore, retrograding drugs could be applied to enable transsynaptic transportation from the ventral hypothalamus to upstream targets when necessary. These novel therapeutic strategies will lead us to a new era conquering obesity and other diseases.

Reference

Abizaid, A., Liu, Z.-W., Andrews, Z.B., Shanabrough, M., Borok, E., Elsworth, J.D., Roth, R.H., Sleeman, M.W., Picciotto, M.R., Tschöp, M.H., et al. (2006). Ghrelin modulates the activity and synaptic input organization of midbrain dopamine neurons while promoting appetite. J. Clin. Invest. *116*, 3229–3239.

Adan, R.A.H. (2013). Mechanisms underlying current and future anti-obesity drugs. Trends Neurosci. *36*, 133–140.

Alhadeff, A.L., Su, Z., Hernandez, E., Klima, M.L., Phillips, S.Z., Holland, R.A., Guo, C., Hantman, A.W., De Jonghe, B.C., and Betley, J.N. (2018). A neural circuit for the suppression of pain by a competing need state. Cell *173*, 140-152.e15.

Alhadeff, A.L., Goldstein, N., Park, O., Klima, M.L., Vargas, A., and Betley, J.N. (2019). Natural and Drug Rewards Engage Distinct Pathways that Converge on Coordinated Hypothalamic and Reward Circuits. Neuron *103*, 891-908.e6.

Alsiö, J., Olszewski, P.K., Norbäck, A.H., Gunnarsson, Z.E.A., Levine, A.S., Pickering, C., and Schiöth, H.B. (2010). Dopamine D1 receptor gene expression decreases in the nucleus accumbens upon long-term exposure to palatable food and differs depending on diet-induced obesity phenotype in rats. Neuroscience *171*, 779–787.

Amami, P., Dekker, I., Piacentini, S., Ferré, F., Romito, L.M., Franzini, A., Foncke, E.M.J., and Albanese, A. (2015). Impulse control behaviours in patients with Parkinson’s disease after subthalamic deep brain stimulation: de novo cases and 3-year follow-up. J. Neurol. Neurosurg. Psychiatr. *86*, 562–564.

Andrews, Z.B., Liu, Z.-W., Walllingford, N., Erion, D.M., Borok, E., Friedman, J.M.,

Tschöp, M.H., Shanabrough, M., Cline, G., Shulman, G.I., et al. (2008). UCP2 mediates ghrelin's action on NPY/AgRP neurons by lowering free radicals. Nature *454*, 846–851.

Aponte, Y., Atasoy, D., and Sternson, S.M. (2011). AGRP neurons are sufficient to orchestrate feeding behavior rapidly and without training. Nat. Neurosci. *14*, 351–355.

Arble, D.M., Ramsey, K.M., Bass, J., and Turek, F.W. (2010). Circadian disruption and metabolic disease: findings from animal models. Best Pract. Res. Clin. Endocrinol. Metab. *24*, 785–800.

Arcis, V., and Desor, D. (2003). Influence of environment structure and food availability on the foraging behaviour of the laboratory rat. Behav. Processes *60*, 191–198.

Astrup, A., Greenway, F.L., Ling, W., Pedicone, L., Lachowicz, J., Strader, C.D., Kwan, R., and Ecopipam Obesity Study Group (2007). Randomized controlled trials of the D1/D5 antagonist ecopipam for weight loss in obese subjects. Obesity (Silver Spring) *15*, 1717–1731.

Atcherley, C.W., Wood, K.M., Parent, K.L., Hashemi, P., and Heien, M.L. (2015). The coaction of tonic and phasic dopamine dynamics. Chem. Commun. *51*, 2235–2238.

Azevedo, E.P., Pomeranz, L., Cheng, J., Schneeberger, M., Vaughan, R., Stern, S.A., Tan, B., Doerig, K., Greengard, P., and Friedman, J.M. (2019). A Role of Drd2 Hippocampal Neurons in Context-Dependent Food Intake. Neuron *102*, 873-886.e5.

Batel, P., Houchi, H., Daoust, M., Ramoz, N., Naassila, M., and Gorwood, P. (2008). A haplotype of the DRD1 gene is associated with alcohol dependence. Alcohol. Clin. Exp. Res. *32*, 567–572.

Baver, S.B., Hope, K., Guyot, S., Bjørbaek, C., Kaczorowski, C., and O'Connell, K.M.S.

(2014). Leptin modulates the intrinsic excitability of AgRP/NPY neurons in the arcuate nucleus of the hypothalamus. J. Neurosci. *34*, 5486–5496.

Beninger, R.J., and Miller, R. (1998). Dopamine D1-like receptors and reward-related incentive learning. Neurosci. Biobehav. Rev. *22*, 335–345.

Berridge, K.C. (2007). The debate over dopamine's role in reward: the case for incentive salience. Psychopharmacology (Berl) *191*, 391–431.

Berrios, J., Li, C., Madara, J.C., Garfield, A.S., Steger, J.S., Krashes, M.J., and Lowell, B.B. (2021). Food cue regulation of AGRP hunger neurons guides learning. Nature *595*, 695–700.

Besharse, J.C., and McMahon, D.G. (2016). The Retina and Other Light-sensitive Ocular Clocks. J. Biol. Rhythms *31*, 223–243.

Betley, J.N., Cao, Z.F.H., Ritola, K.D., and Sternson, S.M. (2013). Parallel, redundant circuit organization for homeostatic control of feeding behavior. Cell *155*, 1337–1350.

Betley, J.N., Xu, S., Cao, Z.F.H., Gong, R., Magnus, C.J., Yu, Y., and Sternson, S.M. (2015). Neurons for hunger and thirst transmit a negative-valence teaching signal. Nature *521*, 180–185.

Beutler, L.R., Chen, Y., Ahn, J.S., Lin, Y.-C., Essner, R.A., and Knight, Z.A. (2017). Dynamics of Gut-Brain Communication Underlying Hunger. Neuron *96*, 461-475.e5.

Blundell, J.E., Goodson, S., and Halford, J.C. (2001). Regulation of appetite: role of leptin in signalling systems for drive and satiety. Int. J. Obes. Relat. Metab. Disord. *25 Suppl 1*, S29-34.

Boekhoudt, L., Roelofs, T.J.M., de Jong, J.W., de Leeuw, A.E., Luijendijk, M.C.M.,

Wolterink-Donselaar, I.G., van der Plasse, G., and Adan, R.A.H. (2017). Does activation of midbrain dopamine neurons promote or reduce feeding? Int J Obes (Lond) *41*, 1131–1140.

Borgland, S.L., Chang, S.-J., Bowers, M.S., Thompson, J.L., Vittoz, N., Floresco, S.B., Chou, J., Chen, B.T., and Bonci, A. (2009). Orexin A/hypocretin-1 selectively promotes motivation for positive reinforcers. J. Neurosci. *29*, 11215–11225.

Bosello, O., Carruba, M.O., Ferrannini, E., and Rotella, C.M. (2002). Sibutramine lost and found. Eat. Weight Disord. *7*, 161–167.

Bray, G.A., and Popkin, B.M. (1998). Dietary fat intake does affect obesity! Am. J. Clin. Nutr. *68*, 1157–1173.

Bromberg-Martin, E.S., Matsumoto, M., and Hikosaka, O. (2010). Dopamine in motivational control: rewarding, aversive, and alerting. Neuron *68*, 815–834.

Bruijnzeel, A.W., Corrie, L.W., Rogers, J.A., and Yamada, H. (2011). Effects of insulin and leptin in the ventral tegmental area and arcuate hypothalamic nucleus on food intake and brain reward function in female rats. Behav. Brain Res. *219*, 254–264.

Cains, S., Blomeley, C., Kollo, M., Rácz, R., and Burdakov, D. (2017). Agrp neuron activity is required for alcohol-induced overeating. Nat. Commun. *8*, 14014.

Cameron, C.M., Wightman, R.M., and Carelli, R.M. (2014). Dynamics of rapid dopamine release in the nucleus accumbens during goal-directed behaviors for cocaine versus natural rewards. Neuropharmacology *86*, 319–328.

Campbell, J.N., Macosko, E.Z., Fenselau, H., Pers, T.H., Lyubetskaya, A., Tenen, D., Goldman, M., Verstegen, A.M.J., Resch, J.M., McCarroll, S.A., et al. (2017). A

molecular census of arcuate hypothalamus and median eminence cell types. Nat. Neurosci. *20*, 484–496.

Cason, A.M., Smith, R.J., Tahsili-Fahadan, P., Moorman, D.E., Sartor, G.C., and Aston-Jones, G. (2010). Role of orexin/hypocretin in reward-seeking and addiction: implications for obesity. Physiol. Behav. *100*, 419–428.

Cavalcanti-de-Albuquerque, J.P., Bober, J., Zimmer, M.R., and Dietrich, M.O. (2019). Regulation of substrate utilization and adiposity by Agrp neurons. Nat. Commun. *10*, 311.

Chaix, A., Lin, T., Le, H.D., Chang, M.W., and Panda, S. (2019a). Time-Restricted Feeding Prevents Obesity and Metabolic Syndrome in Mice Lacking a Circadian Clock. Cell Metab. *29*, 303-319.e4.

Chaix, A., Manoogian, E.N.C., Melkani, G.C., and Panda, S. (2019b). Time-Restricted Eating to Prevent and Manage Chronic Metabolic Diseases. Annu. Rev. Nutr. *39*, 291–315.

Chaput, J.P., Klingenberg, L., Astrup, A., and Sjödin, A.M. (2011). Modern sedentary activities promote overconsumption of food in our current obesogenic environment. Obes. Rev. *12*, e12-20.

Chen, H.Y., Trumbauer, M.E., Chen, A.S., Weingarth, D.T., Adams, J.R., Frazier, E.G., Shen, Z., Marsh, D.J., Feighner, S.D., Guan, X.M., et al. (2004). Orexigenic action of peripheral ghrelin is mediated by neuropeptide Y and agouti-related protein. Endocrinology *145*, 2607–2612.

Chen, Y., Lin, Y.-C., Kuo, T.-W., and Knight, Z.A. (2015). Sensory detection of food

rapidly modulates arcuate feeding circuits. Cell *160*, 829–841.

Cincotta, A.H., and Meier, A.H. (1996). Bromocriptine (Ergoset) reduces body weight and improves glucose tolerance in obese subjects. Diabetes Care *19*, 667–670.

Coccurello, R., and Maccarrone, M. (2018). Hedonic Eating and the “Delicious Circle”: From Lipid-Derived Mediators to Brain Dopamine and Back. Front. Neurosci. *12*, 271.

Cooper, S.J., and Al-Naser, H.A. (2006). Dopaminergic control of food choice: contrasting effects of SKF 38393 and quinpirole on high-palatability food preference in the rat. Neuropharmacology *50*, 953–963.

Cowley, M.A., Smart, J.L., Rubinstein, M., Cerdán, M.G., Diano, S., Horvath, T.L., Cone, R.D., and Low, M.J. (2001). Leptin activates anorexigenic POMC neurons through a neural network in the arcuate nucleus. Nature *411*, 480–484.

Davis, J. (2018). Hunger, ghrelin and the gut. Brain Res. *1693*, 154–158.

Davis, C., Fattore, L., Kaplan, A.S., Carter, J.C., Levitan, R.D., and Kennedy, J.L. (2012). The suppression of appetite and food consumption by methylphenidate: the moderating effects of gender and weight status in healthy adults. Int. J. Neuropsychopharmacol. *15*, 181–187.

Del Corral, P., Bryan, D.R., Garvey, W.T., Gower, B.A., and Hunter, G.R. (2011). Dietary adherence during weight loss predicts weight regain. Obesity (Silver Spring) *19*, 1177–1181.

Denis, R.G.P., Joly-Amado, A., Webber, E., Langlet, F., Schaeffer, M., Padilla, S.L., Cansell, C., Dehouck, B., Castel, J., Delbès, A.-S., et al. (2015). Palatability can drive feeding independent of agrp neurons. Cell Metab. *22*, 646–657.

Dietrich, M.O., Bober, J., Ferreira, J.G., Tellez, L.A., Mineur, Y.S., Souza, D.O., Gao, X.-B., Picciotto, M.R., Araújo, I., Liu, Z.-W., et al. (2012). AgRP neurons regulate development of dopamine neuronal plasticity and nonfood-associated behaviors. Nat. Neurosci. *15*, 1108–1110.

Dietrich, M.O., Zimmer, M.R., Bober, J., and Horvath, T.L. (2015). Hypothalamic Agrp neurons drive stereotypic behaviors beyond feeding. Cell *160*, 1222–1232.

Dodd, G.T., Michael, N.J., Lee-Young, R.S., Mangiafico, S.P., Pryor, J.T., Munder, A.C., Simonds, S.E., Brüning, J.C., Zhang, Z.-Y., Cowley, M.A., et al. (2018). Insulin regulates POMC neuronal plasticity to control glucose metabolism. ELife *7*.

Durst, M., Könczöl, K., Balázsa, T., Eyre, M.D., and Tóth, Z.E. (2019). Reward-representing D1-type neurons in the medial shell of the accumbens nucleus regulate palatable food intake. Int J Obes (Lond) *43*, 917–927.

Eckel, R.H., Kahn, S.E., Ferrannini, E., Goldfine, A.B., Nathan, D.M., Schwartz, M.W., Smith, R.J., and Smith, S.R. (2011). Obesity and type 2 diabetes: what can be unified and what needs to be individualized? J. Clin. Endocrinol. Metab. *96*, 1654–1663.

Ellwood, I.T., Patel, T., Wadia, V., Lee, A.T., Liptak, A.T., Bender, K.J., and Sohal, V.S. (2017). Tonic or Phasic Stimulation of Dopaminergic Projections to Prefrontal Cortex Causes Mice to Maintain or Deviate from Previously Learned Behavioral Strategies. J. Neurosci. *37*, 8315–8329.

Espinosa-Carrasco, J., Burokas, A., Fructuoso, M., Erb, I., Martín-García, E., Gutiérrez-Martos, M., Notredame, C., Maldonado, R., and Dierssen, M. (2018). Time-course and dynamics of obesity-related behavioral changes induced by energy-dense foods in

mice. Addict. Biol. *23*, 531–543.

Felten, D.L., and Sladek, J.R. (1983). Monoamine distribution in primate brain V. Monoaminergic nuclei: anatomy, pathways and local organization. Brain Res. Bull. *10*, 171–284.

Fenselau, H., Campbell, J.N., Verstegen, A.M.J., Madara, J.C., Xu, J., Shah, B.P., Resch, J.M., Yang, Z., Mandelblat-Cerf, Y., Livneh, Y., et al. (2017). A rapidly acting glutamatergic ARC→PVH satiety circuit postsynaptically regulated by α-MSH. Nat. Neurosci. *20*, 42–51.

Ferrario, C.R., Labouèbe, G., Liu, S., Nieh, E.H., Routh, V.H., Xu, S., and O'Connor, E.C. (2016). Homeostasis meets motivation in the battle to control food intake. J. Neurosci. *36*, 11469–11481.

Fields, H.L., Hjelmstad, G.O., Margolis, E.B., and Nicola, S.M. (2007). Ventral tegmental area neurons in learned appetitive behavior and positive reinforcement. Annu. Rev. Neurosci. *30*, 289–316.

Fischer, A.W., Cannon, B., and Nedergaard, J. (2018). Optimal housing temperatures for mice to mimic the thermal environment of humans: An experimental study. Mol. Metab. *7*, 161–170.

la Fleur, S.E., Kalsbeek, A., Wortel, J., Fekkes, M.L., and Buijs, R.M. (2001). A daily rhythm in glucose tolerance: a role for the suprachiasmatic nucleus. Diabetes *50*, 1237–1243.

la Fleur, S.E., Vanderschuren, L.J.M.J., Luijendijk, M.C., Kloeze, B.M., Tiesjema, B., and Adan, R.A.H. (2007). A reciprocal interaction between food-motivated behavior and

diet-induced obesity. Int J Obes (Lond) *31*, 1286–1294.

Florentin, M., Liberopoulos, E.N., and Elisaf, M.S. (2008). Sibutramine-associated adverse effects: a practical guide for its safe use. Obes. Rev. *9*, 378–387.

Freedland, C.S., Poston, J.S., and Porrino, L.J. (2000). Effects of SR141716A, a central cannabinoid receptor antagonist, on food-maintained responding. Pharmacology Biochemistry and Behavior *67*, 265–270.

Fulton, S. (2010). Appetite and reward. Front. Neuroendocrinol. *31*, 85–103.

Fuxe, K., Hökfelt, T., and Ungerstedt, U. (1970). Morphological and functional aspects of central monoamine neurons. In International Review of Neurobiology Volume 13, (Elsevier), pp. 93–126.

Fu, O., Iwai, Y., Narukawa, M., Ishikawa, A.W., Ishii, K.K., Murata, K., Yoshimura, Y., Touhara, K., Misaka, T., Minokoshi, Y., et al. (2019). Hypothalamic neuronal circuits regulating hunger-induced taste modification. Nat. Commun. *10*, 4560.

Gabel, K., Hoddy, K.K., Haggerty, N., Song, J., Kroeger, C.M., Trepanowski, J.F., Panda, S., and Varady, K.A. (2018). Effects of 8-hour time restricted feeding on body weight and metabolic disease risk factors in obese adults: A pilot study. Nutr. Healthy Aging *4*, 345–353.

Garris, P.A., Ciolkowski, E.L., Pastore, P., and Wightman, R.M. (1994). Efflux of dopamine from the synaptic cleft in the nucleus accumbens of the rat brain. J. Neurosci. *14*, 6084–6093.

Gearhardt, A.N., White, M.A., Masheb, R.M., Morgan, P.T., Crosby, R.D., and Grilo, C.M. (2012). An examination of the food addiction construct in obese patients with binge

eating disorder. Int. J. Eat. Disord. *45*, 657–663.

Georgescu, D., Sears, R.M., Hommel, J.D., Barrot, M., Bolaños, C.A., Marsh, D.J., Bednarek, M.A., Bibb, J.A., Maratos-Flier, E., Nestler, E.J., et al. (2005). The hypothalamic neuropeptide melanin-concentrating hormone acts in the nucleus accumbens to modulate feeding behavior and forced-swim performance. J. Neurosci. *25*, 2933–2940.

Grippo, R.M., Tang, Q., Zhang, Q., Chadwick, S.R., Gao, Y., Altherr, E.B., Sipe, L., Purohit, A.M., Purohit, N.M., Sunkara, M.D., et al. (2020). Dopamine Signaling in the Suprachiasmatic Nucleus Enables Weight Gain Associated with Hedonic Feeding. Curr. Biol. *30*, 196-208.e8.

Gudelsky, G.A. (1981). Tuberoinfundibular dopamine neurons and the regulation of prolactin secretion. Psychoneuroendocrinology *6*, 3–16.

Guh, D.P., Zhang, W., Bansback, N., Amarsi, Z., Birmingham, C.L., and Anis, A.H. (2009). The incidence of co-morbidities related to obesity and overweight: a systematic review and meta-analysis. BMC Public Health *9*, 88.

Hahn, T.M., Breininger, J.F., Baskin, D.G., and Schwartz, M.W. (1998). Coexpression of Agrp and NPY in fasting-activated hypothalamic neurons. Nat. Neurosci. *1*, 271–272.

Hamdi, A., Porter, J., and Prasad, C. (1992). Decreased striatal D2 dopamine receptors in obese Zucker rats: changes during aging. Brain Res. *589*, 338–340.

Hansen, D.L., Toubro, S., Stock, M.J., Macdonald, I.A., and Astrup, A. (1998). Thermogenic effects of sibutramine in humans. Am. J. Clin. Nutr. *68*, 1180–1186.

Hariri, N., and Thibault, L. (2010). High-fat diet-induced obesity in animal models. Nutr.

Res. Rev. *23*, 270–299.

Harris, G.C., Wimmer, M., and Aston-Jones, G. (2005). A role for lateral hypothalamic orexin neurons in reward seeking. Nature *437*, 556–559.

Harrold, J.A., and Williams, G. (2003). The cannabinoid system: a role in both the homeostatic and hedonic control of eating? Br. J. Nutr. *90*, 729–734.

Hatori, M., Vollmers, C., Zarrinpar, A., DiTacchio, L., Bushong, E.A., Gill, S., Leblanc, M., Chaix, A., Joens, M., Fitzpatrick, J.A.J., et al. (2012). Time-restricted feeding without reducing caloric intake prevents metabolic diseases in mice fed a high-fat diet. Cell Metab. *15*, 848–860.

Hernandez, L., and Hoebel, B.G. (1988). Food reward and cocaine increase extracellular dopamine in the nucleus accumbens as measured by microdialysis. Life Sci. *42*, 1705–1712.

Heusner, C.L., Beutler, L.R., Houser, C.R., and Palmiter, R.D. (2008). Deletion of GAD67 in dopamine receptor-1 expressing cells causes specific motor deficits. Genesis *46*, 357–367.

Hill, J.O., Melanson, E.L., and Wyatt, H.T. (2000). Dietary fat intake and regulation of energy balance: implications for obesity. J. Nutr. *130*, 284S-288S.

van der Hoek, G.A., and Cooper, S.J. (1994). The selective dopamine uptake inhibitor GBR 12909: Its effects on the microstructure of feeding in rats. Pharmacology Biochemistry and Behavior *48*, 135–140.

Holtzman, S.G. (1979). Suppression of appetitive behavior in the rat by naloxone: lack of effect of prior morphine dependence. Life Sci. *24*, 219–226.

Holt, R.I.G., Barnett, A.H., and Bailey, C.J. (2010). Bromocriptine: old drug, new formulation and new indication. Diabetes Obes. Metab. *12*, 1048–1057.

Hommel, J.D., Trinko, R., Sears, R.M., Georgescu, D., Liu, Z.-W., Gao, X.-B., Thurmon, J.J., Marinelli, M., and DiLeone, R.J. (2006). Leptin receptor signaling in midbrain dopamine neurons regulates feeding. Neuron *51*, 801–810.

Howard, C.D., Li, H., Geddes, C.E., and Jin, X. (2017). Dynamic nigrostriatal dopamine biases action selection. Neuron *93*, 1436-1450.e8.

Huang, W., Ma, J.Z., Payne, T.J., Beuten, J., Dupont, R.T., and Li, M.D. (2008). Significant association of DRD1 with nicotine dependence. Hum. Genet. *123*, 133–140.

Hurt, R.T., Kulisek, C., Buchanan, L.A., and McClave, S.A. (2010). The obesity epidemic: challenges, health initiatives, and implications for gastroenterologists. Gastroenterol Hepatol (N Y) *6*, 780–792.

Isaacs, D., Prasad-Reddy, L., and Srivastava, S.B. (2016). Role of glucagon-like peptide 1 receptor agonists in management of obesity. Am. J. Health Syst. Pharm. 73, 1493–1507.

Jais, A., Paeger, L., Sotelo-Hitschfeld, T., Bremser, S., Prinzensteiner, M., Klemm, P., Mykytiuk, V., Widdershooven, P.J.M., Vesting, A.J., Grzelka, K., et al. (2020). PNOCARC Neurons Promote Hyperphagia and Obesity upon High-Fat-Diet Feeding. Neuron *106*, 1009-1025.e10.

James, W.P.T., Astrup, A., Finer, N., Hilsted, J., Kopelman, P., Rössner, S., Saris, W.H.M., and Gaal, L.F.V. (2000). Effect of sibutramine on weight maintenance after weight loss: a randomised trial. Lancet *356*, 2119–2125.

Jebb, S. (2004). Obesity: causes and consequences. Women's Health Medicine *1*, 38–41.

Jenni, N.L., Larkin, J.D., and Floresco, S.B. (2017). Prefrontal dopamine D1 and D2 receptors regulate dissociable aspects of decision making via distinct ventral striatal and amygdalar circuits. J. Neurosci. *37*, 6200–6213.

Johnson, P.M., and Kenny, P.J. (2010). Dopamine D2 receptors in addiction-like reward dysfunction and compulsive eating in obese rats. Nat. Neurosci. *13*, 635–641.

Joly-Amado, A., Cansell, C., Denis, R.G.P., Delbes, A.-S., Castel, J., Martinez, S., and Luquet, S. (2014). The hypothalamic arcuate nucleus and the control of peripheral substrates. Best Pract. Res. Clin. Endocrinol. Metab. *28*, 725–737.

Joly, J.-S., Osório, J., Alunni, A., Auger, H., Kano, S., and Rétaux, S. (2007). Windows of the brain: towards a developmental biology of circumventricular and other neurohemal organs. Semin. Cell Dev. Biol. *18*, 512–524.

Keiflin, R., and Janak, P.H. (2015). Dopamine prediction errors in reward learning and addiction: from theory to neural circuitry. Neuron *88*, 247–263.

Kern, A., Albarran-Zeckler, R., Walsh, H.E., and Smith, R.G. (2012). Apo-ghrelin receptor forms heteromers with DRD2 in hypothalamic neurons and is essential for anorexigenic effects of DRD2 agonism. Neuron *73*, 317–332.

Kim, E.R., Wu, Z., Sun, H., Xu, Y., Mangieri, L.R., Xu, Y., and Tong, Q. (2015). Hypothalamic Non-AgRP, Non-POMC GABAergic Neurons Are Required for Postweaning Feeding and NPY Hyperphagia. J. Neurosci. *35*, 10440–10450.

Kim, E.R., Xu, Y., Cassidy, R.M., Lu, Y., Yang, Y., Tian, J., Li, D.-P., Van Drunen, R.,

Ribas-Latre, A., Cai, Z.-L., et al. (2020). Paraventricular hypothalamus mediates diurnal rhythm of metabolism. Nat. Commun. *11*, 3794.

Koch, M., Varela, L., Kim, J.G., Kim, J.D., Hernández-Nuño, F., Simonds, S.E., Castorena, C.M., Vianna, C.R., Elmquist, J.K., Morozov, Y.M., et al. (2015). Hypothalamic POMC neurons promote cannabinoid-induced feeding. Nature *519*, 45–50.

Kohsaka, A., Laposky, A.D., Ramsey, K.M., Estrada, C., Joshu, C., Kobayashi, Y., Turek, F.W., and Bass, J. (2007). High-fat diet disrupts behavioral and molecular circadian rhythms in mice. Cell Metab. *6*, 414–421.

Kokorovic, A., Cheung, G.W.C., Rossetti, L., and Lam, T.K.T. (2009). Hypothalamic sensing of circulating lactate regulates glucose production. J. Cell. Mol. Med. *13*, 4403–4408.

Könner, A.C., Hess, S., Tovar, S., Mesaros, A., Sánchez-Lasheras, C., Evers, N., Verhagen, L.A.W., Brönneke, H.S., Kleinridders, A., Hampel, B., et al. (2011). Role for insulin signaling in catecholaminergic neurons in control of energy homeostasis. Cell Metab. *13*, 720–728.

Krashes, M.J., Koda, S., Ye, C., Rogan, S.C., Adams, A.C., Cusher, D.S., Maratos-Flier, E., Roth, B.L., and Lowell, B.B. (2011). Rapid, reversible activation of AgRP neurons drives feeding behavior in mice. J. Clin. Invest. *121*, 1424–1428.

Kreisler, A.D., and Rinaman, L. (2016). Hindbrain glucagon-like peptide-1 neurons track intake volume and contribute to injection stress-induced hypophagia in meal-entrained rats. Am. J. Physiol. Regul. Integr. Comp. Physiol. *310*, R906-16.

Kwon, E., Joung, H.-Y., Liu, S.-M., Chua, S.C., Schwartz, G.J., and Jo, Y.-H. (2020). Optogenetic stimulation of the liver-projecting melanocortinergic pathway promotes hepatic glucose production. Nat. Commun. *11*, 6295.

Lammel, S., Steinberg, E.E., Földy, C., Wall, N.R., Beier, K., Luo, L., and Malenka, R.C. (2015). Diversity of transgenic mouse models for selective targeting of midbrain dopamine neurons. Neuron *85*, 429–438.

Land, B.B., Narayanan, N.S., Liu, R.-J., Gianessi, C.A., Brayton, C.E., Grimaldi, D.M., Sarhan, M., Guarnieri, D.J., Deisseroth, K., Aghajanian, G.K., et al. (2014). Medial prefrontal D1 dopamine neurons control food intake. Nat. Neurosci. *17*, 248–253.

Lean, M.E. (2001). How does sibutramine work? Int. J. Obes. Relat. Metab. Disord. *25 Suppl 4*, S8-11.

Lee, H.S., Giunti, E., Sabino, V., and Cottone, P. (2020). Consummatory, Feeding Microstructural, and Metabolic Effects Induced by Limiting Access to Either a High-Sucrose or a High-Fat Diet. Nutrients *12*.

Leinninger, G.M., Jo, Y.-H., Leshan, R.L., Louis, G.W., Yang, H., Barrera, J.G., Wilson, H., Opland, D.M., Faouzi, M.A., Gong, Y., et al. (2009). Leptin acts via leptin receptor-expressing lateral hypothalamic neurons to modulate the mesolimbic dopamine system and suppress feeding. Cell Metab. *10*, 89–98.

Lindeberg, J., Usoskin, D., Bengtsson, H., Gustafsson, A., Kylberg, A., Söderström, S., and Ebendal, T. (2004). Transgenic expression of Cre recombinase from the tyrosine hydroxylase locus. Genesis *40*, 67–73.

Liu, J.-J., Bello, N.T., and Pang, Z.P. (2017). Presynaptic Regulation of Leptin in a

Defined Lateral Hypothalamus-Ventral Tegmental Area Neurocircuitry Depends on Energy State. J. Neurosci. *37*, 11854–11866.

Liu, T., Kong, D., Shah, B.P., Ye, C., Koda, S., Saunders, A., Ding, J.B., Yang, Z., Sabatini, B.L., and Lowell, B.B. (2012). Fasting activation of AgRP neurons requires NMDA receptors and involves spinogenesis and increased excitatory tone. Neuron *73*, 511–522.

Li, C., Hou, Y., Zhang, J., Sui, G., Du, X., Licinio, J., Wong, M.-L., and Yang, Y. (2019). AGRP neurons modulate fasting-induced anxiolytic effects. Transl. Psychiatry *9*, 111.

Luca, P., Laurin, N., Misener, V.L., Wigg, K.G., Anderson, B., Cate-Carter, T., Tannock, R., Humphries, T., Lovett, M.W., and Barr, C.L. (2007). Association of the dopamine receptor D1 gene, DRD1, with inattention symptoms in families selected for reading problems. Mol. Psychiatry *12*, 776–785.

Luo, S.X., Huang, J., Li, Q., Mohammad, H., Lee, C.-Y., Krishna, K., Kok, A.M.-Y., Tan, Y.L., Lim, J.Y., Li, H., et al. (2018). Regulation of feeding by somatostatin neurons in the tuberal nucleus. Science *361*, 76–81.

Luquet, S., Perez, F.A., Hnasko, T.S., and Palmiter, R.D. (2005). NPY/AgRP neurons are essential for feeding in adult mice but can be ablated in neonates. Science *310*, 683–685.

Lutas, A., Kucukdereli, H., Alturkistani, O., Carty, C., Sugden, A.U., Fernando, K., Diaz, V., Flores-Maldonado, V., and Andermann, M.L. (2019). State-specific gating of salient cues by midbrain dopaminergic input to basal amygdala. Nat. Neurosci. *22*, 1820–1833.

Madisen, L., Zwingman, T.A., Sunkin, S.M., Oh, S.W., Zariwala, H.A., Gu, H., Ng, L.L.,

Palmiter, R.D., Hawrylycz, M.J., Jones, A.R., et al. (2010). A robust and high-throughput Cre reporting and characterization system for the whole mouse brain. Nat. Neurosci. *13*, 133–140.

Mansour, A., Khachaturian, H., Lewis, M.E., Akil, H., and Watson, S.J. (1988). Anatomy of CNS opioid receptors. Trends Neurosci. *11*, 308–314.

Marcellino, D., Kehr, J., Agnati, L.F., and Fuxe, K. (2012). Increased affinity of dopamine for D(2) -like versus D(1) -like receptors. Relevance for volume transmission in interpreting PET findings. Synapse *66*, 196–203.

Marino, R.A.M., McDevitt, R.A., Gantz, S.C., Shen, H., Pignatelli, M., Xin, W., Wise, R.A., and Bonci, A. (2020). Control of food approach and eating by a GABAergic projection from lateral hypothalamus to dorsal pons. Proc Natl Acad Sci USA *117*, 8611–8615.

Mazzone, C.M., Liang-Guallpa, J., Li, C., Wolcott, N.S., Boone, M.H., Southern, M., Kobzar, N.P., Salgado, I. de A., Reddy, D.M., Sun, F., et al. (2020). High-fat food biases hypothalamic and mesolimbic expression of consummatory drives. Nat. Neurosci. *23*, 1253–1266.

Ma, Y., Bertone, E.R., Stanek, E.J., Reed, G.W., Hebert, J.R., Cohen, N.L., Merriam, P.A., and Ockene, I.S. (2003). Association between eating patterns and obesity in a free-living US adult population. Am. J. Epidemiol. *158*, 85–92.

Min, N., Joh, T.H., Kim, K.S., Peng, C., and Son, J.H. (1994). 5’ upstream DNA sequence of the rat tyrosine hydroxylase gene directs high-level and tissue-specific expression to catecholaminergic neurons in the central nervous system of transgenic

mice. Brain Res. Mol. Brain Res. *27*, 281–289.

Mirmohammadsadeghi, Z., Shareghi Brojeni, M., Haghparast, A., and Eliassi, A. (2018). Role of paraventricular hypothalamic dopaminergic D1 receptors in food intake regulation of food-deprived rats. Eur. J. Pharmacol. *818*, 43–49.

Mitchell, C.S., and Begg, D.P. (2021). The regulation of food intake by insulin in the central nervous system. J. Neuroendocrinol. *33*, e12952.

Mitrofanis, J. (2005). Some certainty for the “zone of uncertainty”? Exploring the function of the zona incerta. Neuroscience *130*, 1–15.

Montesi, L., El Ghoch, M., Brodosi, L., Calugi, S., Marchesini, G., and Dalle Grave, R. (2016). Long-term weight loss maintenance for obesity: a multidisciplinary approach. Diabetes Metab. Syndr. Obes. *9*, 37–46.

Moriya, S., and Kuwaki, T. (2021). A13 dopamine cell group in the zona incerta is a key neuronal nucleus in nociceptive processing. Neural Regen. Res. *16*, 1415–1416.

Musselman, L.P., Fink, J.L., Narzinski, K., Ramachandran, P.V., Hathiramani, S.S., Cagan, R.L., and Baranski, T.J. (2011). A high-sugar diet produces obesity and insulin resistance in wild-type Drosophila. Dis. Model. Mech. *4*, 842–849.

de Mutsert, R., Sun, Q., Willett, W.C., Hu, F.B., and van Dam, R.M. (2014).

Müller, T.D., Blüher, M., Tschöp, M.H., and DiMarchi, R.D. (2021). Anti-obesity drug discovery: advances and challenges. Nat. Rev. Drug Discov.

Overweight in early adulthood, adult weight change, and risk of type 2 diabetes, cardiovascular diseases, and certain cancers in men: a cohort study. Am. J. Epidemiol. *179*, 1353–1365.

Nakajima, K., Cui, Z., Li, C., Meister, J., Cui, Y., Fu, O., Smith, A.S., Jain, S., Lowell, B.B., Krashes, M.J., et al. (2016). Gs-coupled GPCR signalling in AgRP neurons triggers sustained increase in food intake. Nat. Commun. *7*, 10268.

Namburi, P., Al-Hasani, R., Calhoon, G.G., Bruchas, M.R., and Tye, K.M. (2016). Architectural representation of valence in the limbic system. Neuropsychopharmacology *41*, 1697–1715.

Narayanan, N.S., Guarnieri, D.J., and DiLeone, R.J. (2010). Metabolic hormones, dopamine circuits, and feeding. Front. Neuroendocrinol. *31*, 104–112.

Negishi, K., Payant, M.A., Schumacker, K.S., Wittmann, G., Butler, R.M., Lechan, R.M., Steinbusch, H.W.M., Khan, A.M., and Chee, M.J. (2020). Distributions of hypothalamic neuron populations coexpressing tyrosine hydroxylase and the vesicular GABA transporter in the mouse. J. Comp. Neurol. *528*, 1833–1855.

Nogueiras, R., Romero-Picó, A., Vazquez, M.J., Novelle, M.G., López, M., and Diéguez, C. (2012). The opioid system and food intake: homeostatic and hedonic mechanisms. Obes. Facts *5*, 196–207.

Olson, O.C., Quail, D.F., and Joyce, J.A. (2017). Obesity and the tumor microenvironment. Science *358*, 1130–1131.

Oswald, K.D., Murdaugh, D.L., King, V.L., and Boggiano, M.M. (2011). Motivation for palatable food despite consequences in an animal model of binge eating. Int. J. Eat. Disord. *44*, 203–211.

Padilla, S.L., Carmody, J.S., and Zeltser, L.M. (2010). Pomc-expressing progenitors give rise to antagonistic neuronal populations in hypothalamic feeding circuits. Nat.

Med. *16*, 403–405.

Palmiter, R.D. (2007). Is dopamine a physiologically relevant mediator of feeding behavior? Trends Neurosci. *30*, 375–381.

Piccinni, A., Bucchi, R., Fini, C., Vanelli, F., Mauri, M., Stallone, T., Cavallo, E.D., and Claudio, C. (2021). Food addiction and psychiatric comorbidities: a review of current evidence. Eat. Weight Disord. *26*, 1049–1056.

Piché, M.-E., Tchernof, A., and Després, J.-P. (2020). Obesity phenotypes, diabetes, and cardiovascular diseases. Circ. Res. *126*, 1477–1500.

Punjabi, M., Arnold, M., Geary, N., Langhans, W., and Pacheco-López, G. (2011). Peripheral glucagon-like peptide-1 (GLP-1) and satiation. Physiol. Behav. *105*, 71–76.

Rathod, Y.D., and Di Fulvio, M. (2021). The feeding microstructure of male and female mice. PLoS ONE *16*, e0246569.

Ravussin, E., and Tataranni, P.A. (1997). Dietary fat and human obesity. J. Am. Diet. Assoc. *97*, S42–S46.

Reichenbach, A., Clarke, R.E., Stark, R., Lockie, S.H., Mequinion, M., Dempsey, H., Rawlinson, S., Reed, F., Sepehrizadeh, T., DeVeer, M., et al. (2022). Metabolic sensing in AgRP neurons integrates homeostatic state with dopamine signalling in the striatum. ELife *11*.

Richfield, E.K., Penney, J.B., and Young, A.B. (1989). Anatomical and affinity state comparisons between dopamine D1 and D2 receptors in the rat central nervous system. Neuroscience *30*, 767–777.

Rodríguez, E.M., Blázquez, J.L., and Guerra, M. (2010). The design of barriers in the

hypothalamus allows the median eminence and the arcuate nucleus to enjoy private milieus: the former opens to the portal blood and the latter to the cerebrospinal fluid. Peptides *31*, 757–776.

Rolls, B.J., Shide, D.J., Thorwart, M.L., and Ulbrecht, J.S. (1998). Sibutramine reduces food intake in non-dieting women with obesity. Obes. Res. *6*, 1–11.

Rolls, B.J., Morris, E.L., and Roe, L.S. (2002). Portion size of food affects energy intake in normal-weight and overweight men and women. Am. J. Clin. Nutr. *76*, 1207–1213.

Rolls, B.J., Roe, L.S., Meengs, J.S., and Wall, D.E. (2004a). Increasing the portion size of a sandwich increases energy intake. J. Am. Diet. Assoc. *104*, 367–372.

Rolls, B.J., Roe, L.S., Kral, T.V.E., Meengs, J.S., and Wall, D.E. (2004b). Increasing the portion size of a packaged snack increases energy intake in men and women. Appetite *42*, 63–69.

Romanov, R.A., Zeisel, A., Bakker, J., Girach, F., Hellysaz, A., Tomer, R., Alpár, A., Mulder, J., Clotman, F., Keimpema, E., et al. (2017). Molecular interrogation of hypothalamic organization reveals distinct dopamine neuronal subtypes. Nat. Neurosci. *20*, 176–188.

Romero-Fernandez, W., Borroto-Escuela, D.O., Vargas-Barroso, V., Narváez, M., Di Palma, M., Agnati, L.F., Larriva Sahd, J., and Fuxe, K. (2014). Dopamine D1 and D2 receptor immunoreactivities in the arcuate-median eminence complex and their link to the tubero-infundibular dopamine neurons. Eur. J. Histochem. *58*, 2400.

Ruan, H.-B., Dietrich, M.O., Liu, Z.-W., Zimmer, M.R., Li, M.-D., Singh, J.P., Zhang, K., Yin, R., Wu, J., Horvath, T.L., et al. (2014). O-GlcNAc transferase enables AgRP

neurons to suppress browning of white fat. Cell *159*, 306–317.

Salamone, J.D., and Correa, M. (2012). The mysterious motivational functions of mesolimbic dopamine. Neuron *76*, 470–485.

Salamone, J.D., Correa, M., Mingote, S., and Weber, S.M. (2003). Nucleus accumbens dopamine and the regulation of effort in food-seeking behavior: implications for studies of natural motivation, psychiatry, and drug abuse. J. Pharmacol. Exp. Ther. *305*, 1–8.

Schultz, W. (1998). Predictive reward signal of dopamine neurons. J. Neurophysiol. *80*, 1–27.

Seagle, H.M., Bessesen, D.H., and Hill, J.O. (1998). Effects of sibutramine on resting metabolic rate and weight loss in overweight women. Obes. Res. *6*, 115–121.

Sharf, R., Sarhan, M., Brayton, C.E., Guarnieri, D.J., Taylor, J.R., and DiLeone, R.J. (2010). Orexin signaling via the orexin 1 receptor mediates operant responding for food reinforcement. Biol. Psychiatry *67*, 753–760.

Small, C.J., Kim, M.S., Stanley, S.A., Mitchell, J.R., Murphy, K., Morgan, D.G., Ghatei, M.A., and Bloom, S.R. (2001). Effects of chronic central nervous system administration of agouti-related protein in pair-fed animals. Diabetes *50*, 248–254.

Stagkourakis, S., Dunevall, J., Taleat, Z., Ewing, A.G., and Broberger, C. (2019). Dopamine release dynamics in the tuberoinfundibular dopamine system. J. Neurosci. *39*, 4009–4022.

Stanhope, K.L. (2016). Sugar consumption, metabolic disease and obesity: The state of the controversy. Crit. Rev. Clin. Lab. Sci. *53*, 52–67.

Statnick, M.A., Tinsley, F.C., Eastwood, B.J., Suter, T.M., Mitch, C.H., and Heiman,

M.L. (2003). Peptides that regulate food intake: antagonism of opioid receptors reduces body fat in obese rats by decreasing food intake and stimulating lipid utilization. Am. J. Physiol. Regul. Integr. Comp. Physiol. *284*, R1399-408.

Sutton, E.F., Beyl, R., Early, K.S., Cefalu, W.T., Ravussin, E., and Peterson, C.M. (2018). Early Time-Restricted Feeding Improves Insulin Sensitivity, Blood Pressure, and Oxidative Stress Even without Weight Loss in Men with Prediabetes. Cell Metab. *27*, 1212-1221.e3.

Szczypka, M.S., Rainey, M.A., Kim, D.S., Alaynick, W.A., Marck, B.T., Matsumoto, A.M., and Palmiter, R.D. (1999). Feeding behavior in dopamine-deficient mice. Proc Natl Acad Sci USA *96*, 12138–12143.

Takahashi, K.A., and Cone, R.D. (2005). Fasting induces a large, leptin-dependent increase in the intrinsic action potential frequency of orexigenic arcuate nucleus neuropeptide Y/Agouti-related protein neurons. Endocrinology *146*, 1043–1047.

Travagli, R.A., and Anselmi, L. (2016). Vagal neurocircuitry and its influence on gastric motility. Nat. Rev. Gastroenterol. Hepatol. *13*, 389–401.

Turek, F.W., Joshu, C., Kohsaka, A., Lin, E., Ivanova, G., McDearmon, E., Laposky, A., Losee-Olson, S., Easton, A., Jensen, D.R., et al. (2005). Obesity and metabolic syndrome in circadian Clock mutant mice. Science *308*, 1043–1045.

Vinué, Á., and González-Navarro, H. (2015). Glucose and Insulin Tolerance Tests in the Mouse. Methods Mol. Biol. *1339*, 247–254.

Volkow, N.D., Wang, G.-J., and Baler, R.D. (2011). Reward, dopamine and the control of food intake: implications for obesity. Trends Cogn Sci (Regul Ed) *15*, 37–46.

Volkow, N.D., Wise, R.A., and Baler, R. (2017). The dopamine motive system: implications for drug and food addiction. Nat. Rev. Neurosci. *18*, 741–752.

Wang, G.J., Volkow, N.D., Logan, J., Pappas, N.R., Wong, C.T., Zhu, W., Netusil, N., and Fowler, J.S. (2001). Brain dopamine and obesity. Lancet *357*, 354–357.

Warwick, Z.S., Synowski, S.J., Rice, K.D., and Smart, A.B. (2003). Independent effects of diet palatability and fat content on bout size and daily intake in rats. Physiol. Behav. *80*, 253–258.

Webb, V.L., and Wadden, T.A. (2017). Intensive lifestyle intervention for obesity: principles, practices, and results. Gastroenterology *152*, 1752–1764.

de Weijer, B.A., van de Giessen, E., van Amelsvoort, T.A., Boot, E., Braak, B., Janssen, I.M., van de Laar, A., Fliers, E., Serlie, M.J., and Booij, J. (2011). Lower striatal dopamine D2/3 receptor availability in obese compared with non-obese subjects. EJNMMI Res. *1*, 37.

Winters, B.D., Krüger, J.M., Huang, X., Gallaher, Z.R., Ishikawa, M., Czaja, K., Krueger, J.M., Huang, Y.H., Schlüter, O.M., and Dong, Y. (2012). Cannabinoid receptor 1-expressing neurons in the nucleus accumbens. Proc Natl Acad Sci USA *109*, E2717-25.

Winzell, M.S., and Ahrén, B. (2004). The high-fat diet-fed mouse: a model for studying mechanisms and treatment of impaired glucose tolerance and type 2 diabetes. Diabetes *53 Suppl 3*, S215-9.

Wise, R.A. (2004). Dopamine, learning and motivation. Nat. Rev. Neurosci. *5*, 483–494.

Wise, R.A. (2009). Roles for nigrostriatal--not just mesocorticolimbic--dopamine in reward and addiction. Trends Neurosci. *32*, 517–524.

Wise, R.A., and Colle, L.M. (1984). Pimozide attenuates free feeding: best scores analysis reveals a motivational deficit. Psychopharmacology (Berl) *84*, 446–451.

Wise, R.A., Spindler, J., and Legault, L. (1978). Major attenuation of food reward with performance-sparing doses of pimozide in the rat. Can. J. Psychol. *32*, 77–85.

World Health Organization. Obesity and overweight. Available at http://www.who.int/mediacentre/factsheets/fs311/en

Yamanaka, A., Beuckmann, C.T., Willie, J.T., Hara, J., Tsujino, N., Mieda, M., Tominaga, M., Yagami, K. ichi, Sugiyama, F., Goto, K., et al. (2003). Hypothalamic orexin neurons regulate arousal according to energy balance in mice. Neuron *38*, 701–713.

Yang, J., Hu, J., and Zhu, C. (2021). Obesity aggravates COVID-19: A systematic review and meta-analysis. J. Med. Virol. *93*, 257–261.

Yip, S.H., York, J., Hyland, B., Bunn, S.J., and Grattan, D.R. (2018). Incomplete concordance of dopamine transporter Cre (DATIREScre)-mediated recombination and tyrosine hydroxylase immunoreactivity in the mouse forebrain. J. Chem. Neuroanat. *90*, 40–48.

Zahodne, L.B., Susatia, F., Bowers, D., Ong, T.L., Jacobson, C.E., Okun, M.S., Rodriguez, R.L., Malaty, I.A., Foote, K.D., and Fernandez, H.H. (2011). Binge eating in Parkinson’s disease: prevalence, correlates and the contribution of deep brain stimulation. J. Neuropsychiatry Clin. Neurosci. *23*, 56–62.

Zhang, X., and van den Pol, A.N. (2016). Hypothalamic arcuate nucleus tyrosine hydroxylase neurons play orexigenic role in energy homeostasis. Nat. Neurosci. *19*,

1341–1347.

Zhang, X., and van den Pol, A.N. (2017). Rapid binge-like eating and body weight gain driven by zona incerta GABA neuron activation. Science *356*, 853–859.

Zhan, C., Zhou, J., Feng, Q., Zhang, J.-E., Lin, S., Bao, J., Wu, P., and Luo, M. (2013). Acute and long-term suppression of feeding behavior by POMC neurons in the brainstem and hypothalamus, respectively. J. Neurosci. *33*, 3624–3632.

Zhu, C., Jiang, Z., Xu, Y., Cai, Z.-L., Jiang, Q., Xu, Y., Xue, M., Arenkiel, B.R., Wu, Q., Shu, G., et al. (2020). Profound and redundant functions of arcuate neurons in obesity development. Nat. Metab. *2*, 763–774.

Bromocriptine: MedlinePlus Drug Information.